ABSTRACT

Title of dissertation: SENSORY-RELATED CHANGES IN TWO-SEGMENT DYNAMICS ON A SWAY-REFERENCED SUPPORT SURFACE

Robert A. Creath, Doctor of Philosophy, 2008

Dissertation directed by: Professor John J. Jeka, Department of Kinesiology

In its simplest form, the human postural control system can be described as a closed-loop control system consisting of a plant (body segments and musculotendon actuators) and feedback. Previous efforts to understand the contributions of plant and feedback employed techniques to “open the loop” which is problematic with the study of posture because the plant is unstable without feedback. In the present experiment, a closed-loop system identification method was used to “open the loop” without removal of sensory feedback.

Subjects stood on a movable platform facing a visual scene, both of which were capable of rotation about an axis coaxial with the subject’s ankles. The visual stimulus (present all trials) consisted of a 10-frequency sum-of-sines while movement of the support surface consisted of the following conditions: 1.

Stationary; 2. Sway-referenced to the subject's body sway; 3. 10-frequency sum-of-sines; 4. Combined sway-referenced and sum-of-sines.

Closed-loop frequency response functions were calculated for visual stimulus to EMG and visual stimulus to body sway angle. The open loop frequency response function for the plant was determined by dividing the frequency response functions, mathematically canceling the effects of feedback. With respect to the visual stimulus, gains for the leg segment showed no differences between the four platform conditions. Phase for the stationary condition was lower at the higher stimulus driving frequencies than for any of the moving platform conditions. In contrast, trunk segment gains were lower for the sway-referenced conditions at lower stimulus frequencies than for the stationary and sum-of-sines conditions. Phase showed a slight lead of the legs over the trunk for the sway-referenced conditions. The phase relationship between the trunk and leg segments, typically in-phase below ~1 Hz and anti-phase above ~1 Hz, showed a gradual transition at a lower frequency for the sway-referenced conditions than for the stationary or sum-of-sines conditions. Complex coherence showed a "legs-leading" coordinative relationship at the phase mode transition for the two sway-referenced conditions.

Differences in the frequency response functions demonstrate that the plant changes with platform condition requiring different postural control strategies to maintain stability.

SENSORY-RELATED CHANGES IN TWO-SEGMENT DYNAMICS ON A SWAY-REFERENCED SUPPORT SURFACE

by

Robert A. Creath

Dissertation proposal submitted to the faculty of the Graduate School of the University of Maryland, College Park in partial fulfillment of the requirements for the degree of Doctor of Philosophy

2008

Advisory Committee:
Professor John Jeka, Chair
Professor Jose Contreras-Vidal
Dr. Timothy Kiemel
Professor William Levine
Professor Jae Shim

Preface

Research activities and achievements

Upon matriculation to the University of Maryland I was introduced to the study of postural control through a project that involved an experimental paradigm which used a rotating platform to perturb quite stance in healthy subjects. Although not involved in the data collection, I performed the analysis which demonstrated the procedures involved in studying human postural control.

Pilot data was taken on four subjects, all students or faculty members, in order to assess the effectiveness of A/P sinusoidal platform rotations as perturbations to quiet stance. The purpose was to compare platform rotations with results obtained from similar studies involving light fingertip contact with a sinusoidal moving touch surface. The results suggested that gain and phase behaved similarly to the light touch paradigm.

My first opportunity to collect data came on a trip to Portland through collaboration with Fay Horak's lab at the Neurological Sciences Institute of the Oregon Health & Sciences University. The project, which yielded two publications (Creath et al., 2002, Horak et al., 2002), examined the effects of profound bilateral vestibular loss using a rotating platform paradigm and light, fingertip touch on a stationary surface. Without the benefit of vestibular information, BVL subjects were unable to reweight vestibular information and therefore tended to follow the platform at higher rotation frequencies, displaying higher gain and variability than control subjects. During trials with light touch, BVL subjects

displayed gain and variability values similar to control subjects. Finally, when asked to hold their “touch” finger in a stationary position above the touch plate, control subjects displayed different strategies to achieve this using a combination of hip and ankle strategies whereas BVL subjects were confined to a single, ankle strategy.

The second project was an extension of the BVL study. We sought to use galvanic stimulation of the vestibular nerve in order to simulate vestibular loss. Although we were able alter vestibular information, we were unable to mimic vestibular loss.

The third project involved looking at how subjects use support surface information to control posture by comparing fixed, foam, and sway-referenced surfaces. Working in collaboration with Robert Peterka and Fay Horak, we produced two publications. The results of the first (Jeka et al., 2004) suggested velocity information was more accurate in controlling posture than position or acceleration. In the second publication (Creath et al., 2005), we characterized posture using a 2-segment model that displayed simultaneous in-phase and anti-phase behavior between the trunk and leg segments.

On the fourth project we chose to look at postural control in subjects with Parkinson’s disease. Parkinsonian subjects suffer from a range of symptoms which vary considerably between subjects. We were looking for evidence of a proprioceptive deficit that affected posture. The results were as varied as the between-subjects symptomatic variability. Some subjects displayed a deficit while others did not. We concluded that a greater number of subjects who

displayed more advanced symptoms (i.e. minimum H&Y level 3) would be needed to characterize the subtle differences in posture caused by a proprioceptive deficit.

The fifth project sought to answer two questions. First, what happens during sway-referencing, and second, how does this affect intersegmental dynamics? Although sway-referencing is a commonly used technique for reducing ankle proprioception, questions remain regarding additional sensory information resulting from contact with the support surface. Our findings suggest that sway-referencing is effective at reducing sensory information that would normally occur due to changes in ankle angle. This includes sway around the ankles at frequencies of less than 1 Hz. Sway attributed to changes in trunk angle, usually in the frequency range above 1 Hz, do not appear to be correlated to sway-referenced platform movement.

The projects I have undertaken have given me the opportunity to explore a wide range of factors that influence postural control. Several of the projects have produced publications which are referenced in the text above. Others, although they haven't culminated in a publication, have given me insight into new ways to address research issues. An example would be a paper we have recently completed that applied our method of two-segment analysis to the BVL data from 2002 which is pending submission to the Journal of Vestibular Research. The motivation for taking another look at the BVL data grew out of our failure to successfully characterize postural deficits in early-stage Parkinsonian patients. The goal of my dissertation project is to extend these research efforts into

understanding how changes in sensory information affect intersegmental dynamics for a two-segment model of human posture.

Table of Contents

Part I. Introduction

Chapter 1

Using sway-referencing to assess postural control

The goal of research in postural control has been to understand the complex relationship between sensory and motor systems by observing the individual and integrated effects of visual, vestibular, and somatosensory information on maintaining upright stance. Sway-referencing is a commonly used technique that tries to render a particular form of sensory information ineffective by moving the normally stationary information source in proportion to the subjects' body sway. For example, when we use vision to help stabilize posture we depend on the fact that the visual scene is earth-fixed which provides a stationary reference. With visual sway-referencing the visual scene moves in proportion to natural body sway, taking away the attenuating effects of a stationary visual reference.

Like its visual analog, support surface sway-referencing (hence forth to be referred to as sway-referencing) tries to eliminate proprioceptive cues obtained from changes in ankle angle that occur during the course of normal body sway. This is accomplished by using a computer-driven servomotor system that uses a sensor to measure the angular deflection of body sway and induces a motor-driven rotation of the support surface in direct proportion to the change in body sway angle. Under ideal conditions, sway-referencing eliminates proprioceptive information by keeping ankle angle constant.

Sway-referencing has become an accepted method of manipulating sensory inputs to posture because it causes a predictable increase in sway. The underlying assumption is that proprioceptive information is eliminated or at least attenuated, but to an unknown degree. This coarse understanding of sway-referencing makes it very difficult to develop models that predict the consequences of sway-referencing, which may serve as a very useful tool to understand the postural control loop. The goal of this project is to critically look at support surface sway-referencing by assessing changes in postural control strategies that occur when the sensory environment changes.

Applications of sway-referencing in the study of postural control

Sway-referencing was a technique developed by Nashner in which various combinations of visual and support surface conditions were introduced to subjects where vision was either present (eyes open), absent (eyes closed), or ineffective (sway-referenced), and the support surface was either fixed or sway-referenced. The idea was to render sensory information obtained through vision and/or ankle proprioception ineffective by having the source of sensory information move in direct proportion to the subject's body sway. The six combinations of sensory conditions, referred to as the sensory organization test (SOT), were used to assess balance and postural disorders (e.g. Nashner et al., 1982).

Researchers have found that sway-referencing is an effective means of causing predictable increases in sway. In a research discipline such as

postural control where most sensory-induced changes in body sway are on the order of a degree or two, sway-referencing was found to increase sway up to an order of magnitude compared to sway on a fixed surface (e.g. Mergner et al., 2005). This suggests that sway-referencing has promise as a clinical diagnostic tool. As a result, sway-referencing has been applied to various patient populations such as diabetics (Horak et al., 2002), individuals with vestibular deficits (Nashner et al., 1982, Black et al., 1983; Peterka and Benolken, 1995, Mergner et al., 2005, Maurer et al., 2005), and individuals with Alzheimer's and Parkinson's diseases (Chong et al., 1999b, 2000) in an effort to diagnose condition-related postural deficiencies.

As a diagnostic tool, sway-referencing is effective in identifying postural deficits, but limitations of the SOT inhibit a thorough understanding of how sensory information is being used. First, vestibular information is always present. This limitation was addressed in several studies which compared normal and BVL subjects (e.g. Black et al., 1983; Peterka and Benolken, 1995; Mergner et al., 2003; Mergner et al., 2005; Maurer et al., 2005), and second, sway-referencing represents a different type of sensory perturbation in that the effects of vision or proprioception aren't absent such as for closing the eyes with vision, but they are instead rendered ineffective. I.e. a visual reference remains stationary relative to eye position instead of being earth-fixed and a proprioceptive reference remains constant relative to ankle angle. This creates a conundrum in that increased sway can result from either absent or ineffective sensory information.

This issue was addressed in the previously cited study by Peterka and Benolken (1995). This study departed from the more "traditional" SOT-based approach of comparing sway ratios between pairs of sensory conditions by using mathematical methods which stressed time series analysis and a feedback control model. The experiment involved a sinusoidally driven visual scene presented at three different frequencies (.1, .2, .5 Hz) and amplitudes up to 10 degrees to vestibular loss and healthy control subjects, on both a fixed and sway-referenced support surface. Vestibular loss subjects were found to increase sway amplitude with increasing visual amplitude while control subjects reached a "saturation" point at a frequency after which their sway amplitude remained constant. Next, the authors presented the simplest possible feedback model based on the assumption that the only source of sensory feedback was due to vision (vestibular and somatosensory information were not included in the model). When the results of their experimental analysis were compared with model simulations, the authors were able to make several qualitative judgments about the function of vestibular and somatosensory feedback even though they weren't included in the model. The first addressed the "saturation" phenomenon (the attenuation of sway with increasing stimulus amplitude) observed in healthy control subjects stated that saturation must be a phenomenon linked to vestibular function, and the second, an unexpected result, suggested that vestibular loss subjects didn't increase somatosensory gain to compensate for their deficit. The strength of using this approach is that it allowed comparisons to be made

which could address the issue of absent or ineffective sensory information, albeit in a qualitative manner.

In another study by Horak et al. (2002), subjects with diabetic peripheral neuropathy were compared to healthy controls using three different methods of sway-referencing. The first method referenced the support surface to the subject's ankle angle, the second, to the subject's center of mass sway angle, and the third to the filtered center of pressure trajectory. The authors found several interesting results. First, postural sway in diabetics was significantly greater than healthy controls on the fixed surface but not on the sway-referenced surfaces, suggesting that sway-referencing was effective at reducing somatosensory information in healthy subjects. Second, controls swayed more on the sway-referenced surface than diabetics standing on the fixed surface demonstrating that sway-referencing affected somatosensory information to a greater degree than was disrupted by severe neuropathy. Third, by comparing center of pressure sway-referencing (the authors assumed this to be most sensitive to tactile information) to the ankle and center of mass methods (assumed to be more sensitive to proprioceptive information), the authors deduced that subjects with diabetic neuropathy have a greater tactile deficit than proprioceptive deficit. In regard to sway-referencing as an experimental technique, the authors demonstrated two important points. First, that tactile information is used during sway-referencing and second, their assumptions about proprioceptive (ankle and center of mass sway-referencing) and tactile (filtered center of pressure)

sensitivity allowed them to use sway-referencing to assess an important question regarding peripheral deficits in subjects with diabetic neuropathy.

The Horak et al. (2002) results demonstrated that proprioception is indeed degraded by sway-referencing and that tactile information is used, but there is still the question of how they are integrated when one is degraded. This issue was addressed in a more recent study by Maurer et al. (2005) where the authors compared experimental data for subjects with vestibular loss and healthy controls to a feedback control model. The experimental paradigm consisted of platform tilts or external torques produced by a force-controlled pull of the subject's body, with and without sway-referencing. The experimental results showed that the transfer function was responsive to the stimulus frequency of the perturbation as a function of proprioceptive and vestibular cues which was an expected result. But, when they compared the experimental results with their modeling results, they found that sway-referencing the support surface caused an increase in the weighting of plantar somatosensory force sensors, suggesting that the postural control system has the ability to increase the weighting tactile information in the absence of ankle proprioception.

In the above cited cases, sway-referencing was used effectively to differentiate between the body sway characteristics of two patient populations and address the issue of how proprioceptive and tactile information were used to control posture. An important point to note is that the differences could be evaluated because the patients exhibited increased sway under

certain experimental conditions. It's possible that they also incorporated different postural strategies, but given the increases in body sway, they weren't necessary to evaluate sensitivity to changes in sensory information.

An example of a study where sway-referencing was less effective in differentiating postural deficits occurred in a study (Chong et al., 1999) comparing Parkinsonian (PD) subjects with Alzheimer's (AD) and control subjects. In this experiment the three subject groups underwent the six conditions of the SOT. The authors made two ambiguous conclusions. First, they stated that AD subjects were unable to suppress the incongruent visual stimuli presented in SOT condition 6 where both the visual scene and the support surface are sway-referenced. They followed this statement by saying that AD subjects weren't dependent on vision because they didn't increase sway with eyes closed. In regard to the PD subjects they stated that they had a "more general balance control problem" that might be related to their inability to change set which may indicate a proprioceptive deficit. The author's assessment, ambiguous in the case of AD subjects and unclear in the case of the PD subjects, was based on changes in the amount of sway induced by the addition of sway-referenced information.

The literature cited above shows some of the limitations of sway-referencing. Efforts have focused on observing sensory-related changes in the amount of body sway for a single variable, usually center of mass or center of pressure, which represents the simplest mechanical description of

human posture. The addition of modeling has shown promise because it allows for comparisons of greater complexity, e.g. control strategies.

In a 2004 study, Peterka and Loughlin, the authors were able to compare two control strategies with experimental results. The interesting thing about this study is that the authors apparently designed the experiment around their feedback model. Rather than allowing for flexion of joints other than the ankle (e.g. hip), they strapped the subjects to a backboard that limited subjects to an ankle strategy. The reason for this is simple. Single-segment models are easier to simulate than multi-segment models.

The experiment involved testing healthy subjects on a support surface that was either sway-referenced (180s trials: 60s fixed surface, 60s sway-referenced, 60s fixed) or reverse sway-referenced (240s trials: 60s fixed, 60s sway-referenced, 60s reverse sway-referenced, 60s fixed). The experimental objective was to observe transient changes in postural stability with the addition or removal of sensory information. The authors found that subjects displayed oscillatory sway with the cessation of sway-referencing which they determined was due to an increase in ankle torque. They were able to model this phenomenon using a feedback control model and determined that the increased ankle torque was due to sensory reweighting rather than increased gain of the compensating torque.

An important distinction regarding their modeling assumptions should be made. By simplifying the mechanical structure of their model to a single-segment, inverted pendulum they were able they were able to determine that

the likely strategy for increasing ankle torque was due to sensory reweighting. But, would this be true for a model that allowed flexion at the hip? It has been shown that a two-segment model which allows for hip and ankle flexion is utilized for large perturbations of the support surface (Horak and Nashner, 1986) as well as during quiet stance (Creath et al., 2005). The reason for the former is to accommodate large excursions of the center of mass and maintain upright stance, while the reason during quiet stance is unknown. It is reasonable to assume that by allowing for flexion at the hip, postural strategies would be exhibited other than those demonstrated by Peterka and Loughlin (2004) for their experimental paradigm.

Characterizing sway-referencing using a two-segment model

Efforts to fully understand the effects of sway-referencing on posture are hindered by the fact that the process isn't fully understood. It causes a predictable increase in sway and is probably the most effective means of rendering proprioceptive information ineffective. But, human posture is a complex process that involves dynamic interactions between multiple segments, some of which are responsive to changing sensory stimuli.

In a study by Creath et al. (2005) the dynamic relationship between trunk and leg segments was explored. Healthy subjects stood quietly with eyes closed for three support-surface conditions: fixed; foam (on fixed); and sway-referenced surfaces. Using frequency-domain analysis techniques, it was discovered that subjects simultaneously exhibited two postural

strategies, swaying with trunk and legs segments in-phase for frequencies below ~1 Hz and anti-phase for frequencies above ~1Hz. During sway-referencing, subjects were found to exhibit a different intersegmental relationship that showed a legs-leading-trunk coordinative relationship at the frequency that corresponded to the transition between in-phase and anti-phase behavior, while for the fixed and foam conditions the coordinative relationship between segments was undefined. An important result of this study is that sway-referencing altered a characteristic of posture, the relationship between segments, other than just causing an increase in sway that was observed in experiments involving single-segment models.

Sway-referencing is a useful experimental method in assessing human posture, but a more comprehensive understanding of its effects is needed. The purpose of this study is to characterize the effects of changing sensory information on a two-segment model of human posture in an effort to understand the dynamic relationship between trunk and leg segments during sway-referencing.

Chapter 2

A review of the postural control literature

The first part of this literature review explores the way in which the sensory modalities affect human upright posture. The purpose of this section is to provide a basic understanding of what is known about the influence of vestibular, visual, and somatosensory information on postural sway. The second part focuses on multisensory integration in an effort to explain the interaction effects of multiple sensory modalities on posture. In both parts, emphasis is placed on experimental paradigms which have provided a clear description of how posture is affected.

The sensory environment influences postural control

Postural sway is affected by sensory information obtained by vestibular, visual, and somatosensory systems. These sensory modalities provide information about the environment that enables us to assess our position, velocity, and acceleration in space, and to subsequently make the corrective moves which allow us to maintain upright stance.

Vestibular

Galvanic stimulation of the vestibular system

The peripheral structure of the human vestibular system, located in the inner ear, consists of otoliths and semicircular canals which are connected to the central nervous system via the VIII cranial nerve (Wilson and Melvill

Jones, 1979) providing information about linear and angular accelerations of the head, respectively.

Vestibular information presents several difficulties in the study of postural control. First, the otoliths have a limited sensitivity in detecting the acceleration of gravity. According to Horak and Macpherson (1996) studies on perceived orientation relative to vertical show the otoliths accurate to +/- 20 degrees for submerged subjects. Considering that a primary goal of posture is to counteract gravity in order to remain upright, this suggests that the otoliths only provide partial information in order to perceive gravitational acceleration (Trousselard et al., 2001; Mittelstaedt, 1992). Second, semicircular canals have a detection threshold of about +/- 1 degree/s (Peterka and Benolken, 1992; Schweigart et al., 1993). Since a large portion of normal postural sway occurs at low frequencies, the vestibular system is unable to detect sway at low frequencies. Third, the vestibular system is always active. Unlike other sensory modalities such as vision which can disrupted by closing of the eyes and proprioception which can be degraded through sway-referencing of the support surface, vestibular information always affects postural control. Despite these difficulties, several areas of research have yielded information on the effects of vestibular information.

Galvanic stimulus of the vestibular nerve has been employed to alter vestibular information in normal subjects (e.g. Coats, 1972; Hlavacka and Njiokiktjien, 1985, 1986). The method induces a low power electric field adjacent to the VIII cranial nerve which alters the characteristics of the tonic

signal transmitted from the inner ear to the central nervous system. By varying current polarity, the normal state of the tonic vestibular signal is disrupted by changes in the induced electric field. This alters the subject's response to the gravitational vector, thereby introducing a probe into the vestibulospinal system that can be used to study vestibular interactions with visual and somatosensory systems. These probes have taken three primary forms.

The first type of probe consists of continuous changes in current polarity. An early study by Coats (1972) using a sinusoidal galvanic probe was able to induce sinusoidal sway along the interaural axis. The importance of this results lies in that only the otoliths seemed to be affected. The apparent result was to simulate sinusoidal variations in the gravitational vector relative to head position that were the equivalent of tilting the head about the roll (naso-occipital) axis.

Two later studies by Hlavacka and Njiokiktjien (1985, 1986), using a similar type of sinusoidal probe, addressed the issue of how variations in vestibular information are used to control posture. In the 1985 study the authors found that rotation of the head relative to the trunk would change the direction of the induced sway. Regardless of trunk orientation, sway was always along the interaural axis. They concluded that neck afferents modulated postural corrections so that upright stance was always maintained regardless of head or trunk orientation. The 1986 study compared two different electrode arrangements, bipolar where the electrodes were placed

on opposite mastoid processes and the current polarity was altered differentially between the two electrodes, and monopolar where electrodes were placed on both mastoids and a ground placed on the subject's hand where the current polarity was altered either between the mastoids or between the mastoids and the ground. The results showed that both bipolar and monopolar stimulation could induce sway along the interaural axis, but that monopolar stimulation could also induce an additional amount of sway along the naso-occipital axis. Since sway along the latter axis was very small compared to interaural axis they concluded that monopolar stimulation had limited usefulness as a probe.

The second type of probe consists of pulsed current of constant polarity (as opposed to switching polarity used in sinusoidal stimuli) in the form of a cosine-bell curve. Hlavacka et al., (1996) used this type of probe in combination with a vibratory stimulus applied to the subject's leg. The purpose was to probe the relationship between vestibular information and leg proprioception. The authors found that subjects leaned in the direction predicted by the linear sum of the two perturbations, a conclusion that demonstrated up-channeling and down-channeling during quiet stance (Mergner was one of the authors). Another study by Horak and Hlavacka (2001) used this method to study the effects of peripheral neuropathy and standing on a foam surface. Two significant results were realized. First, subjects with peripheral neuropathy showed greater sensitivity to vestibular stimuli than control subjects for normal and foam surfaces. Second, kinematic

analyses indicated that trunk sway increased more than body center of mass suggesting that vestibular information is used in control of the trunk.

The third type of probe consists of pulsed current (similar to the second type) except that its timing is specified to coincide with a second probe. This method was employed using platform translations as the second probe (Inglis et al., 1995; Hlavacka et al., 1999). The purpose behind this approach is that it exposes the components of a known task, the platform translations, using a physical perturbation which stimulates both the otoliths (galvanic) and the semicircular canals (platform translations). In the first study the authors found that applying the galvanic stimulus 500 ms before platform movement occurred caused a change in the center of mass and center of pressure trajectories during platform movement and a change to a final equilibrium position predicted by the galvanic stimulus. The second study used the same approach, but altered the timing of the two probes. The authors found that subjects became habituated to the galvanic stimulus if it was applied more than 1 s before the platform moved. Additionally, they found a nonlinear response during the dynamic part of the postural response at approximately 150 ms which occurred before reaching the final equilibrium position. They concluded that the postural response was primarily under vestibulospinal control during the early, dynamic part of the response due to the combined nonlinear effects of sudden acceleration, presumably due to canal-otolith interaction combined with proprioceptive information from the support surface,

but under vestibular control, a linear summation of vestibular and proprioceptive information, later when an equilibrium position was achieved.

Galvanic stimulus provides a useful probe when looking at the relationships between vestibular information and proprioception, but its utility is limited in that the perturbation effects are small and directionally specific relative to other sensory perturbations and therefore provide information that is mostly qualitative. In order to understand the degree to which vestibular information affect postural control without the luxury of being able to disengage the vestibular apparatus it is useful to look to studies performed on subjects who have bilateral vestibular loss (BVL). This approach has its own inherent weakness in that the integrative component of vestibular information is lost in BVL subjects making direct comparisons with vestibular-intact subjects less than perfect.

Vestibular stimulation using support-surface perturbations

Another method of stimulating the vestibular system is by sinusoidal rotations (Allum et al., 1994, 1998; Peterka and Benolken, 1995; Mergner et al, 2000; Horak et al, 2002; Creath et al., 2002) or translations (Buchanan and Horak, 2001-2002; Horak et al, 2002) of the support surface. The rotation/translation paradigms provide a unique opportunity to assess the vestibular contribution of the postural response to surface perturbations based on a work by Nashner (1976) in which he looked at the functional stretch reflex (FSR). When comparing the two paradigms, lower leg muscles

are used such that the gastrocnemius is stretched for the rotation and translation paradigms, but in case of rotation stimulating the stretch reflex would cause the subject to over-rotate in the direction of platform movement and away fro upright vertical, destabilizing posture. On the other hand, backward translations move the feet from under the subject's center of mass, destabilizing posture. In this case, stimulating the stretch reflex would tend to bring subjects back to upright vertical, the opposite effect compared to rotation. Nashner concluded that the FSR is modified through integration with visual and vestibular information such that subjects switching between the two paradigms would adapt their postural set to achieve the same goal of reducing sway during upright stance.

In the case of sinusoidal platform rotations, several studies have been performed comparing BVLs and normal controls (Mergner et al, 2000; Horak et al, 2002; Creath et al., 2002). In all three studies, BVLs and controls were able to maintain upright stance with eyes closed for low frequency rotations by orienting themselves to the platform. As the platform frequency increased, normal subjects attenuated their body sway by shifting from platform information to vestibular information. BVLs, due to their deficiency, were unable to make the shift. As a result, several BVLs fell because they were unable to remain oriented to the platform at the higher rotation frequencies. An interesting point to note is that the BVLs experienced increased trunk sway compared to controls, but not leg sway (Creath et al., 2006) which

suggests that vestibular information plays a dominant role in control of the trunk.

Sinusoidal platform translations have been used infrequently as an experimental perturbation. One such study was performed by Buchanan and Horak (2001-2002) in which the platform was translated in the anterior-posterior direction at various frequencies from .1 to 1.15 Hz. The authors reported that controls and well-compensated BVLs rode the platform by fixing their head and trunk with respect to the platform for frequencies below .25 Hz. At higher frequencies (above .75 Hz), the well compensated BVLs behaved like the controls and tended to orient their trunks in space instead of with the platform. This is an important result that agrees with Nashner's observation regarding the FSR. When compared to the increased trunk sway in BVLs for sinusoidal platform rotations (Creath et al., 2006), the control of the trunk for platform translations is more like that of the controls. BVLs can use information from the FSR without addition vestibular information for platform translations, but not rotations.

While continuous perturbations provide information about the frequency-dependent processes of postural control, repeated exposure to the same motion can lead to habituation effects. While this approach has proven insightful, it doesn't address exposure to sudden "surprise" perturbations such as the type that might cause falls. A paradigm that addresses this issue utilizes discrete platform translations to perturb quiet stance. The general result of this approach has been elucidated by Horak and Nashner (1986)

who have shown that the postural response to sudden translations is dependent on the magnitude of the perturbation and the length of the support surface. For small magnitude perturbations in which the subject has full foot contact with the support surface, subjects exhibit an ankle strategy, but for large magnitude perturbations in which the subject is standing on a shortened surface, a hip strategy occurs.

A study using platform translations by Horak et al. (1990) compared BVLs and controls with the additional constraint of degrading somatosensory information from the lower legs and feet by hypoxic anesthesia. The purpose was to examine the effects of vestibular and somatosensory loss on the implementation of a hip or ankle strategy. EMG and kinematic analyses led the authors to conclude that vestibular information was necessary to implement a hip strategy, but not an ankle strategy. Later studies by members of the same research group (Shupert et al, 1994; Shupert et al, 1996; Runge et al, 1998) cast doubt on this conclusion by changing two components of the experimental protocol and more rigorous screening the BVL subjects. First, they removed the somatosensory constraint. Their conclusions for this change were that vestibular information wasn't necessary during the first 50 ms of the perturbation and that somatosensory clues derived from the platform were used in a similar manner by BVLs and controls. Second, they looked at larger perturbations using a longer surface for the BVLs. The reasoning was that a shortened support surface decreased the only remaining source of information available to BVLs (after closing their

eyes) which made falls inevitable. They found that BVLs exhibited what appeared to be a hip strategy, but had different EMG firing patterns. Third, some BVLs were categorized as “well compensated.” This seems to be an arbitrary designation based on clinical observation associated with performance on screening tests. Subjects who were designated as well compensated exhibited the apparent hip strategy described above while others did not. An important result of these studies was that EMG patterns were different in the BVLs than controls despite the appearance of a hip strategy, suggesting that vestibular information plays an important role in modulating muscle excitation during medium and long latency segments of the postural response to platform translations.

Interestingly enough, one study compared single rotations and translations of the support surface (Allum et al., 1994). EMG data was recorded to compare BVLs with controls. The results indicate that initial onset latencies were unchanged between the two groups, but that BVLs were unable to modulate muscle activity later in the postural correction (compare to similar findings of Hlavacka et al., 1999 using galvanic stimulus) which made the BVLs’ response seem slower compared to the controls. The authors further concluded that EMG responses of the legs were enhanced and responses of the trunk were inhibited by vestibular information. This last result explains an apparent contradiction between two studies (Horak et al., 1990; Runge et al., 1998), the first that stated BVLs didn’t exhibit a hip strategy and the second which said they did. Allum et al.’s (1994) observations suggested

that the specific characteristics of the support surface are the reason for the discrepancy. Responses to translations appear similar for both groups, albeit with differences appearing later during the postural correction for the BVLs, while responses to rotations appear different between the two groups.

Integrating vestibular information and proprioception

A final note regarding continuous sinusoidal rotations should be made for a method employed by Thomas Mergner's group (Schweigart et al., 1993; Mergner et al., 1997, 1998). Their approach was to rotate a subject's trunk (subjects were seated in a chair) and head (using a bite block) around the same vertical axis at various frequencies using combinations of the head and/or trunk. The subjects would then express (verbally or using a pointing device) which segment, head or trunk (or both), that they thought was being manipulated. Normal subjects (Mergner et al., 1997) would perceive the correct segment rotation provided the rotation frequency was high enough to exceed the vestibular threshold while BVLs (Schweigart et al., 1993) would only express the correct segmental rotation if the head was stationary (i.e. the only time their vestibular information was correct). The results demonstrated how the perception of movement changes by fusing information from the vestibular system and neck proprioceptors to establish a perception of position-in-space based on information that is up-channeled from neck proprioceptors and down-channeled from the vestibular system.

Vision

Vision affects postural control

In the previous section I discussed how vestibular information affects posture by detecting accelerations of the head. The other head-based sensory contribution to posture is from vision. Unlike vestibular information, vision provides an absolute, earth-fixed reference that serves to stabilize posture.

In an effort to understand how vision is used for postural control, Dornan et al. (1978) conducted a study on lower-leg amputees. Lacking proprioceptive and somatosensory inputs from the lower body, subjects showed decreased body sway when vision was present. When compared to control subjects, the amputees' dependence on vision was shown to be much greater than control subjects, a fact that the authors attributed to their dependence on visual and vestibular information.

Experiments designed to explore visual contributions to quiet stance frequently require the subject to direct their gaze at a fixed position, but when we interact with the environment our attention is usually directed at activities other than posture. In a study by Paulus et al. (1984) the authors sought to quantify the components of vision that contribute to postural control. First, they showed that postural stability decreased with the log of visual acuity until it reaches a threshold value of .03 (20/20 vision is a visual acuity of 1.0). Second, the authors found that foveal vision dominates over peripheral contributions, especially for mediolateral sway, a result that has come into

question in more recent studies. Third, when the visual scene is presented intermittently (using a strobe), continuity of visual information isn't required to stabilize posture. With exception of the foveal contribution result, the authors determined that a relatively minimal amount of visual information is required to assist in stabilizing posture. In a more recent study by Berencsi et al. (2005), central and peripheral visual contributions to posture were studied using a visual stimulus that consisted of a stationary random dot pattern that was presented to the subjects' central or peripheral vision fields. The authors found (in contrast to Paulus et al., 1984) that peripheral vision plays the dominant role in stabilizing posture.

Another point to consider is that the visual scene always contains movement. Even when standing quietly, self-motion ensures that our visual receptors will be observing what appears to be a non-stationary visual scene. In an effort to understand how moving visual information affects posture, Stoffregen (1985) performed a series of experiments designed to compare the effects of radial and lamellar optic flow. The first result was that lamellar flow in the peripheral field of view affected posture to a greater degree than radial flow in the central field of view. In order to test if the converse application of lamellar and radial flow had an effect, the subjects turned their heads so that lamellar flow was presented to their central field of vision and radial flow to their peripheral field of view. The result of this comparison was that radial flow in the peripheral field had no effect on posture, but that lamellar flow in the central field had a slight effect.

Visual information from a moving source

As an experimental method, moving the visual scene has proven to be a useful tool in probing posture. Referred to as the moving room paradigm (Lee & Aronson, 1974), the technique, as the name implies, consists of moving the visual scene, using either a physical room mounted on wheels, a computer generated virtual scene (e.g. Oie et al., 2002), or in the case of sway-referencing a scene that rotates along an axle collinear with the subject's ankles (e.g. Peterka, 2002).

Assessing the visual contribution to postural control becomes much more complex when movement of the visual scene is considered. In an experiment by van Asten et al. (1988) the effects of visual-scene rotation on postural sway was observed for two conditions accomplished in one of two ways, sinusoidally or at random angular velocities. The authors found that rotations of the visual scene induced similar rotations in subjects about the ankles joints for frequencies below .3 Hz, but that the induced sway appeared to be independent of the visual stimulus for angular velocities above 5 degrees/sec (sinusoidal rotations) or 10 degrees/sec (random angular velocities).

As a source of sensory information, vision helps attenuate body sway. But, the more effectively vision is used, the less sway is exhibited and the harder it is to observe sensory-related changes in posture. The results of van Asten et al. (1988) suggest a method to address this problem. Visually-

induced body sway provides an effective, non-mechanical probe for studying postural control.

In a study by Peterka and Benolken (1995) subjects with bilateral vestibular loss and healthy controls were presented with sinusoidal rotations of the visual field while standing on a platform that was either fixed or sway-referenced. Rotations of the visual scene occurred at frequencies of .1, .2, and .5 Hz for amplitudes between .2 and 10 degrees. The results showed that all subjects followed the visual stimulus in a similar manner at the lower visual amplitudes, but that controls reached a saturation point after which they realized no increases in sway amplitude. Vestibular loss subjects did not experience saturation. The results demonstrate that visual information is an effective sensory probe for small-amplitude perturbations.

In another study by Peterka (2002), subjects with bilateral vestibular loss were compared with healthy controls using a pseudorandom ternary sequence (PRTS) applied to the visual scene and support surface. The visual sensory conditions included PRTS, fixed (stationary), and eyes closed while the platform conditions included fixed, sway-referenced, and PRTS. The experimental results showed similar responses to the visual stimulus for all platform conditions. Gains increased with increasing stimulus frequency to approximately .3 Hz and decreased such that the lowest gains were at the highest frequencies. The condition dependence of gain was such that the smaller amplitudes produced higher gains than larger amplitudes, a difference that became minimal at higher stimulus frequencies. Phase angles at low

frequencies were between 0 and 90 degrees, decreasing with increasing stimulus frequency although there appeared to be no effect due to amplitude.

Somatosensation

The third type of sensory information, somatosensation, consists of proprioceptive and tactile information and differs from the other two types of sensory information in that information is derived from direct contact with the environment. Unlike visual or vestibular information, contact with the environment introduces a mechanical component that doesn't exist for the other sensory modalities.

Proprioception

Proprioception has been identified as crucial to maintaining upright posture because in the absence of visual and vestibular information, it's the only sensory modality necessary to maintain upright posture (Horak & Macpherson, 1996).

Proprioception refers to the ability to sense position and movement. Muscle spindle fibers, golgi tendon organs, and joint receptors are specialized peripheral neurons that respond to changes in limb position, transmitting information to the central nervous system (CNS). Once in the CNS, proprioceptive information is integrated with other sources of sensory information in order to translate the raw proprioceptive stimuli into a perceived movement within a body-centered coordinate system.

An application of this mechanism that relates to posture was elucidated by Nashner (1976) in an experiment that compared postural responses for different applications of the stretch reflex in the lower leg (Although this experiment was described earlier in this review I would like to refresh the details). In one case, the support surface was translated backwards causing a stretch in the gastrocnemius and moving the feet anterior to the center of mass, placing the subject in an unstable postural position. In the other scenario the support surface was rotated toes-up around an axis that was co-linear with the subject's ankle joints causing a similar stretch of the gastrocnemius. In the first case, the reflexive response to muscle stretching would facilitate a return to a stable, upright position, but in the second case the reflexive response would cause further backward rotation of the subject away from a stable upright position by contracting the gastrocnemius. Since healthy subjects were able to maintain upright posture when presented with either perturbation, the stretch reflex must be treated differently by the postural control system depending on the task, and modified by additional sensory information supplied from visual or vestibular sources. Nashner referred to this modified response the functional stretch reflex (FSR).

In addition to modifying the stretch reflex for use in postural control, the CNS performs an essential role in the processing of proprioceptive information used to derive estimates of body position in space. Experimental evidence comes from a study that utilized vibration to stimulate muscle spindles and alter the tonic signal used by the CNS to derive changes in

position. Lackner et al. (1979) placed vibrating mechanisms on postural muscles of the lower legs of subjects standing in a darkened room. When presented with touch or pressure cues, subjects would perceive motion despite being stationary. The authors termed this phenomenon “propriogyral illusion” because they were able to elicit the perception of rotation,

The above studies demonstrate that proprioception involves in interpretation by the CNS in order to decode information received from peripheral receptors. The next point to consider is how this information is used to maintain upright posture. The first study cited in this section (Nashner, 1976) demonstrated that the FSR involves interpretation of the stretch reflex depending on task conditions and sensory input from other sources, but considering the complexity of postural control, questions arise regarding the circumstances that affect the modification of the peripheral signal. For instance, how much vestibular or visual information is necessary and under what task conditions is it applied?

In a study by Diener at al. (1984) subjects had ischemic blocking of afferent nerves at the level of the ankle or the thigh and were then exposed to either sudden ramp tilts or .3 Hz AP sinusoidal rotations of the support surface. Results showed that subjects were not affected by ischemic blocking for sudden tilts, but showed a strong effect for slow oscillations. The authors determined that proprioceptive information derived from skin, pressure, and joint receptors was not used to compensate for sudden perturbations, but played an important role for slower movements. The results further suggest

that the characteristics of the task play a role in the selection of sensory information used.

An understanding of how proprioceptive and vestibular information are integrated can be seen in two studies that looked at subjects with vestibular loss. In the first study, Horak et al. (1990) compared subjects with bilateral vestibular loss and healthy controls for a series of backward translations of normal (full foot contact) and shortened (partial foot contact) support surfaces. An important point to note in this experiment is that the authors were able to observe proprioceptive information used in the absence of vestibular information. The expected result for normal subjects, an ankle strategy for the normal surface (slower translation velocities) and a hip strategy (faster velocities) for the shortened surface, was observed, but the results also showed that the vestibular loss subjects were unable to perform the hip strategy despite EMG data that suggested muscles were recruited in response to the perturbations in a manner similar to control subjects. The authors concluded that cutaneous and joint receptors play a role in determining the nature of the perturbation, but that vestibular information is necessary to execute the hip strategy. Compare the results of a subsequent experiment by Shupert et al. (1994) in which an experiment was performed that was similar with one exception. Vestibular loss subjects had full foot contact for all backward translation velocities. The results showed that vestibular loss subjects exhibited a hip strategy to the faster perturbations that was kinematically similar to controls, but different in terms of the EMG

responses. The authors concluded that vestibular information plays a bigger role than previously thought which includes selecting the correct subset of muscles and modulating their activity to successfully execute a hip strategy.

The two previous studies demonstrate that proprioceptive and vestibular information are codependent for maintaining upright posture in healthy subjects. In a later study, Buchanan and Horak (2001-2002) performed an experiment that showed the frequency dependence on the vestibular-proprioception interaction between the two sensory information sources. The authors compared subjects with vestibular loss to healthy controls for a series of sinusoidal AP platform translations at various frequencies. Results showed that two postural strategies were elicited by the translations that were dependent on the stimulus frequency. For low frequency oscillations (<=.25 Hz), all of the subjects followed the platform, swaying at the ankles. At higher frequencies (>=.75 Hz), control subjects fixed their heads in space while their legs followed the platform. At frequencies in between, the better compensated vestibular loss subjects were able to maintain balance on the moving platform, presumably because they were able to derive adequate information about platform velocity from proprioceptive sources. The authors concluded that vestibular information has a greater effect on trunk control, but that the postural control system was able to differentiate between vestibular and proprioceptive information, allowing for two control strategies to be exhibited at higher platform frequencies.

Light touch

Besides contact that is a result of standing on the support surface, contact with the environment can involve light touch contact with a stationary surface. This may be in the form of resting an arm on your desk or using a cane for support. Either method provides contact with the environment that helps us orient ourselves in space. The way in which we use touch contact has been explored through various studies that have focused on the neural component by limiting the contact forces to a small, non-mechanical value.

A common experimental approach used to explore somatosensation is through light finger tip contact with a stationary surface. Light touch has been shown to reduce body sway (Holden et al., 1994; Jeka and Lackner, 1994) which suggests that it has great potential as a substitute for individuals with balance problems needing assistance in maintaining postural control (Jeka, 1997). Indeed, studies have shown that light touch improves postural stability in subjects with vestibular deficits (Lackner et al., 1999, Horak et al., 2002, Creath et al., 2002), blind subjects (Jeka et al., 1996) and subjects who experience peripheral neuropathy (Dickstein et al., 2001, 2003).

The way in which light touch attenuates postural sway is a little less clear. Is it because of proprioceptive information due to changes in arm position or because of tactile clues that occur in fingertip sensors that detect pressure or shear forces? A study performed by Jeka and Lackner (1995) addressed this issue by looking at differences in postural sway due to light

touch on rough or slippery surfaces and found no differences. This result suggests that proprioception from changes in arm position may play the dominant sensory role. But, a study done by Rogers et al. (2001) which looked at passive contact also found that sway was reduced. In this study, tactile information was maintained by means of a device that was held against the skin at different points on the subjects' bodies. Sway was reduced sway regardless of the point of contact, but to a greater degree when applied at the shoulder than when applied to the lower leg. They concluded that the magnitude of the tactile stimulus (i.e. the amount of movement against the stationary contact surface) was the main factor in reducing sway. Furthermore, they stated that the postural control process was able to adapt to changing experimental conditions suggesting that somatosensation, whether proprioceptive or tactile, provides information about body position relative to the environment.

Using light touch to study somatosensation has an advantage in that the amount of mechanical contact can be altered by increasing or decreasing the amount of contact force making it possible to assess the mechanical contribution to postural sway. The extremes of this point were addressed in a study by Jeka and Lackner (1994) where conditions were compared where subjects used either light touch (<1 N) or as much force as they desired. The authors concluded that both conditions achieved a similar degree of sway reduction. The mechanical effects of force seemed only to matter in the phase relationship between fingertip contact forces and center of pressure.

When the contact force was greater, the finger contact forces and center of pressure were in phase due to mechanical support at the fingertip, but when contact force was reduced, body sway lagged fingertip contact forces suggesting that sensory information was being utilized to make postural adjustments (Jeka and Lackner, 1994).

When compared to other forms of sensory information, light touch causes a similar reduction in body sway, but the degree to which somatosensory information influences postural control is difficult determine from this paradigm because the observable variable (e.g. body sway, COP) decreases for stronger sensory stimuli making stronger stimuli harder to observe. A solution to this conundrum was employed by Jeka et al. (1997, 1998) who used a moving touch plate with a sinusoidal drive as a somatosensory probe. Using this paradigm it's possible to look at the effects of larger stimuli without the observable variable diminishing.

Three results stand out from these studies. First, subjects tended to entrain their body sway to the driving stimulus with gains of approximately 1 (but sometimes greater) and phases which indicated a phase lead at lower frequencies and a phase lag at higher frequencies. Second, the phase relationship between drive and response indicated that subjects coupled mainly to the velocity of the stimulus, but also to its position as well. And third, stimulus velocity was the primary variable used by the postural control system.

Multisensory integration

The postural control system operates on several levels. Neural sensors detect stimuli from an environmental source, the information is transmitted through a complex network of neurons to higher levels in the central nervous system where it's integrated and used to make corrective movements. The last step, the integration of sensory information from multiple sources, has proven to be the most difficult to understand. The search for answers has taken two forms, experimental and modeling.

Experimental studies

Efforts to elucidate the effects of changing sensory information on posture are confounded by the presence of redundant information from competing sources making it difficult to isolate a single modality. One approach to understanding multisensory integration has been through studies which compare combinations of sensory modalities, a method commonly referred to as dynamic posturography. The method was presented as a means of diagnosing balance deficits using combinations of vision, vestibular, and somatosensory information (Nashner et al., 1982; Black et al., 1983). Visual or somatosensory modalities are either present, absent, or rendered ineffective. For vision this meant that the eyes were open, closed, or the visual scene referenced to the subjects' body sway (likewise for somatosensory information with the support platform). The idea was to use

the six possible combinations of the three modalities to clinically evaluate balance deficits (Mirka and Black, 1990).

It was obvious that a better understanding of sensory fusion was needed to address variations that occur within a condition. The integration of vestibular and proprioceptive inputs was examined (Mergner et al., 1997, Mergner and Rosemeier, 1998) where the authors used horizontal rotations of the trunk and head around a common vertical axis. Subjects estimated their position by using the sum of the head and trunk rotations such that their perceived position was a combination of the two rotations. When the frequency of head rotation was below the threshold of vestibular detection, subjects made errors in estimating position suggesting that it was necessary to have the fused vestibular and proprioceptive signals in order to estimate position.

When performing a simple task, such as Mergner's head and trunk rotations, a clear picture of sensory fusion emerges, but when sensory information from different sources conflict with each other a method for resolving the ambiguity is needed. A concept that addresses this issue, sensory reweighting, involves looking at how the relative priority placed on a particular sensory modality by the postural control system varies with changing sensory conditions.

The idea behind sensory reweighting is that the postural control system can change the emphasis it places on input from a specific sensory

modality depending on changes that occur in the sensory environment (Horak and Macpherson, 1996).

In an experiment performed by Creath et al. (2002), subjects with bilateral vestibular loss were compared to healthy control subjects while standing with eyes closed on a moving platform that rotated sinusoidally in the AP direction at frequencies ranging from .01 to .4 Hz. At the lower platform frequencies, center of mass sway angle gains for both groups were similar, but as platform frequency increased, the gains reported for the healthy subjects decreased while the gains reported for the vestibular loss subjects increased. The gain similarities between the two groups suggest that proprioception dominates postural control at low frequencies while at higher frequencies the gain differences show that vestibular information becomes increasingly important for maintaining upright posture, and that the control subjects were able to reweight somatosensory and vestibular information as platform frequency increased while the vestibular loss subjects were not.

The frequency-dependent gain decrease observed in the control subjects is a phenomenon that has been observed in other experiments that utilized a similar driving signal (e.g. Jeka et al., 1997, 1998) which suggests that gain is somehow influenced by the driving signal. A problem in assessing reweighting using this format is that changes in driving frequency may be simply demonstrating the frequency dependencies observed between proprioceptive and vestibular sensory modalities (Creath et al., 2002). This

issue was addressed by Oie et al. (2002) in a study that employed two drives and two sensory modalities. In their experiment, touch and visual driving signals were presented simultaneously where one was held constant while the other varied and vice versa. The authors found two interesting results. First, the center of mass gains decreased for both touch and vision when the stimulus amplitude increased indicating that intra-modality reweighting occurred, and second, that visual gain was also dependent on touch amplitude indicating that inter-modality reweighting had also occurred.

Modeling studies

Experimental studies provide a limited view of sensory integration because the processes that occur in the central nervous system can only be observed through their expression as an observable variable such as center of pressure or center of mass sway angle. Studies that involve mathematical modeling allow for an in-depth analysis of "hidden" processes, but have their own inherent strengths and weaknesses.

Models are simplified representations of complex processes that express the state of a system based on a set of assumptions. For example, the equations that define the motion of a pendulum can be derived from assumptions based on physical principles which are readily observable such as gravity and the moment of inertia. In the case of the pendulum, the model agrees well with observable phenomena. But, when we look at the postural control system, many of the processes that occur are hidden from view in the

cortical areas of the central nervous system. In order to model these processes, assumptions are often made based on experimental observations, and as a result, tend to follow trends based on the experimental outcomes that inspired them. Never the less, modeling has proven to be useful in elucidating the possible underlying mechanisms that drive sensory integration.

An example of a sensory integration model based on experimental data was presented by Jeka et al. (1997, 1998). The model expressed the postural control system as a second order system with noise in which coupling coefficients were used to express the degree to which a subject's sway was entrained to the driving stimulus. Based on this observation, the estimated coupling coefficients characterized the degree to which sway was entrained to the velocity and position of the stimulus motion. The strength of this model was that the authors' assumptions captured the essence of observable body sway phenomena relative to the driving stimulus, in this case the relative degree to which body sway was entrained to the position and velocity of the stimulus.

Another experimentally-inspired model was developed by Mergner et al. (1997) and enhanced by Mergner and Rosemeier (1998) which examined the integration of vestibular and sensory information from neck proprioceptors. The experiment that inspired this model, described earlier in this review, involved rotations of the trunk and head around a common vertical axis. In this model, sensory integration is expressed as a sum of the

information from vestibular and neck proprioceptors which provided an estimate of position in space.

While the model up/down channeling model described by Mergner seems to accurately capture the sensory fusion process, it is unable to describe the more complex processes that use the fused sensory information. This issue was explored in two studies (Mergner et al., 2003; Maurer et al., 2005), both of which employed feedback control models to demonstrate a mechanism for sensory feedback and cortical control of ankle torque. The authors were able to demonstrate how sensory fusion from up/down channeling could be used to form global set points which were then fed into the control model to initiate the ankle torque needed to remain upright.

Part II. Previous research projects

Chapter 3

Limited Control Strategies with the Loss of Vestibular Function

Creath R, Kiemel T, Horak F, Jeka JJ

Exp Brain Res. (2002); 145(3): 323-33

Introduction

One of the properties considered essential for flexible control of upright stance is reweighting of the sensory information from the visual, vestibular, and somatosensory systems. As we move about in the environment, sensory conditions continually change, potentially in ways that make certain sources of sensory information unreliable for the maintenance of upright stance. For example, if we move from a light to a dark environment, our previous reliance upon vision is no longer relevant. It is assumed that in such situations (although not definitively shown in the literature), the nervous system increases the sensitivity to other forms of sensory information or recruits additional forms of sensory information to generate reasonable estimates of the center of mass. The common behavior of seeking out additional hand contact with rigid surfaces or objects in a dark room accentuates this point. In the present study, we illustrate how both reweighting and use of an additional source of sensory information are effective strategies to deal with changing environmental conditions. Moreover, we show how the lack of vestibular information influences the process of reweighting.

One form of additional sensory information that is commonly used is light touch contact of the fingertip or hands with surrounding support surfaces. A series of studies have demonstrated that fingertip contact with a rigid surface at very low force levels is as effective in stabilizing postural sway as when the applied forces are mechanically supportive (Holden et al., 1994; Jeka & Lackner, 1994; 1995; Jeka, et al., 1996). The experimental paradigm consists of subjects standing quietly, typically in a challenging stance (such as heel-to-toe), while touching a small metal plate with embedded force transducers. A feedback circuit sounds an alarm when an adjustable force threshold is exceeded. At a threshold of 1 Newton (≅ 100 gm), subjects easily learn (within 1 practice trial) to keep the alarm off while standing quietly. More importantly, when subjects stand with “light touch contact”, body sway amplitude decreases by 50-60% when compared to standing without touch. When the alarm is turned off and subjects are allowed to apply mechanically supportive forces, sway amplitude is equivalent to that measured with light touch contact. This suggests that touch contact improves stability by providing reliable somatosensory feedback rather than mechanical support.

Despite numerous investigations, the role of somatosensory information in postural control is not fully understood. Somatosensory information can take the form of deep pressure and cutaneous information from the bottom of the feet that can provide information about support surface properties such as width, texture, sliding friction, as well as information about

surface contact forces. Through proprioception from the muscles, somatosensation also provides information about the movement of the body and the relative position of body segments (Dietz, 1992; Horak & Macpherson, 1996). Somatosensory information from the feet and legs is thought to dominate control of postural sway whenever information from the support surface is available and reliable (Mergner, Huber & Becker, 1997; Horak, Nashner & Diener, 1990; Magnussen, Johansson & Wiklund, 1990; Dietz, 1992). However, when subjects stand on unstable (i.e., narrow, compliant, or moving) surfaces, vestibular and visual information become more important for the control of posture (Buchanan and Horak, 1998; Fitzpatrick & McCloskey, 1994; Horak, Shupert, Dietz & Horstmann, 1994; Maurer, Mergner, Bolha & Hlavacka, 2000; Mergner, Huber & Becker, 1997; Nashner, Black & Wall, 1982).

Compliant and short surfaces not only result in altered somatosensory feedback, but they also produce changes in postural control strategies. Because these surfaces do not permit the use of torque about the ankle to control the position of the body's center of mass, stance on narrow and compliant surfaces is unstable and is associated with the use of large hip and trunk movements ("hip strategy") to control posture (Horak & Nashner, 1986; Runge, Shupert, Horak, & Zajac, 1999). Presumably, it is the altered somatosensory information generated by the narrow or compliant force surface, in combination with visual and vestibular information signaling increased instability that triggers the switch to the hip strategy. Sensory

information from the vestibular and visual systems also seems especially critical for the control of the head and trunk in space during postural control. Loss of vestibular information compromises the ability to perform the hip strategy on short support surfaces (Horak et al., 1990), and vestibular loss subjects are unable to control head and trunk position during stance on an oscillating platform when vision is not available (Buchanan & Horak; 1999).

In the present study, we compared how bilateral vestibular loss subjects control postural sway compared to healthy control subjects when standing on a sinusoidally moving support surface with eyes closed. The intent was to investigate how individuals adjust to different frequencies of platform movement at constant amplitude. With increasing frequency at constant amplitude, the strength of the velocity-dependent component of the platform stimulus also increases. We asked whether subjects showed evidence of reweighting to another source of sensory information with increasing frequency of the support surface. In addition, we investigated whether subjects could use an external reference to compensate for the influence of support platform movements on postural sway. Two forms of external reference were studied: 1) light touch contact of the fingertip to a rigid earth-fixed surface; and 2) maintenance of the fingertip at a virtual location just above the touch surface (no contact). Previous studies have shown that light touch contact compensates for the loss of vestibular information during quiet stance (Lackner et al., 1999). The question in the current study was whether a controlled position of the fingertip in space was

as effective as an actual external reference during a dynamic balancing task standing on a sinusoidally moving support surface.

Methods

Subjects

The experimental protocol was approved by the Institutional Review Boards of the Oregon Health Sciences University and the University of Maryland and was performed in accordance with the 1964 Helsinki Declaration. All subjects gave their informed consent prior to participation in this study.

Five bilaterally deficient vestibular subjects, three females and two males, and six healthy control subjects matched by age and gender participated in the study.[1] Vestibular function was assessed by a combination of methods to determine the degree of deficit, as shown in Table 1.[2] Dynamic otolith function was determined from the modulation component of horizontal eye movements recorded during off-vertical axis rotations (OVAR) (Haslwanter et al., 2000). Static otolith function was determined by measuring the peak-to-peak amplitude of counter-rolling eye movements during left and right slow-roll tilts (OC) (Miller, 1970). Horizontal semicircular canal function (HVOR) was determined by fitting an exponential function, $A*\exp(-t/T_c)$, to the slow-component velocity of HVOR eye movements for constant velocity rotations about an earth-vertical axis (Honrubia et al., 1982). DC gain of the HVOR relative to acceleration was estimated from the product of the time

constant, T_c, and the gain constant. The gain constant was determined by dividing the response amplitude, A, by the velocity of rotation. Pitch and yaw VOR gain were derived in a similar manner (Peterka et al., 1990).

Apparatus

Subjects were instructed to stand on a variable pitch platform that rotated $\pm 1.2^{O}$ in the anterior-posterior direction, as shown in Figure 1. Subjects stood in a standard parallel stance with their ankles directly above the axis of rotation.[3] In the touch condition, subjects maintained contact with a touch plate with their right index fingertip. The touch plate consisted of a circular aluminum disk that was mounted horizontally on top of a 97.8 cm pedestal. Force sensors mounted between the disk and pedestal determined touch forces in the anterior-posterior, medial-lateral, and vertical directions. The pedestal stood on a supportive metal structure that straddled the platform in order to isolate the touch plate from platform vibrations. The center of the touch plate was adjusted so that it was directly in front of the subject's right shoulder. The distance between the subject and the touch plate was adjusted so that the subject could reach the touch plate with their right index finger in a comfortable manner. Subjects wore a safety harness that was secured to a movable ceiling mount by a connecting strap. The connecting strap was adjusted to allow subjects to lower their body approximately 30 cm before becoming taut. The platform rotation signal was sampled at 120 Hz.

Kinematic data was recorded using a Motion Analysis data acquisition system at a sampling rate of 30 Hz. Markers were located on the right side of the subjects' bodies as shown in Figure 1. Additionally, reference markers were placed on the pedestal and a stationary position on the non-rotating part of the platform.

Measures

Center of mass (CoM) was estimated using a three-segment model (Kane & Levinson, 1985). CoM angular displacement was defined as the angle formed by the CoM, the ankle, and vertical. Fingertip angular displacement was defined as the angle formed by the fingertip, the ankle, and vertical. Positive angles refer to forward movements from upright vertical.

Procedures

The platform rotation stimulus consisted of a sinusoidal waveform at five frequencies: 0.01, 0.03, 0.10, 0.20, and 0.40 Hz. Two sensory conditions were employed: (1) Light (non-supportive) touch. Subjects were instructed to maintain contact of the center of the touch plate with their right index fingertip. An auditory alarm sounded when touch force exceeded 1 Newton; (2) No touch. Subjects were instructed to hold their right index finger in a stationary position in space, slightly above the point they believed to be the center of the touch plate.

Subjects were instructed to stand facing a visual target. Before the light touch trials, subjects were instructed to place their right index finger at the center of the touch bar. Before the no touch trials, subjects were instructed to place their finger directly above the center of the touch bar without making contact. This hand position accomplished two things. First, it mimicked the arm position and any biomechanical effects due to changes in the center of mass during light touch trials. Second, it allowed measurement of the perception of finger position in space relative to the touch bar. After positioning the finger, but prior to the start of each trial, subjects were instructed to close their eyes. Trials were initiated with the movement of the support surface.

All trials were 100 seconds in duration. All subjects completed three, randomized 10-trial blocks, consisting of 5 frequency conditions x 2 sensory conditions. The total experiment lasted approximately 1.5 hours.

Analysis

A linear systems spectral analysis was performed on each trial by calculating the Fourier transforms of the platform and the subjects' body sway. The transfer function at the platform driving frequency was calculated as the Fourier transform of the response divided by the Fourier transform of the input at the driving frequency. Since the platform motion is deterministic, the calculation of the transfer function as the ratio of the response (body sway) to the input (platform motion) is consistent with the definition of the

transfer function in terms of the power spectra. We recovered gain and phase as the absolute value and the argument of the transfer function.

Phase is a measure of the temporal relationship between body sway and stimulus motion. A phase > 0 means that the body sway is leading the platform. Gain is the ratio of the amplitude of the response to the amplitude of the stimulus at the driving frequency. A gain = 1 means the response and drive amplitudes are equal.

To estimate body sway variability, the mean value was first subtracted from the postural sway trajectory in each trial. The component of body sway due to the platform rotation was then removed by subtracting the sinusoid corresponding to the Fourier transform of the trajectory at the platform frequency. This procedure is valid because the response to platform motion is approximately linear. The variability of body sway was defined as the root mean square (standard deviation) of the residual postural sway trajectory.

In addition, for the no touch condition we calculated three measures comparing the finger to the CoM: finger variability divided by CoM variability, finger gain divided by CoM gain, and finger phase minus CoM phase. These measures provide information about whether the finger and CoM movements were rigidly linked. For example, if the body above the ankle was kept rigid, then the variability and gain ratios would be 1 and the phase difference would be 0. These measures were not informative for the light touch condition because the finger variabilities and gains were usually low and the finger phase could not be reliably estimated.

Statistical Analysis

A repeated-measures (2x2x5) MANOVA compared variability, gain, and phase for subject group (BVL subjects, control subjects), sensory condition (no touch, light touch), and frequency (5 frequencies) for CoM and finger displacements. The statistical analysis was based on the average across trials. BVL subjects did not repeat trials in which they lost equilibrium. The reason for this was to minimize fatigue effects realized over the duration of the experiment. Controls never lost their balance during a trial. A primary concern was how subjects maintained the fingertip in space during the no touch condition. Thus, we tested for differences in individual results with a repeated measures Subject x Frequency MANOVA to help explain variation within groups for the no touch condition. Below we report results at the $p < .05$ level of significance.

Results

Figure 2A-D shows CoM time series from exemplar light touch and no touch trials from a BVL and control subject at 0.01 and 0.2 Hz, which illustrate a number of differences. First, in the no touch condition, the sway response of the BVL subject was similar to that of the control subject at 0.01 Hz, but much larger than the control subject at 0.2 Hz. Below we show how the overall amplitude response consists of two components: the response at the driving frequency (gain) and the response at frequencies other than the drive (variability). Both components are larger in BVL subjects than control

subjects, but only at higher platform frequencies. Second, when provided with light touch information, the sway response of BVL subjects is similar to control subjects at all frequencies, essentially eliminating any deficit in their postural response. These effects were also observed in the group results. A Group x Condition x Frequency MANOVA on gain, phase, and variability was found to be significant ($p < .01$). Univariate results are reported individually below.

CoM Displacement

Figure 3 shows the group means for CoM variability, gain, and phase as a function of frequency for each touch condition. BVL subjects showed generally higher CoM variability and gain than control subjects in the no touch condition. With the addition of light touch, CoM variability and gain were equivalent between subject groups.

A statistical analysis supported these effects: Variability showed a distinct frequency effect ($p < .02$) in BVL subjects for the no touch condition, increasing with frequency. Variability remained relatively constant across frequency for the control subjects for both touch conditions. The latter effect was more prevalent in the no touch condition than the light touch condition, an effect that was probably due to the lower overall variability observed for the light touch condition.

CoM gain showed a significant 3-way Group x Condition x Frequency interaction ($p < .02$). This interaction effect supports the observation that the BVL subjects maintained their orientation to the platform for the no touch

condition as the platform frequency increased in the no touch condition, but behaved in a manner similar to the control subjects in the light touch condition.

Phase averaged approximately zero with a slight decrease as a function of frequency ($p < .001$). This was consistent with previous results (Jeka et al., 1996; Maurer et al., 2000).

An increase in phase at 0.4 Hz for the light touch condition led to a significant Condition x Frequency interaction ($p < .005$). The importance of this result is not known since it was not observed in the BVL subjects. Otherwise, differences between groups and conditions were minimal.

Figure 4 shows CoM variability, gain and phase means for individual subjects as a function of frequency and touch condition. The individual results are generally consistent with the group results. BVL subjects showed consistently higher levels of CoM gain than most control subjects with no touch, supported by a significant Subject x Frequency effect for gain ($p < .05$). Lower gain indicates that control subjects were better at compensating for the platform drive than BVL subjects. Two control subjects showed an exception to this result. Post-hoc analysis showed that CoM gain of control subject C5 was higher than all other control subjects ($p < .05$). Subject C3 showed gain levels similar to BVL subjects and had significantly higher gain than control subjects C4 and C6. By contrast, post-hoc analysis of individual subject variability essentially supported the group results: higher variability of BVL

subjects than control subjects. No meaningful differences arose between individual subjects for phase.

The high gain and low variability of subjects C5 and C3 suggest that their center of mass moved more than other control subjects, but only at the driving frequency. These results were the first indication of multiple control strategies for control subjects, while all BVL subjects showed a similar pattern of gain results (see Discussion).

Finger displacement

Figure 5 shows the group means for finger variability, gain, and phase as a function of frequency for each touch condition. Finger variability showed significant Condition x Group ($p < .03$) and Condition x Frequency ($p < .02$) interactions. Similar to the CoM result, finger variability was higher for the BVL subjects for the no touch condition and showed an increasing trend with increasing frequency.

Finger gain showed a significant 3-way Group x Condition x Frequency interaction ($p < .011$). Note that the mean finger gain for the control subjects in the no touch condition decreased to a value approximately equal to that of the light touch condition. This indicates that the control subjects were able to decouple from the platform motion and estimate finger position in space with a level of accuracy approaching that of the light touch condition. Mean finger gain for the BVL subjects was approximately equal to 1 across frequency indicating that they remained coupled to the platform motion.

The finger variability and gain interaction effects arose primarily because finger gain was: 1) higher in the no touch condition when compared to the light touch condition; 2) higher with BVL subjects when compared to control subjects in the no touch condition; and 3) lowest at the slower platform frequencies.

Finger variability and gain were close to zero in the light touch condition in all subjects, as expected from the instructions to maintain the fingertip in a stationary position on the touch plate. The positive levels of finger gain and variability, which were slightly greater than zero, indicate that the finger did slip slightly with the subjects' body sway.

Finger phase, averaged across all frequencies, was approximately zero with a decreasing trend similar to the reported result for CoM phase ($p < .001$) for the no touch condition. Finger phase was not well estimated in the light touch condition because gain was very low.

The individual results in Figure 6 are consistent with the group results. Statistical analysis of individual subjects did not indicate any meaningful differences within subject groups.

Finger/CoM ratio

Finger/CoM ratio results show that certain control subjects were able to uncouple finger from CoM movements, while movements of the finger were always linked to movements of the CoM with BVL subjects. Figure 7 shows the individual results of finger/CoM variability ratio, gain ratio, and phase

difference in the no touch condition. A Subject x Frequency MANOVA was found to be significant ($p < .01$). Subject x Frequency ANOVAs showed significant effects for variability ratio ($p < .05$), gain ratio ($p < .01$), and phase difference ($p < .01$).

Four control subjects (C1, C2, C4 & C6) showed similar finger/CoM gain ratio results to the BVL subjects. The gain ratios of Subjects C3 and C5 were lower than other subjects, indicating reduced movements of the finger relative to the CoM at the platform driving frequency. Subjects C3 and C5 also showed higher CoM gains (see Figure 4) than other control subjects. Together, these results indicate that subjects C3 and C5 were able to minimize fingertip motion even though their CoM moved at relatively large amplitudes. Other subjects, both control and BVL, did not show such uncoupling of the finger from the CoM.

The behavior of subjects C3 and C5 is even more interesting when the finger/CoM variability results are considered. Post-hoc analysis showed that the variability ratios of subjects C3 and C5 were no different than the majority of other subjects ($p's < .05$), indicating that their finger was moving with similar amplitude as other subjects at frequencies other than the drive. Thus, despite similar levels of overall variability, subjects C3 and C5 were able to selectively reduce the amplitude of their finger movement at the driving frequency. No other subjects showed such independent control of the fingertip and the CoM. Phase difference showed no differences between subjects.

Discussion

Driving the postural sway of subjects with a moving platform allowed analysis of sway components, which were linked (gain, phase) and unlinked (variability) to platform movement. Three important results were observed. First, CoM gain and variability of BVL subjects was distinctly higher than control subjects with no touch contact, particularly at the higher platform frequencies. Second, with light touch contact, BVL and control subjects showed equivalent gain, variability and phase. Third, multiple relationships between the finger and the CoM were observed in control subjects, while BVL subjects implemented a single finger/CoM control scheme, indicating a less flexible control system. The implications of each result are discussed below.

Center of Mass Behavior

The CoM of control subjects loosely tracked the platform movement at low frequencies (gain $\approx$ 1, phase < 40 deg), but showed a distinct change at 0.2 and 0.4 Hz, with gain decreasing to well below 1, even without touch contact. In contrast, the BVL subjects showed gains increasing from nearly 1 to 2 as platform rotation frequency increased, indicating twice as much sway of the CoM compared to the platform motion at .4 Hz. Only with the addition of light touch contact were the BVL subjects able to reduce CoM gain to levels equivalent to the control subjects. The touch plate provided an earth-based reference that enabled all subjects to uncouple from the platform driving signal, resulting in minimal body movement at the platform frequency.

At the lowest platform frequency of .01 Hz, calculation of average CoM peak velocity was approximately 0.1 deg/s for healthy control subjects, indicating that control subjects were well above the vestibular threshold of 0.05 deg/s (Fitzpatrick & McCloskey, 1994). Because CoM peak velocity increased with platform frequency, control subjects were clearly above vestibular threshold at all platform frequencies. Consequently, the CoM gain results of BVL and control subjects may be explained partially as a function of the transfer function characteristics of the vestibular system, which is known to have low gain at lower head movement frequencies and increased gain at higher head movement frequencies (Wilson & Melville-Jones, 1979). Low gain at low frequencies suggests that the vestibular system is playing a minimal role in providing information about CoM dynamics. With eyes closed, the implication is that an estimate of CoM dynamics is most likely due to somatosensory information derived from low-frequency platform movement. As the frequency of the platform increases, head/body movements enter the frequency range of high vestibular gain (> .1 Hz), resulting in a more prominent vestibular role in estimating CoM dynamics. The reliable vestibular information at high platform frequencies can then be used to counteract body sway induced by platform movement. With eyes closed and without access to vestibular information, BVL subjects have no alternative and remain coupled to the platform. The relatively small decreases in CoM gain observed for BVL subjects at higher platform frequencies were likely due to the inertial properties of the body, which act to effectively filter higher oscillation

frequencies. This inertial influence partially contributes to decreased CoM gain in control subjects at higher frequencies as well.

However, while the vestibular transfer function explanation may account for CoM behavior at the frequency of platform movement, it cannot account for behavior at frequencies other than the drive. Our measure of CoM variability becomes important here because it showed larger values for BVL subjects at higher platform frequencies. We suggest that an additional reweighting mechanism is responsible for this effect. A common feature of most models that integrate sensory information for postural control (e.g., Johansson et al., 1988; Kiemel et al., in press; Oie et al., in press; Kuo, 1995) is that whenever a sensory source is diminished (e.g., due to pathology or a change in environmental conditions), a corresponding increase in body sway is predicted because the estimate of body dynamics is now less accurate. Thus, flexible balance control requires a continual updating of sensory weights to current conditions so that muscular commands are based on the most precise and reliable sensory information available. An inherent advantage of having at least three sensory sources available (visual, vestibular, and somatosensory) for posture is that as one sensory source is weighted down, the weighting of an alternative source can be increased to maintain a relatively constant sway level. Such a reweighting mechanism has been considered a crucial component of postural control ever since it was first suggested by Nashner and colleagues over twenty years ago (cf., Black et al., 1988; Horak et al., 1989; Nashner, 1976; Nashner, Black & Wall 1982).

Despite its relative importance, evidence in support of sensory reweighting for posture has been indirect at best. Only recently has direct evidence for such sensory reweighting been shown in the form of inverse gain reweighting of vision and touch (Oie et al., in press).

We speculate that in the present study, the ability of control subjects to maintain constant CoM variability across all platform frequencies is due to a sensory reweighting mechanism. As the platform frequency increases, the corresponding increase in the strength of the platform stimulus allows the nervous system to distinguish platform motion from body motion. Consequently, the weight of proprioceptive information derived from the platform is decreased while increasing the weight of vestibular information to keep sway variability relatively constant. Without the available vestibular information, BVL subjects obviously cannot reweight accordingly, resulting in higher CoM variability when compared to control subjects.

Only with the addition of light touch contact were BVL subjects able to reduce CoM gain and variability to levels equivalent to control subjects. The touch plate provided an earth-based reference that enabled all subjects to uncouple from the platform driving signal, resulting in minimal body movement at the platform frequency. The touch reference is substantial enough to compensate for even the lack of vestibular information, consistent with previous results in quiet stance (Lackner et al., 1999). It should be noted that light touch contact produces a torque of about 0.5 N*m around the ankle joint. This value is on the order of spontaneous torque observed about the

ankle during quiet stance. However, this value is well below the values reported with the addition of platform motion (Runge et al., 1999) and is not a significant contribution to overall ankle torque.

Reweighting of sensory information during support surface movements is consistent with previous experimental results (Buchanan & Horak, 1998) and a conceptual model of sensory integration for postural control recently developed by Mergner and his colleagues (Mergner & Rosemeier, 1998). The underlying hypothesis of this model is that somatosensory information channeling up from the body is integrated in the central nervous system with sensory information channeling down from the head senses (i.e., the visual and vestibular systems) to provide an accurate internal model of both the position and movement of the body in space, and also the characteristics of the support surface. According to this model, as long as the support surface is firm and reliable, estimates of body position in space and postural control responses are dominated by somatosensory information from the trunk and lower extremities. If, however, the support surface is unstable, narrow, or compliant, the central nervous system relies more heavily on information from the visual and vestibular systems. In combination with somatosensory information from the neck, such vestibular and visual information can accurately signal trunk movement in space. The “reweighting” mechanism underlying the up-channeling and down-channeling effects presently stands at a conceptual level and has not been specified formally.

Independent Control of the Finger

Subjects were instructed to maintain fingertip position at a virtual point above the touch plate surface. The motivation was to test whether the ability of subjects to uncouple from the moving support surface was due to the additional sensory information provided by contact of the touch plate or whether it was due to the instructed task of maintaining fingertip position at a specific location. It is possible that focusing the control strategy on maintaining the fingertip at a specific location in space could serve to decouple body movement from the support surface. Moreover, it was of interest to observe whether vestibular information influenced this task.

In general, control subjects showed two different strategies for controlling the finger in the no touch condition. Four of the control subjects (C1, C2, C4 & C6) controlled finger position by simultaneously reducing CoM and finger amplitude, which kept the finger in a position above the touch plate.[4] When compared to the BVL subjects, the gains of the CoM and the finger were much lower in these control subjects, indicating better perception and control of the finger to a virtual location in space. Interestingly, these control subjects showed no difference from BVL subjects in terms of finger/CoM variabililty ($\approx$ 1), gain ratio ($\approx$ 1) or phase difference ($\approx$ 0). Movements of the finger and the CoM were also coupled in BVL subjects. Thus, the strategy implemented by these control subjects (C1, C2, C4 & C6) was similar to that of BVL subjects, but with more precise perception of body movement and subsequent attenuation of the finger and the center of mass.

Results from the other control subjects (C3 & C5) indicated a different control strategy. These subjects were distinguished by a low finger/CoM gain ratio (see Figure 7b) indicating smaller changes in finger position despite greater CoM sway amplitude at the platform driving frequency. These subjects also showed higher CoM gains relative to the other control subjects, which were more equivalent to the CoM gains of BVL subjects. Similar levels of finger/CoM variability across all subjects (Figure 7a) emphasize that control of the finger was specific to the platform frequency in these control subjects. These control subjects did not maintain finger position in a perfectly fixed location relative to their body, but minimized finger movement in space by generating arm movements that compensated for body movement relative to the platform. Such precise control of the finger relative to the body suggests that subjects may rely on an internal model of platform movement, which is used to control finger position in a feed-forward manner by predicting and compensating for platform movement (see Figure 7b, finger/CoM gain ratio). Although these control subjects had an excellent representation of platform movement, they did not use it to minimize CoM movement in space, but focused more directly on the task of minimizing finger movement in space.

Conclusion

Results from the present study have two important implications. First, the loss of vestibular information is more than just loss of information about head movement, to which vestibular information is classically referenced. As many

have stressed before, vestibular information is merely one piece of a sensory mosaic whose loss changes the manner in which individuals flexibly adapt to changing environmental conditions (e.g., Lackner, 1992). The lower gain and variability of control subjects, when compared to BVL subjects, were interpreted to be due to: 1) the shift from low to high gain of the vestibular transfer function as platform driving frequency increased; and 2) a reweighting mechanism which emphasized somatosensory information from the feet/ankles at low platform frequencies and vestibular information at higher platform frequencies. Without a vestibular system, BVL subjects were unable to take advantage of these mechanisms, resulting in much larger movements of the body and finger than control subjects, and for fast frequencies of surface motion, outright loss of equilibrium.

The loss of vestibular information also has implications for independent control of body segments. BVL subjects were unable to show any evidence of controlling the finger independently of the center of mass. Their control strategy suggested that all body parts were coupled and driven by movements of the support platform across all frequencies. In contrast, control subjects showed evidence of different control strategies, one of which suggested independent control of the finger from the center of mass. Uncoupling different degrees of freedom (DoF) as a control strategy has been recently formalized by Scholz and colleagues with the concept of an uncontrolled manifold (Scholz et al., 1999; 2000). While the explicit formalization of the uncontrolled manifold is beyond the scope of this paper,

the essential idea is that when the nervous system is confronted with a more difficult task, less relevant DoFs are released from control. The benefit of this release is that mechanical perturbations inherent to those DoFs no longer influence the movement, thus simplifying the control task. Consistent with this idea, the control subjects who showed low finger/CoM ratios (C3 & C5 – Figure 7b) also showed larger CoM gain (Figure 4b) than other control subjects. One may argue that in order to control the finger precisely, the CoM, and thus perturbations of the CoM, was released from control. The increased CoM sway amplitude may be viewed as a cost of this scheme, however, it is important to note that the task was to control the finger in a position in space. Nothing was specified about overall body movement. The other control subjects were able to attenuate both the finger and the CoM sway equally making the release of the CoM unnecessary to perform the task. With the loss of vestibular information, only the control strategy of linking body parts together was possible, suggesting a more limited repertoire of control strategies. Without proper knowledge of body movement, vestibular loss subjects are forced to use a control strategy of coupling all body components together, which may not be optimal for precise and flexible control of upright stance.

Footnotes

1. The results for an additional control subject, C5, were included in the analysis of individual results but not in the group averages used for statistical comparison. C5 was not an age match to any of the BVL subjects.

2. The determination of normal parameters for vestibular function was based on accumulated data from the laboratory of R.J. Peterka of the Neurological Sciences Institute of the Oregon Health Sciences University.

3. Translation of the ankle in the A-P direction occurs as a result of the axis of rotation of the ankle being slightly above the axis of rotation of the platform. The maximum possible effect of ankle translation was calculated to be < 1.7% of total body sway for the light touch condition at .01 Hz platform frequency. The percent contribution of this ankle translation decreased for all other frequencies and sensory conditions. The possible contribution to sway, as a function of increased variability or through postural response, was a small fraction of overall variability, and therefore contributed minimally over the frequency range used in this study (see Buchanan & Horak, 1999).

4. It is unclear whether subjects controlled the CoM and finger independently or whether the CoM was controlled with the finger held fixed relative to the CoM.

Table 1 Characteristics of the Vestibular Deficient Subjects

(Data provided by R.J. Peterka)

Subject	BVL1	BVL2	BVL3	BVL4	BVL5	Normal
Gender	m	f	f	f	m	n/a
Age	70	47	54	53	50	n/a
Duration of Loss (months)	22	60	49	27	24	n/a
Cause of Loss	ototoxic	idiopathic	idiopathic	ototoxic	ototoxic	n/a
HVOR Sensitivity[a] (sec)	0.029	0.0	0.0	0.193	1.37[b]	>6.0
Pitch VOR Gain	0.029	0.08	0.0431	0.07	b	>0.4
Yaw VOR Gain	0.061	0.065	0.04	0.22	0.45	>0.43
OVAR Amplitude (deg/s) (dynamic otolith)	3.75	4.72	1.98	1.69	b	>3.52
Ocular Counter-rolling (deg) (static otolith)	2.65	4.49	1.29	3.29	b	>9 deg

a HVOR sensitivity calculated from 100 deg/s velocity step stimulus. Equal to the area under slow phase eye velocity exponential decay curve.

b HVOR sensitivity for BLV5 was calculated (product of VOR gain constant and time constant, Gc*Tc) from values derived from sum of sines stimulus.

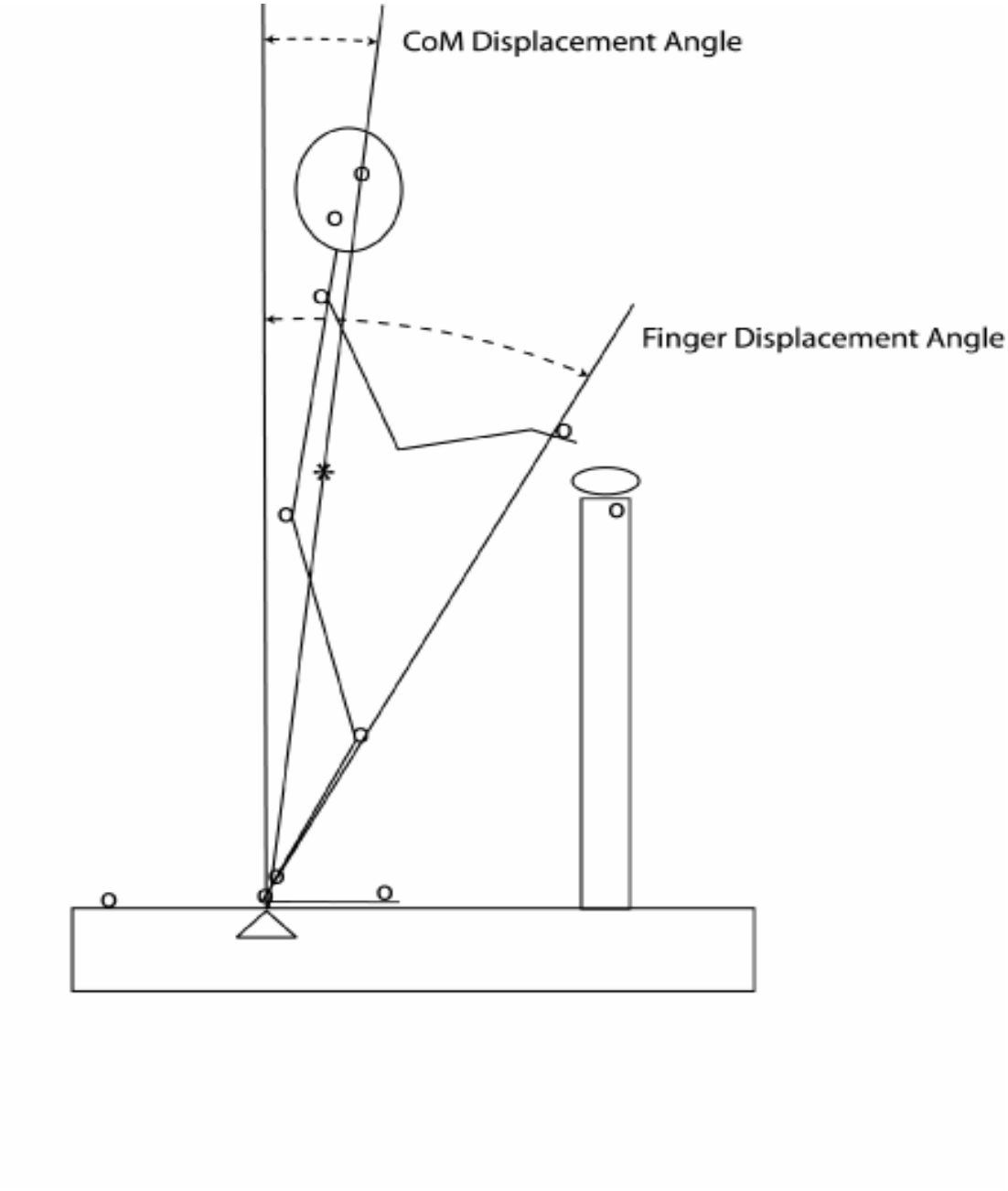

Figure 1 Sagittal view of a subject in a side-by-side stance on the force platform with their right index finger positioned above touch surface. CoM and finger displacements were defined as the angular displacement with vertical. Apex of triangle designates platform axis of rotation. "o" designates placement of kinematic markers. "*" designates calculated CoM position.

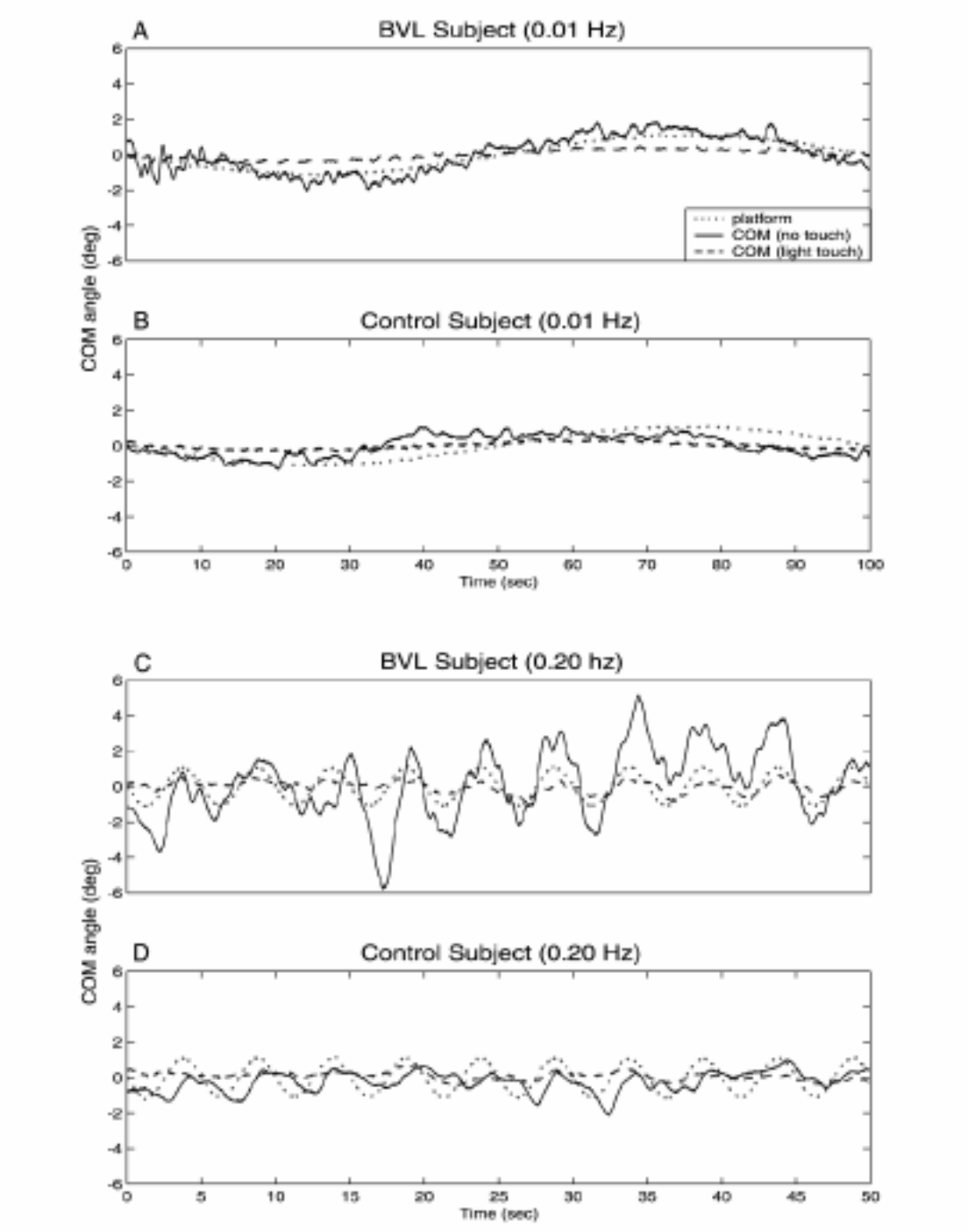

Figure 2 CoM angular displacement vs. time for BVL (A & C) and control (B & D) subjects for the no touch and light touch sensory conditions for platform driving frequencies 0.01 Hz (A & B) and 0.20 Hz (C & D).

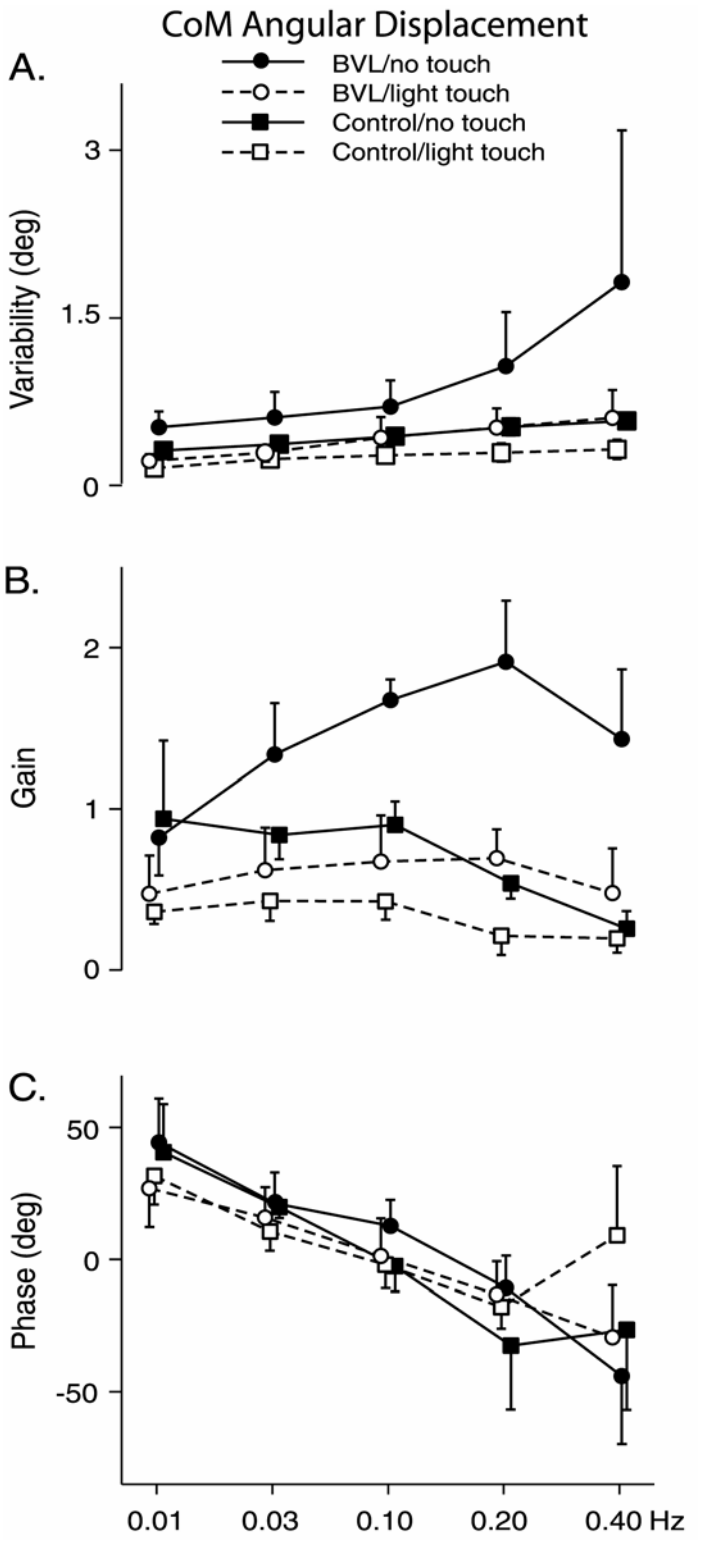

Figure 3 Group averages for variability (A), gain (B), and phase (C) for CoM displacement angle. Error bars = standard error (all plots).

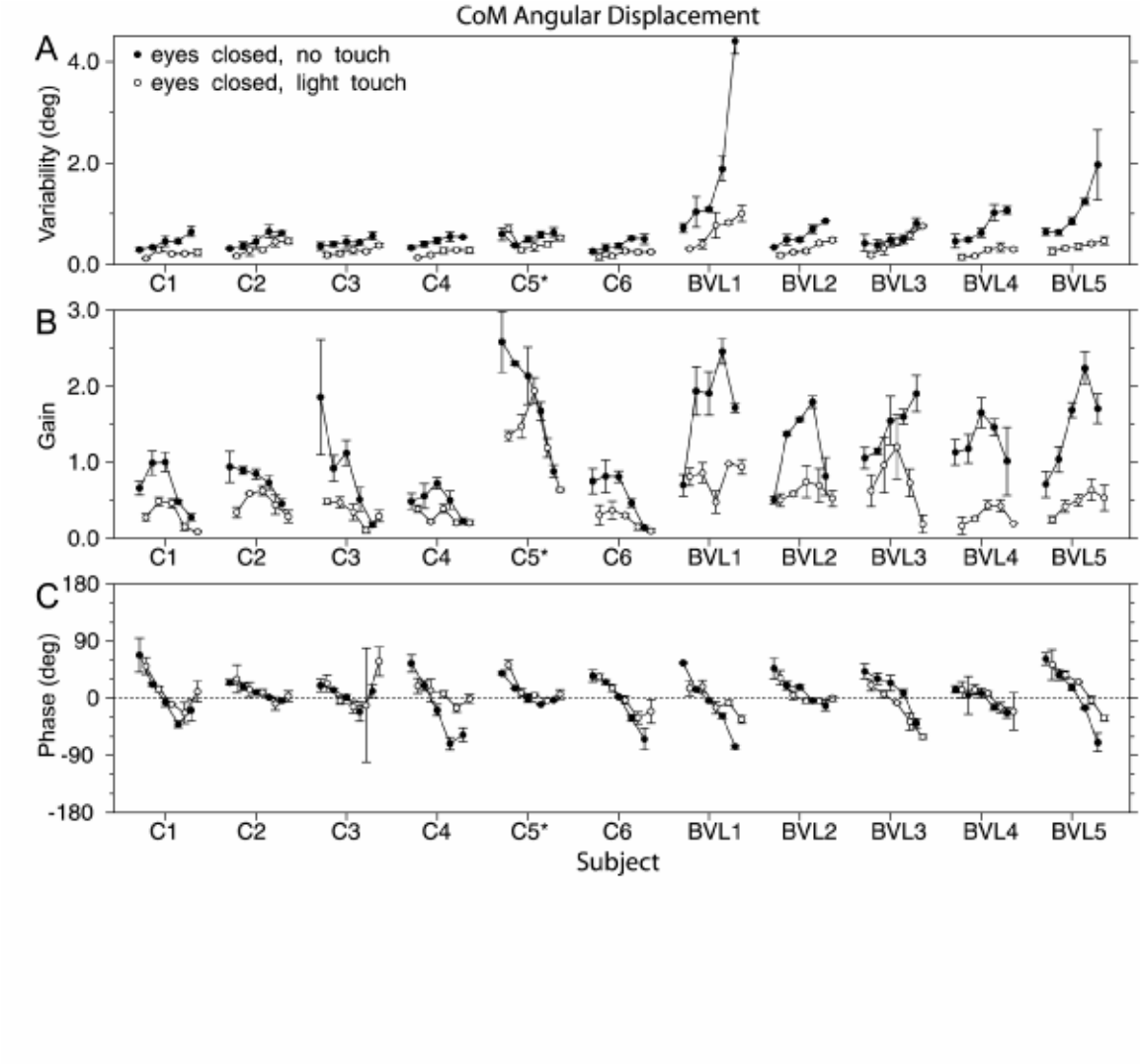

Figure 4 Individual results for variability (A), gain (B), and phase (C) for CoM displacement angle. Increasing frequency conditions are shown from left to right (0.01, 0.03, 0.1, 0.2, and 0.4 Hz). *C5 was included in individual results only (see footnote 1).

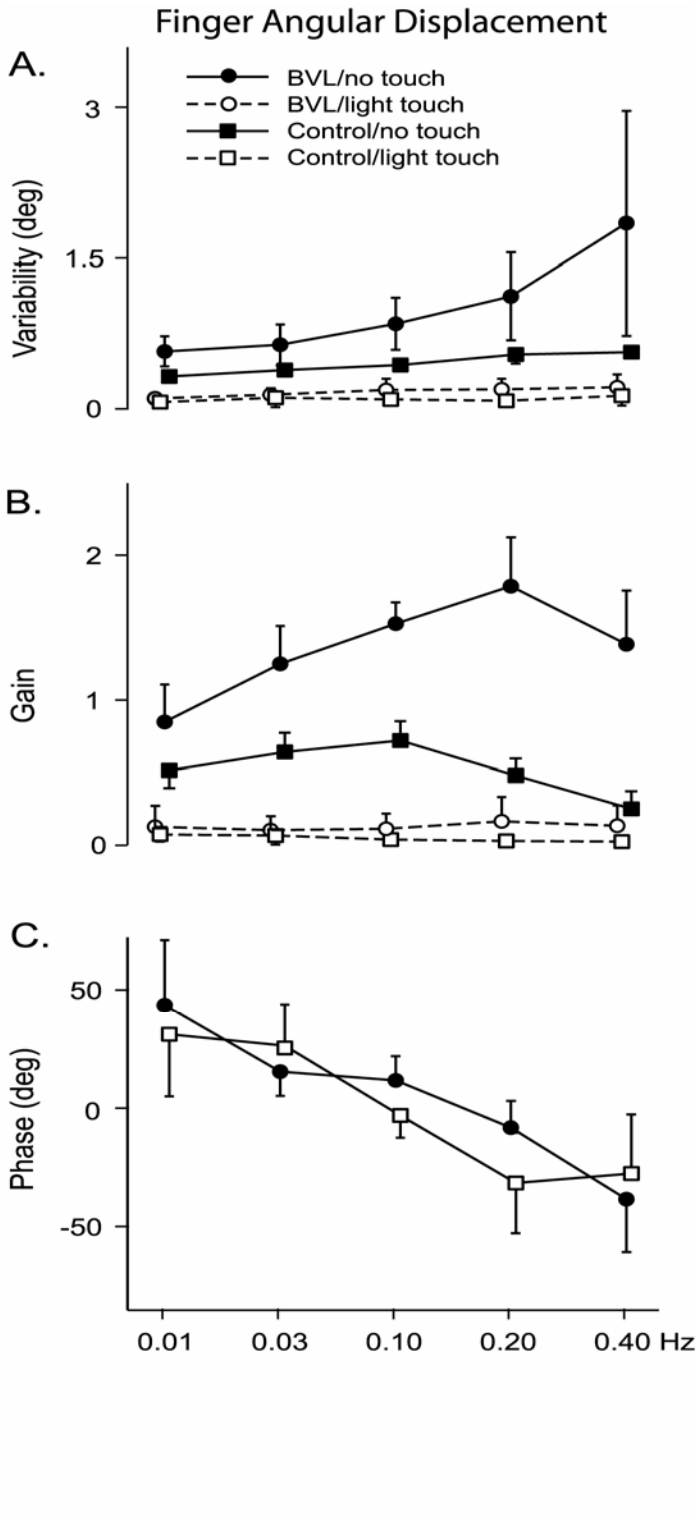

Figure 5 Group averages for variability (A), gain (B), and phase (C) for finger displacement angle.

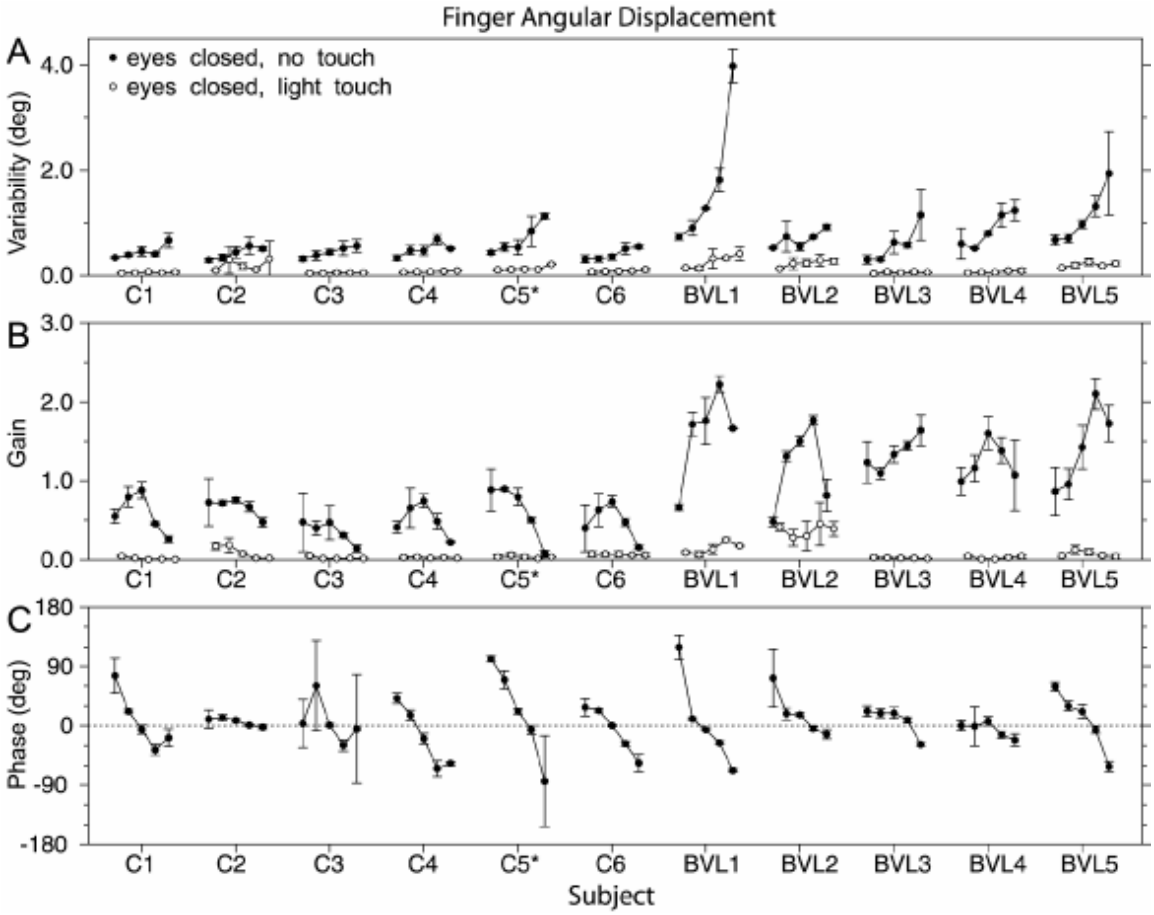

Figure 6 Individual results for variability (A), gain (B), and phase (C) for finger displacement angle. Increasing frequency conditions are shown from left to right (0.01, 0.03, 0.1, 0.2, and 0.4 Hz). * C5 was included in individual results only.

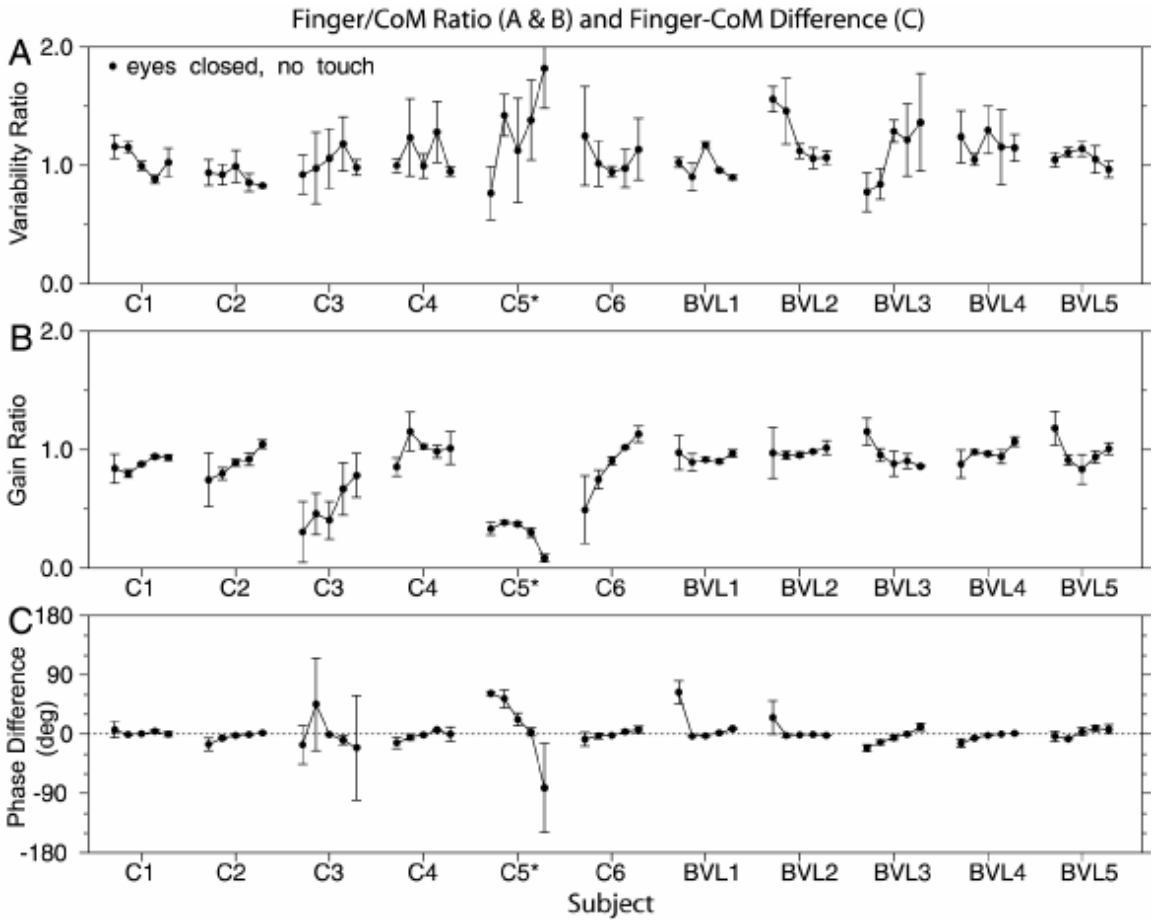

Figure 7 Individual results for variability (A) and gain (B) ratios (finger/CoM), and phase difference(C) (finger-CoM). Increasing frequency conditions are shown from left to right (0.01, 0.03, 0.1, 0.2, and 0.4 Hz). * C5 was included in individual results only.

Chapter 4

Controlling Human Upright Posture: Velocity Information is More Accurate than Position or Acceleration

Jeka J, Kiemel T, Creath R, Horak F, Peterka R

J Neurophysiol. (2004); 92(4): 2368-79

Introduction

A common experimental technique in the postural control literature is to remove or at least attenuate a particular sensory modality and measure how this changes sway behavior. Such changes can then be used to determine how that sensory information is instantiated in the underlying control system. Removing sensory information with a healthy adult population typically leads to an increase in mean sway amplitude (e.g., Woollacott et al., 1986), although certain populations (e.g., children) do not consistently display this result (Ashmead & McCarty, 1991; Chiari et al., 2000; Lacour et al., 1997; Newell et al., 1997). Reduced sensory information means that the nervous system has less information to accurately estimate center of mass dynamics (i.e., position and velocity) and consequently, sway control is less precise. However, an increase in mean sway amplitude due to reduced sensory information is not particularly helpful to understand the underlying control system for posture because most models predict this relationship (e.g., Peterka, 2002; Schöner, 1991; van der Kooij, 1999). Additional

properties/constraints are necessary if modeling is to be used to understand the mechanisms underlying the estimation and control of posture. In this paper, we illustrate a much richer view of how the removal/attenuation of sensory information can lead to changes in postural sway behavior.

Properties of Sensory Information

It is relevant to ask what information is lost when a sensory modality is removed or degraded due to injury or an experimental manipulation. Studies on the psychophysical properties of a particular sensory modality, such as tactile afferents, categorize neurons in terms of rapidly-adapting and slowly-adapting properties, referring to the time taken to return to a baseline activity after stimulation (Kandel et al, 1991). More detailed classification schemes identify the physical aspects of the stimulus to which a neuron responds (Burgess & Perl, 1973; Esteky & Schwark, 1994). For example, slowly adapting neurons are generally considered sensitive to position, responding tonically throughout an entire ramp displacement and displaying sensitivity to the size of the displacement. Many rapidly-adapting neurons respond primarily during a ramp stimulus and increase their firing rate with increasing stimulus velocity regardless of displacement, indicating sensitivity to stimulus velocity. Other rapidly-adapting neurons respond vigorously to rapid/high frequency stimuli and are considered transient detectors, more tuned to the acceleration of a stimulus. These classification schemes do not necessarily

separate afferents into distinct groups, because neurons often respond to more than one physical property.

When investigating the properties of sensory receptors associated with human postural control, it is important to bear in mind that the information conveyed by individual receptors is less relevant than the collective activity transmitted through large populations of receptors distributed throughout the body and then integrated by the central nervous system. Consequently, stimulus properties are often described in terms of the role they play in functional behavior. For instance, the classical view of somatosensation is that it provides information concerning: 1) contact surface forces and properties such as texture and friction; and 2) the relative configuration of body segments (Dietz, 1992; Horak & Macpherson, 1996). Despite their intuitive appeal, such descriptions do not lend themselves easily to quantitative models.

Most models that focus on multisensory integration and postural control assume that the sensory modalities provide information about the dynamics (position, velocity & acceleration) of body sway (e.g., Kiemel et al., 2002; van der Kooij et al., 1999; 2001). The primary methods to investigate stimulus properties relevant for posture stem from linear systems theory. Subjects are typically “driven” by an oscillating pattern of sensory information at different frequencies to determine gain and phase. The shape of the gain and phase curves provide information about coupling properties of postural sway to vestibular (Wilson & Melville Jones, 1979), visual (Berthoz et al.,

1979; Dijkstra et al, 1994a; 1994b; Lee & Lishman, 1975; Peterka & Benolken, 1995; Soechting et al., 1979) and somatosensory stimuli (Jeka et al., 1997; 1998; 2000). Such techniques have shown that the vestibular, visual and somatosensory systems provide position and rate (velocity and acceleration) information in some form. It is of interest to investigate whether any particular physical property dominates collectively. Here we test whether the removal of sensory information is consistent with predictions from a recent model (Kiemel et al., 2002) suggesting that velocity information is the most accurate form of sensory information used to stabilize posture during quiet stance.

Accurate Velocity Information

In Kiemel et al. (2002), we analyzed the stochastic structure of postural sway and demonstrated that this structure imposes important constraints on models of postural control. To briefly summarize our approach, we first analyzed experimental postural sway trajectories using an ARMA technique, to derive descriptive model parameters (i.e., stochastic parameters) that can then be used to create postural sway trajectories that are statistically equivalent to the experimental sway trajectories. We then tested whether these descriptive results could be reproduced by a mechanistic model, such as optimal control models commonly used in the postural control literature (e.g., Kuo, 1995). We found that such models reproduce the stochastic structure of postural sway only when noise is added to the process of fusing

sensory information from multiple modalities, which we refer to as the “noisy-computation” model (Kiemel et al., 2002), whose main features are described in the Appendix.

An important prediction from the noisy-computation model was that the postural control system (during quiet stance) operates in a parameter regime in which sensory input provides more accurate information about the body’s velocity than its position or acceleration. The models considered in Kiemel et al. (2002) did not associate different forms of sensory information (position, velocity, and acceleration) with specific sensory modalities. Instead, the emphasis was that the behavior of a postural control model depends on which form of sensory information is assumed to be most accurate, regardless of the sensory modalities involved.

Of the five stochastic postural sway measures (see Methods below) considered in Kiemel et al. (2002), the noisy-computation model predicts that three measures should depend on the degradation of velocity information. However, when vision and/or light touch information at the fingertip were manipulated in Kiemel et al (2002), only the sway variance showed a statistically significant dependence on sensory condition. We hypothesize that predictions from the noisy computation model were not observed because the support surface was stable in all conditions. With a fixed surface, proprioception through the feet/ankles provides accurate velocity information, and may limit the overall degradation in velocity information when vision or light touch information is removed. Thus, a further test of the noisy-

computation model would be to create experimental conditions that produce a greater degradation in velocity information. If the degradation is sufficiently large, then additional measures beyond sway variance would be predicted to show changes large enough to be detected.

Here we show results from an experiment designed to test the idea that velocity information is most accurate for the control of quiet stance by removing/attenuating **two** primary sensory modalities that provide velocity information about center of mass dynamics, namely vision and proprioception from the feet/ankles. Stochastic measures derived from both experimental sway trajectories and the noisy computation model will be compared. Use of the term "degraded" is motivated by the fact that we cannot assume that all sources of velocity information can be removed entirely through experimental manipulation. Vestibular input also provides velocity information in our experimental setting, although arguably less salient than that provided by proprioception during stance on a fixed surface (see Discussion).

Methods

Subjects

Eight healthy subjects participated in the study, four male and four female between the ages of 22 and 37 with no known musculoskeletal injuries or neurological disorders that might have affected their ability to maintain balance. All subjects were given both oral and written task instructions and gave written consent according to guidelines implemented by the Internal

Review Board at Oregon Health & Science University before undergoing the experimental protocol.

Apparatus

Subjects stood on a variable pitch platform using a shoulder-width parallel stance so that the rotational axis of the ankles coincided with the rotational axis of the platform, as shown in Figure 1. Shoulder and hip displacements were measured using rigid rods attached to a fixed position on one end and attached to the subjects by a harness on the opposite end. The rods could rotate freely about the fixed end in the anterior-posterior plane. The amount of displacement was determined by the change in voltage of potentiometers located on the fixed ends of the shoulder and hip rods. Center of mass angular displacement was estimated from linear displacement of the shoulder and hip using a procedure developed by Peterka (2002). A 120-s calibration trial was performed where subjects slowly leaned forward and backward using different combinations of leg and trunk rotations and minimizing knee flexion. A least-squared error curve fit of the equation

$$x_{cop}(t) = b + a_h x_h(t) + a_s x_s(t) \quad (1)$$

was used to obtain estimates of the coefficients a_h, a_s, and b, where x_{cop} is AP COP displacement, x_h is AP body displacement at hip level, x_s is AP body displacement at shoulder level, and t is time. Because body movements were very slow, x_{cop} is essentially equal to AP COM displacement (except for small rapid oscillations about the local COM position indicative of AP body

acceleration) (Brenière 1996; Winter et al. 1998). In subsequent trials, equation (1) was used to calculate AP COM displacement from measures of $x_h(t)$ and $x_s(t)$. An estimate of the subject's COM height (based on anthropometric measures) above the ankle joint was then used to calculate the COM rotation angle. Thus, CoM sway angle was defined as the angle between the subject's center of mass, the ankle (also the rotational axis of the platform), and vertical.

Subjects wore a safety harness that was secured to fixed brackets by two connecting straps. The straps were adjusted to allow for the subjects' body sway before becoming taut. The platform displacement signal and potentiometer voltages were sampled at 100 Hz.

Procedures

Subjects stood upright with feet shoulder-width apart and eyes closed in three conditions: 1) fixed surface; 2) sway-referenced surface; and 3) foam surface. Three trials of 364 seconds apiece were run in each condition. The platform position was stationary on the fixed surface and foam surface trials. For the sway-referenced trials, the platform rotated in the A-P direction an amount equal to the angular hip displacement as determined by the hip rod potentiometer signal. For the foam surface trials, subjects stood on a 4" thick piece of Sunmate Temper medium density foam placed on the platform. Because of the long trials, the sway-referencing condition was run after the fixed surface condition to minimize any possible effects of fatigue. The foam

surface was run last because it required repositioning the rigid rods to accommodate the increased height of the foam surface. Prior to performing the sway-referenced trials, subjects completed two shorter practice trials to familiarize themselves with the condition in order to minimize any learning effects that might occur as a result of the long trial duration and the unfamiliar nature of the task. Background sound was masked with a tape-recorded text played through ear-covering headphones. One trial was discarded due to technical difficulties and one trial was shortened to 300 seconds due to a loss of balance near the end.

Analysis

ARMA models

For every subject and condition, an autoregressive moving-average (ARMA) model (Wei 1990) was used to characterize the statistical properties of the anterior-posterior center of mass (COM) angular displacement trajectories. Every tenth point of the trajectories was used for analysis, corresponding to a time step *h* of 0.1 s. Increasing the time step in this way reduces the effect of any low-amplitude high-frequency components of the measured sway trajectories, which presumbably are due mainly to measurement noise (see statistical methods below). The three trials were used together to fit parameters in the (*p, q*) ARMA model

$$X_{1,k}^{(j)} = \bar{x}_1^{(j)} + \phi_1(X_{1,k-1}^{(j)} - \bar{x}_1^{(j)}) + \mathcal{L} + \phi_p(X_{1,k-p}^{(j)} - \bar{x}_1^{(j)}) + a_k^{(j)} - \theta_1 a_{k-1}^{(j)} - \mathcal{L} - \theta_q a_{k-q}^{(j)},$$

where $X_{1,k}^{(j)}$ is the *k*th value of the sway time series on the *j*th trial. The subscript '1' indicates position (see Appendix). The $a_k^{(j)}$ are independent normally-distributed random variables with standard deviation σ_a. The integers *p* and *q* are the autoregressive order and moving-average order, respectively, ϕ_1,K,ϕ_p are the autoregressive coefficients and $\theta_1,\mathrm{K},\theta_q$ are the moving average coefficients. The parameters $\bar{x}_1^{(j)}$ are the asymptotic means for each trial. Sampling one variable from a *p*th-dimensional linear (in the narrow sense) stochastic differential equation (Arnold 1974) at fixed time intervals produces a (*p*, *p* – 1) ARMA process. Therefore, we let *q* = *p* – 1.

Parameters were fitted for models of order *p* = 1,…,5 using the method of maximum likelihood. No assumption was made that the process was initially in its equilibrium state. Thus, our fitting procedure allowed for the possible existence of transients. In particular, a slow trend in the data could be interpreted by the fitting procedure as a slowly-decaying transient rather than stochastic variation. See Kiemel et al. (2002) for additional details.

The 5th-order model was compared to the models of orders *p* = 1,…,4 using a likelihood-ratio test at significance level 0.05. In all but one case (the 3 trials combined from subject 4 in the foam condition), the 5th-order model was significantly better than all lower-order models. In these cases, the 5th-order model was selected. In the remaining case, the 5th-order model was better than the 3rd-order model, but not the 4th-order model. In this case, the 4th-order model was selected.

For the selected model, we computed the coefficients $\kappa_1, \mathcal{K}, \kappa_p$ and eigenvalues $\lambda_1, \mathcal{K}, \lambda_p$ of its autocovariance function

$$E[(X_1^{(j)}(t) - \bar{x}_1^{(j)})(X_1^{(j)}(t+\tau) - \bar{x}_1^{(j)})] = \kappa_1 e^{\lambda_1|\tau|} + \mathcal{L} + \kappa_p e^{\lambda_p|\tau|}, \quad (2)$$

where $X_{1,k}^{(j)} = X_1^{(j)}(hk)$ and $\square$ is a multiple of *h*. The terms on the right-hand side of (2) were arranged so that $\left|\kappa_1 e^{\lambda_1 h}\right| \geq \mathcal{L} \geq \left|\kappa_p e^{\lambda_p h}\right|$. We then denoted the first real-valued eigenvalue by λ_{r} and the first pair of complex-conjugate eigenvalues by λ_{c} and $\bar{\lambda}_{\mathrm{c}}$. The corresponding coefficients were denoted by κ_{r}, κ_{c} and $\bar{\kappa}_{\mathrm{c}}$, respectively. Typically, $\kappa_{\mathrm{r}} e^{\lambda_r|\tau|}$, $\kappa_{\mathrm{c}} e^{\lambda_c|\tau|}$ and $\bar{\kappa}_{\mathrm{c}} e^{\bar{\lambda}_c|\tau|}$ were the first three terms on the right-hand side of (2), although not necessarily in that order, and the remaining terms were small. The term $\kappa_{\mathrm{r}} e^{\lambda_r|\tau|}$ represents a first-order decay component of the autocovariance function and $\kappa_{\mathrm{c}} e^{\lambda_c|\tau|} + \bar{\kappa}_{\mathrm{c}} e^{\bar{\lambda}_c|\tau|}$ represents a damped-oscillatory component. Thus, the autocovariance function can be decomposed into a first-order decay component, a damped-oscillatory component, and a remaining component that is typically small. With this decomposition in mind, we define the following six measures that (at least partially) characterize the *stochastic structure* of postural sway:

- The slow-decay rate $\beta = -\lambda_{\mathrm{r}}$, which describes how quickly the first-order decay component of the autocovariance function decays with time delay τ. Note that based on its definition, the slow-decay rate β is not necessarily slow. The term “slow-decay rate” is based on the experimental results from Kiemel et al. (2002). The slow-decay

process can be thought of as a deviation from the baseline level of sway that exponentially relaxes back to a mean position.

- The damping, $\alpha = -(\lambda_c + \overline{\lambda}_c)$, which describes how quickly the damped-oscillatory component of the autocovariance function decays with time delay τ. The rate constant of the decay is $\alpha/2$.
- The eigenfrequency $\omega_0 = \sqrt{\lambda_c \overline{\lambda}_c}$, which is the approximate angular frequency of the damped-oscillatory component if α is small.
- The standard deviation $\sigma_{COM} = \sqrt{\kappa_{tot}}$ of the model's sway trajectories, where $\kappa_{tot} = \kappa_1 + \Lambda + \kappa_p$ is the variance. Typically, $\sigma_{COM} \approx \sqrt{\kappa_r + \kappa_c + \overline{\kappa}_c}$. In most cases, σ^2_{COM} is also approximately equal to the average variance of the three sway trajectories used to fit the ARMA model. However, slow trends in the data that are not modeled as stochastic variation do not contribute to σ_{COM} (see discussion of slow trends above).
- The slow-decay fraction κ_r / κ_{tot}, which describes the relative size of the slow-decay component of the autocovariance function.
- The damped-oscillatory fraction $2|\kappa_c| / \kappa_{tot}$, which describes the relative size of the damped-oscillatory component of the autocovariance function.

These measures are different than those reported in Kiemel et al. (2002) in two respects; the previous study used sway variance instead of sway standard deviation and did not report values of the damped-oscillatory

fraction. Because the absolute value of κ_c is used in the definition of the damped-oscillatory fraction, the sum of the slow-decay and damped-oscillatory fractions can be greater than 1. Therefore, these measures cannot be simply interpreted as a partition of the sway variance. However, roughly speaking, if the slow-decay fraction is near 1 and the damped-oscillatory fraction is near 0, then the slow-decay component of postural sway accounts for most of the sway variance.

The ARMA fitting procedure described above is the same as that used in Kiemel et al. (2002) except in two respects. In the previous study we used (p, p) ARMA models. Here we use (p, p –1) ARMA models, because their autocovariance function (2) has a simpler form. Also, in the previous study we tested models up to order 8, rather than up to order 5. Although higher-order models often provide statistically-significant improvements in the quality of the fit, the measures computed from such models are, in some cases, less consistent across subjects.

COM variability

In addition to the sway standard deviation σ_{COM} based on ARMA model parameters, three measures of variability were computed directly from filtered COM angular displacement trajectories: the standard deviation of position, the standard deviation of velocity, and the mean speed. A forward-reverse cascade of a 2nd-order Butterworth filter was applied to each trajectory using the Matlab function filtfilt, resulting in a 4th-order zero-phase filter with a cutoff

frequency of 3 Hz (Winter, 1990). (We chose the cutoff frequency based on the shape of the power spectral densities; see statistical methods below.) Finite differences where used to compute velocity and speed (the absolute value of velocity).

COM Power Spectral Density.

The average power spectral density (PSD) of the COM angular displacement was calculated from three trials in each condition for each subject (one subject had only two foam trials) using the Matlab spectrum function which implements Welch's averaged periodogram method (Marple, 1987). PSD calculations used a 100-second Hanning window with a one-half window overlap. Means were subtracted from each trial before computing the PSD. Spectral density was plotted on a log-log scale to make it easier to observe the distribution of power at higher frequencies, which is typically small and difficult to resolve visually on a linear scale.

Statistics

Each of our six measures based on ARMA parameters were analyzed separately at significance level 0.05. We first used the Hotelling T^2 statistic to test for significant differences among the three surface conditions. If a significant difference was found, paired *t*-tests were used to make pairwise comparisons among the conditions. Because there are only three conditions,

this procedure controls the familywise type I error rate (Hochberg and Tamhane, 1987).

For each condition, the log of the PSD was averaged across subjects and paired t-tests were used to detect differences between conditions. Tests were performed at 300 equally-spaced frequencies from 0.01 to 3 Hz. (Above 3 Hz the PSDs begin to level off, presumably because of measurement noise.) For each of the three types of condition effects (fixed vs. foam, fixed vs. sway-referenced, and foam vs. sway-reference) we used the procedure of Benjamini and Hochberg (1995) to control the false discovery rate (FDR) at significance level 0.05. The FDR is the expected value of the ratio n_{false}/n_{tot}, where n_{false} is the number of null hypotheses falsely rejected and n_{tot} is the total number of null hypotheses rejected. When $n_{tot} = 0$, the ratio is defined to be 0. Controlling the FDR is more liberal than the traditional approach of controlling the familywise type I error rate but is more conservative than controlling the per-comparison error rate. The Benjamini and Hochberg procedure controls the FDR in the case of independent test statistics. In our case of dependent test statistics, the control of the FDR is only approximate.

For each of the three sway variability measures (position SD, velocity SD & mean speed), each individual subject was tested for condition effects with a one-way ANOVA. Analyses were based on the log of each measure to reduce differences in inter-trial variance across conditions. (Because coefficients of variation were small, the log transformation had only a small effect on the skewness of the distributions.) A Bonferroni test was applied to

the eight resulting *p*-values to select those subjects that showed a significant condition effect. For those subjects, unpaired *t*-tests were used to test for pairwise differences between conditions. Because there were only three conditions, this procedure controls the familywise type I error rate for each subject.

Results

Figure 2 shows an example of the COM sway angle time series for each Surface condition from one representative subject. As many other studies have found, center of mass amplitude increases when standing on a foam (e.g. Rogers et al., 2001; Hytonen et al., 1993) or sway-referenced surface (e.g. Horak et al;., 2002; Kuo et al., 1998; Nashner et al., 1982; Peterka and Benolken, 1995) when compared to the fixed surface condition. Measures from the noisy-computation model below illustrate more detailed differences in the structure of postural sway trajectories between conditions.

Model Predictions

Figure 3 illustrates the predictions of the noisy-computation model as position, velocity or acceleration sensory information is degraded. The assumptions underlying these predictions are described in the Appendix. Moving right along the horizontal axis in Figure 3 represents increasing

degradation of position, velocity or acceleration information. The model predicts that as velocity information is degraded (i.e., σ_2 is increased):

- The slow decay rate (β) will increase (Fig 3a).
- The damping (α) and eigenfrequency (ω_0) are not dependent upon velocity information and will remain constant (Fig. 3b & 3c).
- The standard deviation of COM position (σ_{COM}) will increase (Fig 3d).
- The damped-oscillatory fraction ($2|\kappa_c|/\kappa_{tot}$) will increase (see Fig 3f & Appendix).

There is no prediction concerning the slow-decay fraction (κ_r/κ_{tot}), it can either increase or decrease as velocity information is degraded, depending on the values of the other model parameters. With our choice of model parameters, the slow-decay fraction remains roughly constant (Fig. 3e). Note that the predictions for degrading position and acceleration information are markedly different than those for degrading velocity information. For example, the slow-decay rate and the damped-oscillatory fraction are predicted to decrease as position and acceleration information degrade, contrary to the increase predicted with degraded velocity information.

Model Measures

Figure 4a-f shows the average results across subjects for each of our six measures. On the left side of Figure 4 are three measures based on the eigenvalues of the descriptive model: the slow-decay rate (β), the damping (□), and the eigenfrequency (□$_0$). On the right side of Figure 4 are three

measures based on the coefficients of the model's autocovariance function (2): the sway standard deviation (σ_{COM}), the slow-decay fraction (κ_r/κ_{tot}), and the damped-oscillatory fraction ($2|\kappa_c|/\kappa_{tot}$).

Of the six measures, the slow-decay rate, the sway standard deviation and the damped-oscillatory fraction showed significant differences across the three surface conditions (*p*s < .05). Pairwise tests revealed that the slow-decay rate and the damped-oscillatory fraction were larger on the foam surface (*p*s < 0.01) and sway-referenced surface (*p*s < 0.05) than on the fixed surface. Sway standard deviation was significantly greater in the sway-referenced condition than in the fixed and foam conditions (*p*s < 0.05). Damping and eigenfrequency showed no significant change across surface condition. All of these results are consistent with model predictions in the case of degraded velocity information. The mean slow-decay fraction also showed no significant change across surface condition. This measure was much more variable across subjects in the foam and sway-referenced conditions than in the fixed condition (compare error bars in Fig. 4e).

COM Variability & Power Spectral Density

Figure 5a shows the standard deviation of COM displacement for each of the 8 subjects. Only 5 of the 8 subjects (1–4 and 7) showed a significant dependence of COM displacement on Surface condition (Bonferroni-adjusted *p*s < 0.05, see methods). In addition, subject 2 did not exhibit a significant difference between the foam and sway-referenced conditions, and subject 7

exhibited a significantly lower standard deviation of position in the foam condition than in the fixed and sway-referenced conditions. Thus, only 3 of the 8 subjects showed a significant condition ordering of the form fixed < foam < sway-referenced (*p*s < 0.05).

The lack of consistency across subjects in COM standard deviation is reflected in the distribution of COM spectral power at low frequencies. Figure 5b-c shows log-log plots from two different subjects representing the averaged spectral density of the COM angular displacement from three trials in each condition. At low frequencies, there is no consistent ordering of spectral density across condition in the two subjects. However, in a middle range of frequencies, spectral density is consistently highest in the sway-referenced condition and lowest in the fixed condition for both subjects. This condition hierarchy for spectral density was observed for all subjects in a middle frequency band from 0.37–1.79 Hz. Recall that the variance of COM position is the integral of the COM power spectral density (PSD). Since most of the power of COM position is at the low frequencies, it is the PSD at low frequencies that largely determines the variance, and hence the standard deviation, of COM position.

Figure 6a shows the geometric mean PSDs across subject for each condition. There were no significant differences among conditions at the lowest frequency of 0.01 Hz. At higher frequencies, the mean PSDs were significantly different with a condition ordering of Fixed < Foam < Sway-Referenced (false discovery rate < 0.05: Fixed < Foam for 0.03–2.95 and

2.98–3.00 Hz; Fixed < Sway-Referenced for 0.02–3.00 Hz; Foam < Sway-Referenced for 0.10–3.00 Hz).

Figures 6b-d illustrate PSDs predicted from the noisy computation model based upon changing levels of position, velocity and acceleration noise. The three values of the sensory-noise level correspond to the three experimental conditions. The pattern of spectral power differences across condition based upon changing velocity noise are most similar the experimental PSDs in Figure 6a in that the differences of the three PSDs are smallest at low frequencies and largest in the mid-frequency range. PSDs based upon position or acceleration noise levels are largest at low frequencies and smallest in the mid-frequency range, contrary to the pattern observed in the experimental mean PSDs.

COM Velocity

Because the PSD of COM velocity is $(2\pi f)^2$ times the PSD of COM position, where f is frequency, the variance of velocity (the integral of the velocity PSD) depends very little on the position PSD at low frequencies and is largely determined by the position PSD at higher frequencies. Since the subjects showed consistent condition effects in the position PSD at higher frequencies, this suggests that the standard deviation of velocity will also show consistent condition effects. Figure 7a shows that this was the case. All subjects showed a significant dependence of velocity standard deviation on

condition (Bonferroni-adjusted *p*s < 0.01) and a significant condition ordering of the form Fixed < Foam < Sway-Referenced (*p*s < 0.01).

Another measure that has been used to quantify sway variability is mean path length per unit time (Hufschmidt et al., 1980). This measure is often used to describe sway in two dimensions (anterior-posterior and medial-lateral) but can also be used in one dimension (in our case, anterior-posterior). Mean path length per unit time is equal to mean speed. Since speed is the absolute value of velocity, one would expect that mean speed and the standard deviation of velocity would show similar condition effects. This was true (Figure 7b); the statistical results for the standard deviation of velocity also held for mean speed.

Discussion

Here we tested the prediction of the noisy computation model (Kiemel et al., 2002) that the stochastic properties of sway will change if the major sources of sensory information related to velocity are degraded, namely, by removing/attenuating vision and proprioception. Our results showed that three of the six model measures, the slow-decay rate, the damped-oscillatory fraction, and the sway standard deviation showed a significant increase from the fixed surface to the foam and/or sway-referenced conditions, as predicted. Two other parameters, the damping and eigenfrequency, showed no significant change as a function of surface condition, also as predicted. The results were not consistent with predictions based upon degrading position or

acceleration information, suggesting that our experimental manipulation was successful in primarily degrading velocity information.

Regimes of Accurate Sensory Information

The motivation of this study was based on the suggestion of Kiemel et al. (2002) that the postural control system (during quiet stance) operates in a parameter regime in which sensory input provides more accurate information about the body's velocity than its position or acceleration. This suggestion was based on comparing the behavior of the noisy-computation model to experimental data. Figures 3 and 4 illustrate this comparison. ARMA modeling of sway trajectories yielded measures for the fixed condition that were compatible with those under conditions of accurate velocity information. For example, the slow-decay rate was found to be small, indicating a long time constant. Likewise, the damped-oscillatory fraction was found to be small, suggesting that the damped-oscillatory component of sway accounts for only a small proportion of the total sway variance. These two results are more compatible with the assumption of accurate velocity information than accurate position or acceleration information.

In Kiemel et al. (2002), only total amount of sway showed a statistically significant dependence on the experimental conditions tested. The current experiment was designed to produce a greater degradation of velocity information so that predicted changes in additional postural sway measures would be observed. In particular, the noisy-computation model predicts that

the slow-decay rate will become faster and the damped-oscillatory fraction will increase if velocity information is sufficiently degraded (Figure 3a,f), which is what we observed experimentally (Figure 4a,f). In contrast, degrading position or acceleration information is predicted to produce the opposite behavior in both measures.

Damping and eigenfrequency for the noisy-computation model show no change as a function of degrading any form of sensory information. The reason is that the damping (α) and eigenfrequency (ω_0) depend only on the control-function coefficients c_1 and c_2 and the inverted-pendulum parameter □ and not on any of the sensory-noise levels (see Appendix). Since our experimental manipulations were aimed at varying sensory information, the prediction would then be that damping (α) and eigenfrequency (ω_0) should be constant across our experimental conditions. Our experimental results, which did not show a significance dependence of α and ω_0 on experimental condition, are consistent with this prediction.

Many studies have found an increase in mean sway amplitude when sensory information was removed (for reviews, see Dietz, 1992; Horak & Macpherson, 1996; Nashner, 1981). However, mean sway amplitude is not a very useful measure to distinguish different mechanisms underlying postural control because most models predict such an increase. Figure 3d illustrates this idea; any form of sensory loss is predicted to increase sway standard deviation. Our results supported the prediction that sway SD would increase as velocity information was degraded, although this result was inconsistent

across subjects. In contrast, the standard deviation of COM velocity displayed systematic condition effects for all subjects; lowest on a fixed surface and highest on a sway-referenced surface (see Fig. 7b,c). Consistent with the COM velocity SD results, power spectral densities showed a systematic ordering across condition in the middle frequency range. Such results indicate that foam and sway-referenced support surfaces do not necessarily increase the amount of sway, but influence the dynamics of sway by increasing sway velocity.

Accurate Velocity Information

The basis for the accuracy of velocity information may be due to the underlying physiology of sensory receptors related to postural control, which generally favor rate information rather than absolute position information. The proprioceptive, tactile and visual systems are all thought to be velocity sensitive (Esteky and Schwark, 1994; Matthews, 1972; Dijkstra et al., 1994a; Jeka et al., 1997; 1998). Position information is clearly available from proprioceptive and otolith information, but may not play as prominent a role as velocity in the small corrections required during quiet stance (Masani et al., 2003).

Considering that subjects relied primarily on vestibular information during the sway-referencing condition and to a lesser extent, the foam condition, in the present study, it is useful to consider what information is provided about body sway by the vestibular system. Semicircular canals are

effectively integrating angular accelerometers due to their biophysics, and therefore convey angular velocity information to the CNS over a broad range of frequencies (Fernandez & Goldberg, 1971; Goldberg & Fernandez, 1971a; 1971b; Miles & Braitman, 1980). At very low frequencies, the canal response conveys angular acceleration although this signal is thought to be noisy. One source of the noise is the wide range of head movements over which the canals are designed to operate essentially linearly (up to several hundred deg/s) in order to accurately encode head motion for the generation of compensatory eye movements (VOR). Body sway velocities in our results were approximately 1 deg/s or lower on all surfaces (see Figure 7). This is on the order of one percent of the dynamic range of the canals. Therefore, it would be reasonable to expect that the signal-to-noise ratio of the canal signal would be fairly low during operation in the restricted range of motions associated with spontaneous body sway, although compensation for this deficit may be achieved by combining otolith and canal information (Schmid-Priscoveanu et al., 2000).

A second source of noise is due to their anatomical location in the head; the canals sense head velocity and not COM velocity. Therefore, some transformation of this canal information would be necessary to obtain COM velocity. The simplest transformation would be to combine the vestibular head-in-space information with proprioceptive head-on-body information in order to estimate trunk-in-space information. A more complicated transformation would be the down-channeling and up-channeling mechanism

proposed by Mergner and Rosemeier (1998) that would include additional proprioceptive-based transformations. Assuming the simplest model, these transformations would be additive, and therefore the noise properties of the various sensory processes would also be additive. Therefore, the noisy vestibular information would become more noisy in the process of estimating COM velocity in space.

In summary, stance on foam or sway-referencing requires an increased reliance on vestibular-derived motion information (increased weighting of the vestibular channel, see Peterka & Loughlin, 2004). This increased weighting of vestibular information reveals the relatively high noise level of the vestibular signal at the low frequencies of stimulation during quiet stance and sway-referencing. In contrast, subjects rely primarily on proprioceptive cues during stance on a fixed surface (Peterka, 2002), whose noise level is low relative to vestibular cues (Mergner et al., 1993; van der Kooij et al., 2001). The observed differences between stance on foam versus a sway-referenced surface (e.g., see Figure 6) can be attributed to a higher vestibular weighting during sway-referencing than during stance on foam. There is ankle joint motion during stance on foam and thus some useful proprioceptive information can contribute to postural reactions. Sway-referencing is never quite ideal but comes very close to stabilizing ankle joint motion, providing less useful proprioceptive information than a foam surface.

Limitations of the Noisy-Computation Model

Our modeling approach has been to obtain multiple measures of postural sway across different experimental conditions and then identify a simple mechanistic model whose behavior is *qualitatively* consistent with these measures. This approach led us to the noisy-computation model (Kiemel et al. 2002). Even though the present results are consistent with the predictions of this model, there are potential deficiencies in our modeling approach worth addressing. For example, our simple model lacks features found in more complicated models of the postural control system such as sensory time delays, sensory dynamics, and multiple body segments (see, for example, Kuo 1995; van der Kooij et al. 1999, 2001; Peterka 2000, 2002). We have chosen to forgo these features, because they are not required to obtain qualitative agreement with the data we have considered. However, it will be important to compare our model to more detailed models to investigate whether they can be thought of as refinements of our simple model, or whether they offer fundamentally different interpretations of experimental data.

Another possible deficiency of our modeling approach concerns how we have interpreted our model's parameters. One important parameter is the inverted pendulum parameter, □, which determines the amount of torque that needs to be counteracted from acceleration due to gravity. The question is the extent to which this torque is produced by passive (e.g., tendon) or active (e.g., neurally-mediated muscle activity) components of the ankle-foot

muscle/joint complex. Presently, our model assumes that the counteracting force is mediated only by active changes in muscle force due to changes in sensory noise levels. However, this assumption would be erroneous if passive ankle forces play a significant role. Winter et al (1998) proposed that passive ankle muscle stiffness alone was capable of maintaining upright stance. However, a number of studies have argued against purely passive control (Loram & Lakie, 2002; Morasso & Schieppati. 1999; Morasso & Sanguineti, 2002; Peterka, 2002). For example, Loram and Lakie (2002) used small mechanical perturbations to the foot to measure intrinsic ankle stiffness (stiffness not due to neurally-mediated feedback) during quiet stance. They found that intrinsic ankle stiffness was, on average, 91% of that necessary to minimally counteract the torque produced by gravity. Peterka (2002) developed a PID control model for human postural control which argued for much lower levels of the passive ankle component (10% passive vs 90% active). While the actual contribution of passive ankle stiffness remains controversial, the important point is that attributing the inverted pendulum parameter (to purely active control is most likely an overestimate and may affect the qualitative behavior of the model. Moreover, intrinsic ankle stiffness may play less of a role during sway referencing than during quiet stance. If so, the effective might be different for the different experimental conditions in the current study. This would be counter to our assumption that differences between experimental conditions are primarily sensory in nature and can be modeled by changing only sensory-noise levels.

Conclusions

These results support previous findings (Kiemel et al., 2002) suggesting that velocity information is the most accurate form of sensory information used to stabilize posture during quiet stance. We are not suggesting that position and acceleration information are unimportant for postural control, but rather that healthy postural behavior reflects the availability of accurate velocity information. Reflecting the inherent redundancy of sensory information for postural control, velocity information is derived from more than one sensory modality. As long as velocity information is available, the noisy computation model predicts that the qualitative stochastic structure of sway should not change. If one source of velocity information is lost while another remains available, sway variability may increase because the nervous system cannot estimate center of mass velocity as precisely, but the fundamental characteristics of sway remain unchanged. Only severe degradation of velocity information is predicted to change the basic structure of sway.

APPENDIX

Here we briefly summarize the noisy computation model of Kiemel et al. (2002). The model has four variables: the position x_1, the velocity x_2, the estimated position $\hat{x}_1$, and the estimated velocity $\hat{x}_2$. In this paper, position x_1 is the anterior-posterior angle of the center of mass. The time derivatives of the variables are given by

$$\dot{x}_1 = x_2, \tag{3a}$$

$$\dot{x}_2 = \gamma x_1 - c_1\hat{x}_1 - c_2\hat{x}_2 + \sigma\xi(t), \tag{3b}$$

$$\dot{\hat{x}}_1 = \hat{x}_2 + K_{11}(z_1 - \hat{x}_1) + K_{12}(z_2 - \hat{x}_2) + K_{13}(z_3 - \gamma\hat{x}_1) + \sigma_{c1}\xi_{c1}(t), \tag{3c}$$

$$\dot{\hat{x}}_2 = \gamma\hat{x}_1 - c_1\hat{x}_1 - c_2\hat{x}_2 + K_{21}(z_1 - \hat{x}_1) + K_{22}(z_2 - \hat{x}_2) + K_{23}(z_3 - \gamma\hat{x}_1) + \sigma_{c2}\xi_{c2}(t), \tag{3d}$$

where

$$z_1 = x_1 + \sigma_1\xi_1(t), \tag{3e}$$

$$z_2 = \dot{x}_1 + \sigma_2\xi_2(t), \tag{3f}$$

$$z_3 = \ddot{x}_1 + \sigma_3\xi_3(t) + c_1\hat{x}_1 + c_2\hat{x}_2, \tag{3g}$$

$\xi(t)$, $\xi_1(t)$, $\xi_2(t)$, $\xi_3(t)$, $\xi_{c1}(t)$ and $\xi_{c2}(t)$ are independent white-noise processes, and the K_{jk} are chosen to minimize the estimation performance index

$$J = E[d_1(x_1 - \hat{x}_1)^2 + d_2(x_2 - \hat{x}_2)^2], \tag{3h}$$

where d_1 and d_2 are positive.

Equations (3a) and (3b) describe the dynamics of an inverted pendulum. The right-hand-side of (3b) consists of γx_1, the acceleration

produced by gravity, and $-c_1\hat{x}_1 - c_2\hat{x}_2 + \sigma\xi(t)$, the acceleration produced by muscle activity, where $u(\hat{x}_1, \hat{x}_2) = -c_1\hat{x}_1 - c_2\hat{x}_2$ is the control function and $\sigma\xi(t)$ is process noise.

Equations (3c) and (3d) describe the dynamics of estimating position and velocity based on noisy sensory measurements defined in equations (3e)-(3g); z_1 is a noisy measurement of position, z_2 is a noisy measurement of velocity, and z_3 is a noisy measurement of acceleration, transformed by subtracting the control function $u(\hat{x}_1, \hat{x}_2)$. The coefficients K_{jk} are sensory weights. They are chosen to minimize the weighted sum of squared estimation errors given by the performance index (3h). The weighting of position and velocity errors does not effect the choice of sensory weights. Therefore, we set the performance-index coefficients d_1 and d_2 both equal to 1 in their respective units.

When the sensory weights K_{jk} are zero, (3c) and (3d) are an internal model of the inverted pendulum. The terms $\sigma_{c1}\xi_{c1}(t)$ and $\sigma_{c2}\xi_{c2}(t)$ describe computation noise. Computation noise is meant to model errors made by the neural systems that fuse sensory information to produce the state estimates $\hat{x}_1$ and $\hat{x}_2$. It differs from measurement noise in that it effects the dynamics of estimation even in absence of the sensory information. When the computation-noise levels σ_{c1} and σ_{c2} are zero, (3c) and (3d) are a Kalman filter (Bryson & Ho, 1975).

The model has a total of 9 parameters□ the inverted-pendulum parameter γ; the control-function coeffcients c_1 and c_2; the process-noise

level σ; the sensory-noise levels σ_1, σ_2 and σ_3; and the computation-noise levels σ_{c1} and σ_{c2}.

The autocovariance function of the model has the form

$$E[x_1(t)x_1(t+\tau)] = \kappa_{e1}e^{\lambda_{e1}|\tau|} + \kappa_{e2}e^{\lambda_{e2}|\tau|} + \kappa_{c1}e^{\lambda_{c1}|\tau|} + \kappa_{c2}e^{\lambda_{c2}|\tau|}.$$

The eigenvalues λ_{e1} and λ_{e2} are called the "estimation eigenvalues"; they describe the dynamics of estimation errors and depend only on γ and the noise-level parameters. The eigenvalues λ_{c1} and λ_{c2} are called the "control-function eigenvalues"; they depend only on γ and the control-function coeffcients c_1 and c_2:

$$\lambda_{c1,2} = -c_2/2 \pm i\sqrt{c_1 - \gamma - c_2^2/4}.$$

Based on comparisons of the model to experimental data (Kiemel et al., 2002), we hypothesize that $c_1 > \gamma + c_2^2/4$ so that the control-function eigenvalues are complex-valued, corresponding to a damped-oscillation. We further hypothesize that the postural control system under normal sensory conditions resides in a parameter regime in which the process-noise level σ, the velocity sensory-noise level σ_2, and the position computation-noise level σ_{c1} are all small. This hypothesis is stated mathematically by assuming that these parameters are of order ε, where ε is a small parameter. Then one estimation eigenvalue, λ_{e1}, is of order ε, indicating a slow rate constant; and the other estimation eigenvalue, λ_{e2}, is of order $1/\varepsilon$, indicating a fast rate constant. The control-function eigenvalues λ_{c1} and λ_{c2} are of order 1, indicating dynamics on an intermediate time scale.

The largest coefficient of the autocovariance function is the estimation coefficient κ_{e1}, which is of order ε. The control-function coefficients κ_{c1} and κ_{c2} are of order ε^2, and the second estimation coefficient κ_{e2} is of order ε^5. Therefore, the eigenvalues of a descriptive ARMA model (see methods) can be related to the eigenvalues of the mechanistic noisy-computation model: the real-valued eigenvalue λ_r corresponds to the estimation eigenvalue λ_{e1}, and the complex-valued eigenvalues λ_c and $\bar{\lambda}_c$ correspond to the control-function eigenvalues λ_{c1} and λ_{c2}.

The default values of the parameters are γ = 8 s^{-2}, c_1 = 14.25 s^{-2}, c_2 = 3 s^{-1}, σ = 0.25 deg $s^{-3/2}$, σ_1 = 1 deg $s^{1/2}$, σ_2 = 0.05 deg $s^{-1/2}$, σ_3 = 2 deg $s^{-3/2}$, σ_{c1} = 0.03 deg $s^{-1/2}$, and σ_{c2} = 5 deg $s^{-3/2}$.

Figure 1. Experimental apparatus showing subjects standing on a sway-referenced platform.

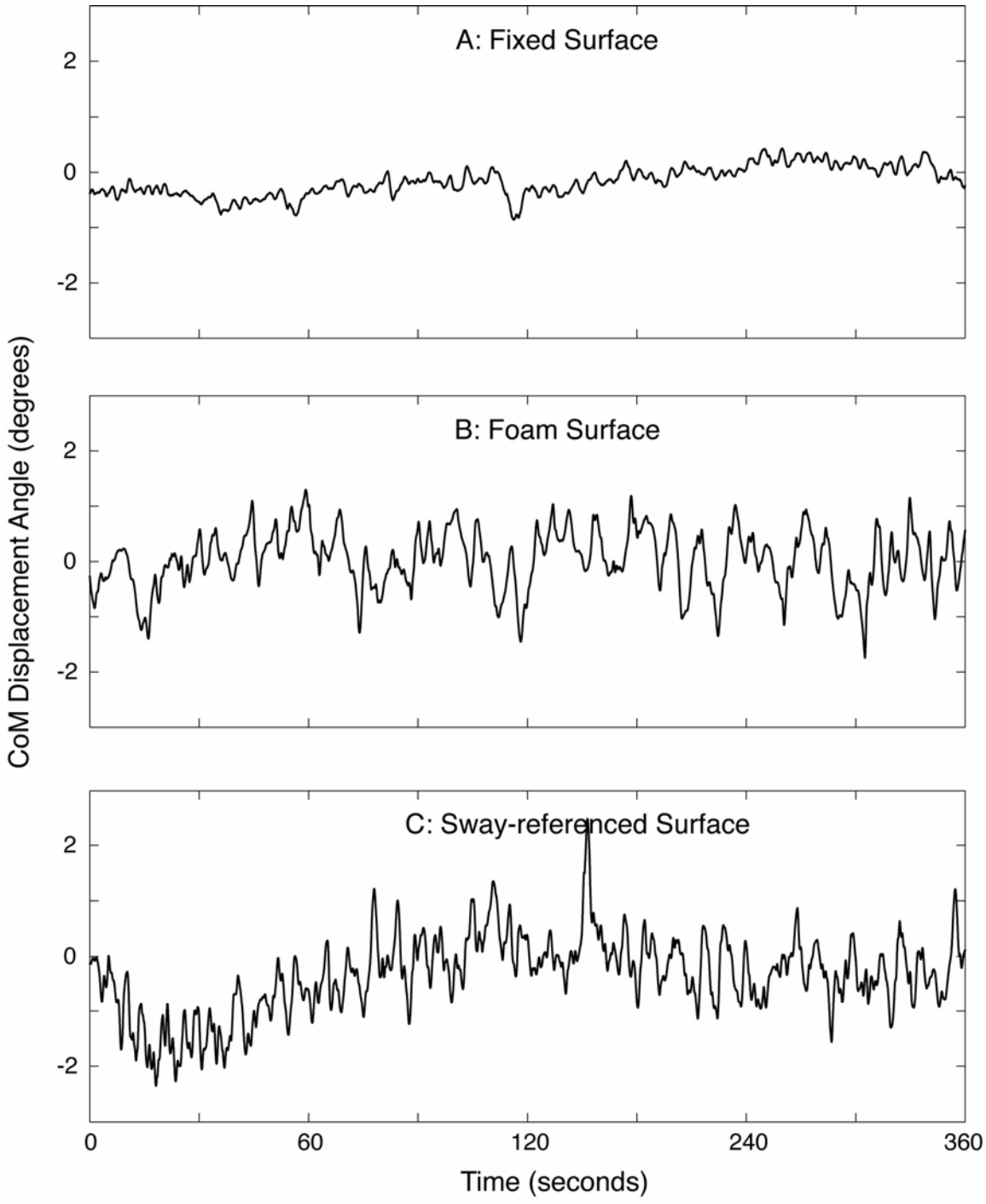

Figure 2. Exemplar time series from Subject 1 in the (A) fixed B) foam C) sway-referenced surface conditions.

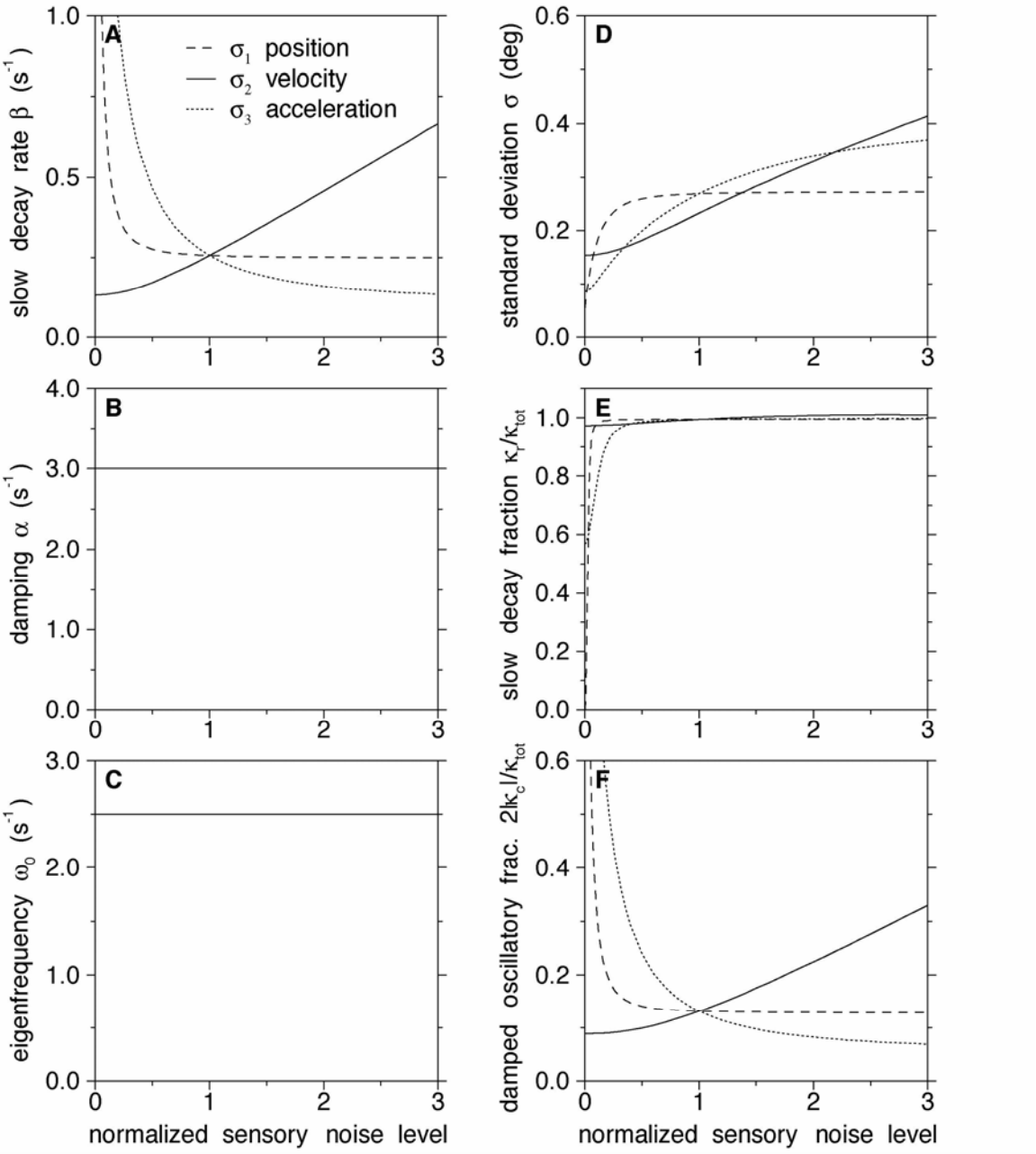

Figure 3. The effect of degrading sensory information in the noisy-computation model. Dashed lines show the effect of varying the position sensory-noise level σ_1; solid lines show the effect of varying the velocity sensory-noise level σ_2; dotted lines show the effect of varying the acceleration sensory-noise level σ_3. Moving right along the horizontal axis is

equivalent to experimentally reducing sensory information. The damping α and eigenfrequency ω_0 do not depend on the sensory noise levels and thus remain constant. The sensory-noise level being varied is normalized by dividing by its default value. All other parameter values are set to their default values (see Appendix).

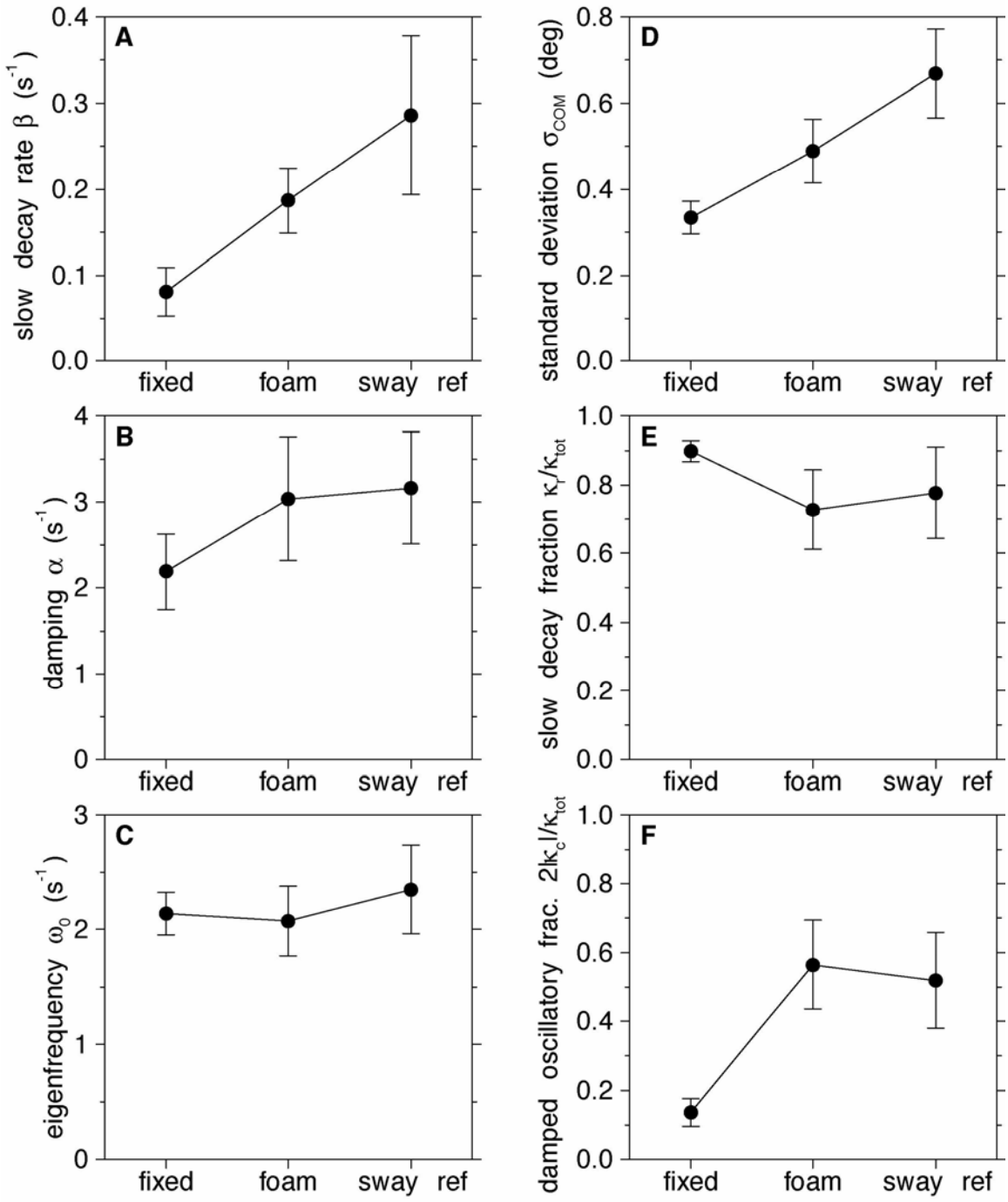

Figure 4. Average model measures across subjects for each condition. Error bars denote SE of the mean.

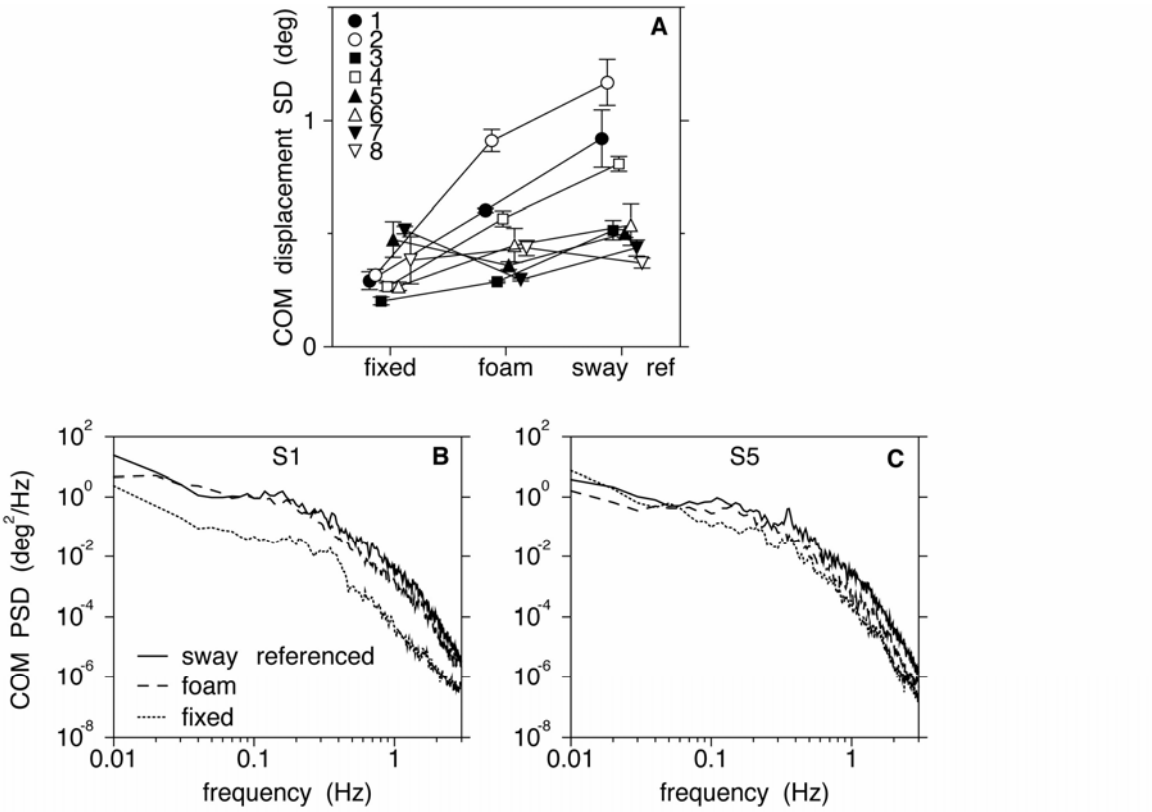

Figure 5. (A) Average COM angular displacement SD for individual subjects show that there was not a consistent increase across conditions for all subjects. COM PSD plots for (B) S1 and (C) S5 show that there was no consistent pattern of spectral power distribution at low frequencies. At higher frequencies, a consistent ordering of fixed<foam<sway-referenced spectral power is observed. Error bars denote SE of the mean.

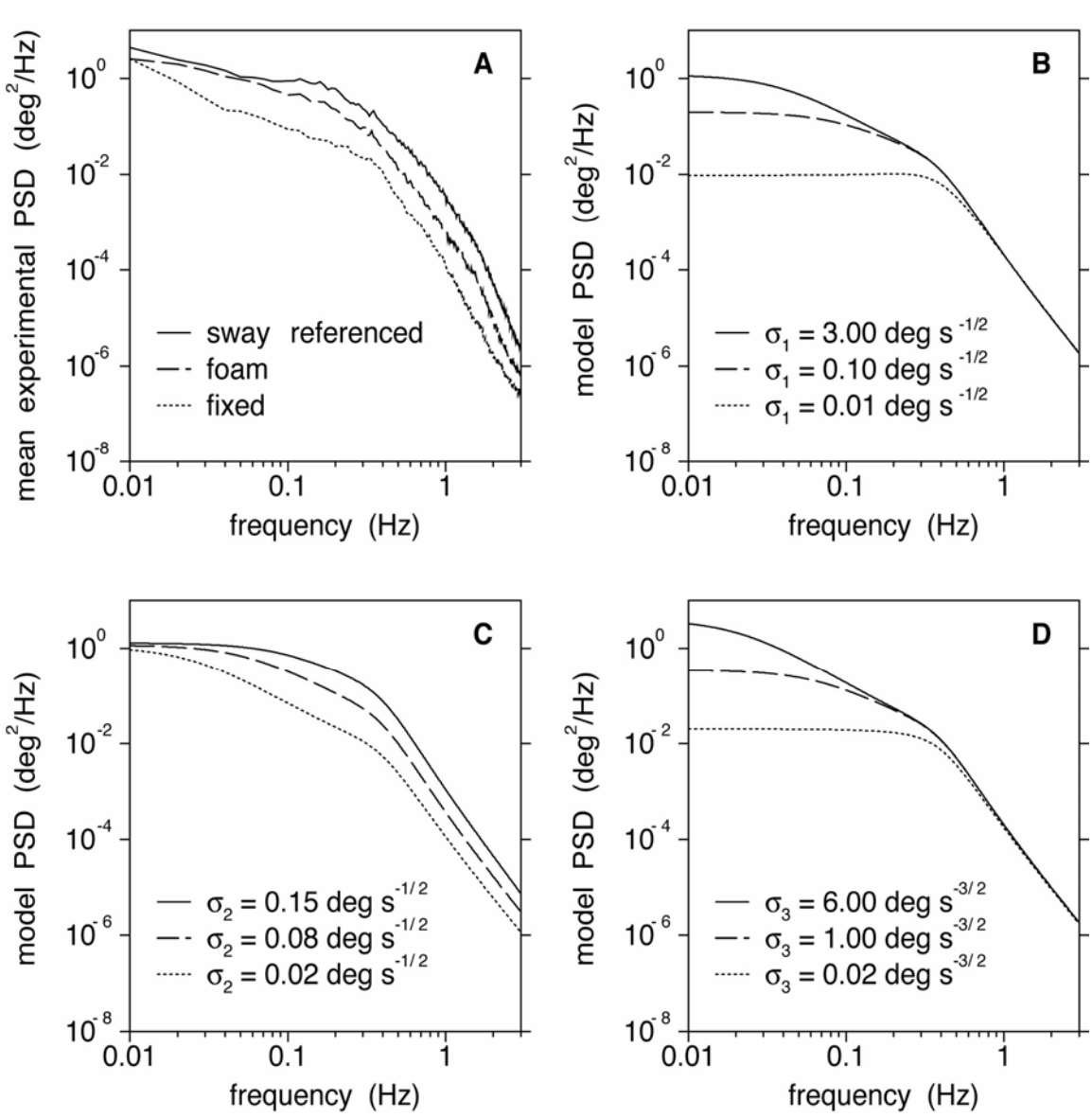

Figure 6. (A) Geometric mean across subjects of the power spectral density for COM angular displacement in the three surface conditions. B-D) Power spectral densities of the noisy-computation model for three values of the position sensory-noise level σ_1, velocity sensory-noise level σ_2, acceleration

sensory-noise level σ_3. The three parameter values are meant to represent the three experimental conditions in (A). Note the similarity between experimental PSDs in (A) and model PSDs based on velocity noise levels in (C). See Appendix for other parameter values.

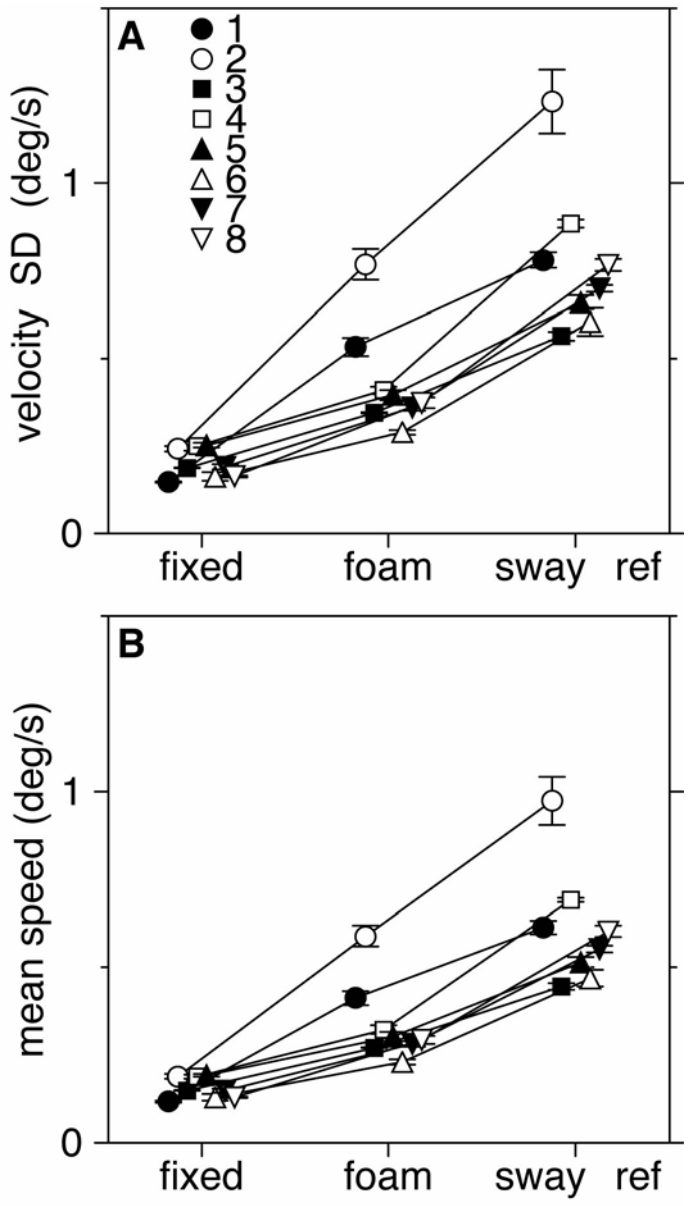

Figure 7. Average COM (A) SD of velocity and (B) speed for each subject and each surface condition. Unlike COM SD of displacement (see Fig 5A), all subjects showed the same pattern of results for both velocity SD and speed. Error bars denote SE of the mean.

Chapter 5

A Unified View of Quiet and Perturbed Stance:

Simultaneous Co-existing Excitable Modes

Creath R, Kiemel T, Horak F, Peterka R, Jeka J

Neurosci Lett. (2005); 377(2): 75-80

Introduction

When standing quietly, human upright stance is often approximated as an inverted pendulum, pivoting around the ankle (Jeka et al. 2004, Peterka 2002). Under more strenuous conditions, such as when support surface perturbations are imposed, multiple coordination patterns are observed (Horak & Macpherson, 1996). The ankle and hip strategies are considered two of the three primary coordinative patterns (along with stepping) implemented by the nervous system to maintain upright stance in response to perturbations (Horak & Nashner 1986). As their names imply, the ankle and hip strategies are characterized by rotation primarily about the ankle and hip, respectively. The current thinking is that a “pure” ankle or hip strategy is observed in response to specific perturbations. For example, the ankle strategy persists during small perturbations consisting of low-amplitude, low-velocity or low-frequency stimuli. With larger perturbations, the hip strategy predominates (Alexandrov at al. 2004, Horak & Nashner 1986, Park et al. 2004). Other factors such as the length of the support surface (Horak &

Nashner 1986), central set (Horak et al. 1989) and neurological pathologies (Horak et al. 1990) influence the prevalence of the ankle or hip strategy. These results have led to a conceptual framework in which postural responses are chosen from a continuum of ankle-hip strategy mixtures, with the “pure” strategies at opposite extremes. The generally accepted idea is that these basic patterns are centrally selected from a set of motor programs, arising from high-level neural strategies and implemented by complex sensorimotor control processes to most effectively counteract the physical characteristics of the perturbation (Horak & Macpherson 1996).

Central selection, however, may not be the primary determinant of the postural response strategy. From a biomechanical perspective, these patterns arise from the dynamics of a multi-link inverted pendulum. Early attempts to characterize a biomechanical influence simplified the problem of controlling an inverted pendulum by analyzing gravitationally-driven, non-inverted pendulums with properties based upon anthropometric measures of the human body (McCollum & Leen 1989). Assuming the adult human body could behave as a two-link pendulum where the links could oscillate in-phase as a single-segment system or anti-phase as a double pendulum, the authors predicted oscillation frequencies of .52 Hz for a single pendulum and 1.45 Hz for a double pendulum, consistent with experimental results (e.g., Park et al. 2004).

More recently, Alexandrov et al. (2001a, 2001b, 2004) used a three-joint (ankle, knee and hip) inverted pendulum model to account for postural

responses during fast-forward bending at the waist on narrow and wide surfaces and in response to platform perturbations. Ankle, hip and knee eigenmovements were derived from the mechanical properties of the body, where each eigenmovement is named after the joint that contributes most to the movement. For a non-inverted version of the model, these eigenmovements have eigenfrequencies of 0.48, 1.13 and 3.47 Hz, respectively[1]. Most important, the authors (Alexandrov et al. 2001a, 2001b, 2004) did not presuppose the existence of any particular pattern. The three patterns emerged as solutions to the three-joint model which co-exist with varying amounts of power during the voluntary bending task.

Finally, recent accounts by Bardy et al. (1999, 2002) have stressed that the inherent “stability” of the ankle-hip patterns determine the postural response, rather than a process of central selection. Based upon a task in which subjects voluntarily tracked a visual sinusoidal stimulus that increased in frequency over the trial, two stable modes were found: one at lower frequencies where the trunk and legs oscillated in-phase; and an anti-phase mode at higher frequencies. Their view argues against the idea that coordinative patterns are “selected”. Instead, transitions between postural states are due to loss of stability. Bipedal stance is an emergent, self-organizing double pendulum with two stable modes (Bardy et al. 1999, 2002).

It is notable that all previous analyses of ankle and hip patterns involved a perturbation of some form. The implicit assumption is that quiet stance can be approximated by a single-segment inverted pendulum and the

hip strategy is invoked when the postural system is perturbed. However, we propose that both patterns are observable during quiet stance. If quiet stance behavior can be represented by a combination of ankle and hip eigenmovements (i.e. assuming there is little or no contribution from the knee eigenmovement) then we hypothesized that spectral analysis will reveal an in-phase relationship between the trunk and leg angles at low frequencies and an anti-phase relationship at higher frequencies. This hypothesis is based on the recognition that (1) the ankle eigenmovement represents in-phase motion of the leg and trunk angles, (2) the hip eigenmovement represents anti-phase motion of the leg and trunk angles, and (3) the hip eigenfrequency is higher than the ankle eigenfrequency,

We investigated the coordination between upper and lower body segments in a behavioral situation in which an in-phase relationship (i.e., ankle strategy) between the trunk and legs has typically been assumed; unperturbed upright stance. Moreover, because the availability of somatosensory information at the feet is known to influence which postural strategies are adopted (Horak et al. 1990), we also tested how altering the support surface with foam and by rotating the surface in proportion to the subject's body sway (i.e., sway-referencing) influences the observed coordination patterns.

Methods

Subjects

Eight healthy subjects participated in the study, four male and four female between the ages of 22 and 37 with no known musculoskeletal injuries or neurological disorders that might have affected their ability to maintain balance. All subjects were given both oral and written task instructions and gave written consent according to guidelines implemented by the Internal Review Board at Oregon Health & Science University and the Declaration of Helsinki before undergoing the experimental protocol.

Apparatus

Subjects stood on a variable pitch platform using a shoulder-width parallel stance so that the rotational axis of the ankles coincided with the rotational axis of the platform (Jeka et al. 2004). Shoulder and hip displacements were measured using rigid rods attached to a fixed position on one end and attached to the subjects by a harness on the opposite end. The rods could rotate freely about the fixed end in the anterior-posterior plane. The amount of displacement was determined by the change in voltage of potentiometers located on the fixed ends of the shoulder and hip rods. Subjects wore a safety harness that was secured to fixed brackets by two connecting straps. The straps were adjusted to allow for the subjects' body sway before becoming taut. The platform displacement signal and potentiometer voltages were sampled at 100 Hz.

Procedures

Subjects stood upright with feet shoulder-width apart and eyes closed in blocks of three 364 second trials on a: 1) fixed surface; 2) foam surface; and 3) sway-referenced surface. The platform position was stationary on the fixed surface and foam surface trials. For the sway-referenced trials, the platform rotated in the A-P direction an amount equal to the angular hip displacement as determined by the hip rod potentiometer signal. For the foam surface trials, subjects stood on a 4" thick piece of Sunmate Temper medium density foam placed on the platform. Because of the long trials, the sway-referencing condition was run after the fixed surface condition to minimize any possible effects of fatigue. The foam surface was run last because it required repositioning the rigid rods to accommodate the increased height of the foam surface. Prior to performing the sway-referenced trials, subjects completed two shorter practice trials to familiarize themselves with the condition in order to minimize any learning effects that might occur as a result of the long trial duration and the unfamiliar nature of the task. Background sound was masked with a tape-recorded text played through ear-covering headphones. One trial was discarded due to technical difficulties and one trial was shortened to 300 seconds due to a loss of balance near the end.

Analysis

Spectral Analysis

Trunk and leg segment angles, relative to earth vertical, were determined by trigonometric methods using the measures of A-P shoulder and hip displacement for the trunk segment, and A-P hip displacement for the leg segment (Peterka 2002). Mean power spectral density (PSD) and mean cross spectral density (CSD) of the trunk and leg segment angular displacements were calculated for each subject as the average of three trials (one subject had only 2 foam trials) in each condition for each subject using the Matlab PSD and CSD functions respectively which implement Welch's averaging method (Marple 1987). Calculations used a 20 second Hanning window with a one-half window overlap after subtracting the mean angular displacement from the raw data. Between-subjects averages for CSD, PSD, and coherence were calculated as the arithmetic mean of the subjects' CSDs, PSDs, and coherence estimates. Estimated cophase between trunk and leg segment angles was calculated as the argument of the between-subjects average CSD. Estimated coherence was calculated for each subject as the absolute value of the average across trials of the CSD, squared and divided by the product of the average across trials of trunk and leg PSDs. Spectral density was plotted on a log-log scale to make it easier to observe the distribution of power in the sway trajectory which is typically concentrated at low frequencies.

Statistics

Trunk and leg PSDs were analyzed for frequencies from 0.05 to 5 Hz in increments of 0.05 Hz. We chose 5 Hz as the maximum frequency, because of the increasing influence of measurement noise at higher frequencies. The log(PSD) values were analyzed using repeated-measures ANOVA with 3 conditions x 2 segments x 100 frequencies at a 0.05 level of significance where $p<.05$ was considered significant. Pairwise comparisons between conditions and segments were performed using Tukey HSD at a significance level of .05. For each pair of PSDs that were determined to be significantly different by the posthoc test, we performed paired t-tests at each of the 100 frequencies to determine the frequency range of the differences. The method of Benjamini and Hochberg (1995) was applied to the resulting p-values to control the false discovery rate (FDR) at a level of 0.05. Controlling the FDR is more liberal than controlling the familywise error rate, but is more conservative than controlling the per-comparison error rate. Because the p-values are correlated, control of the FDR is approximate.

Results

The relationship between the trunk and leg segment angles during quiet stance is visible in the exemplar plots of trunk and leg segment angular displacements in Figure 1A-C. First, notice that the trunk and leg trajectories are primarily moving in unison with large excursions of the trunk mirrored by those of the legs. This suggests that an in-phase pattern accounts for most of

the sway variance of the two segments. However, in-phase behavior does not fully characterize the trunk-leg relationship. Mean power spectral density plots for trunk and leg angles in Figures 1D-F show small, frequency-dependent differences in trunk and leg PSDs. At frequencies above approximately 1 Hz, trunk power was greater than leg power, shown as the frequency range within the dotted rectangle. Conversely, leg power was greater than trunk power for the foam and sway-referenced conditions in the frequency range between .1-.7 Hz, shown as the frequency range within the solid rectangle. Such differences in leg and trunk power suggest double pendulum behavior.

Second, consistent with previous studies, the overall amount of sway increased when sensory information was altered in the foam and sway-referenced conditions (Allum et al. 2002). Figures 2A-B show that the average spectral power for the leg and trunk angles was greatest for the sway-referenced condition followed by the foam and fixed surface conditions ($p < .05$). Leg and trunk spectral power decreased with increasing frequency for all three sensory conditions ($p < .05$). Frequency-by-frequency comparisons for each pair of conditions showed significant differences across almost the entire frequency range (false discovery rate < 0.05). One exception was that none of the pairs of conditions were significantly different at 0.05 Hz for the trunk segment (Figure 2A).

A concise picture of the coordinative relationship between trunk and leg segments was assessed by analyzing the cophase, or the phase angle between the trunk and legs, as shown in Figure 2C. The cophase for all

conditions is approximately zero degrees (in-phase) for lower frequencies and approximately 180 degrees (anti-phase) at the highest frequencies. The in-phase and anti-phase relationships are indicative of the ankle and hip synergies, respectively, demonstrating the simultaneous existence of these patterns during quiet stance. The spectral power at the frequencies corresponding to the anti-phase motion is several orders of magnitude lower than the power in the frequency range corresponding to in-phase motion. Thus, while both patterns exist simultaneously, the majority of sway variance is associated with the ankle pattern.

All three conditions demonstrated a shift from in-phase to anti-phase behavior as sway frequency increased, as shown in Figure 2C. Cophase in the fixed and foam surface conditions shifted downward, suggesting a trunk-lagging shift. Cophase in the sway-referenced condition shifts in an upward direction, suggesting a trunk-leading shift. Cophase settles at essentially the same anti-phase pattern in all three conditions. The shift from in-phase to anti-phase is less clear, however, when coherence in Figure 2D is considered. During the shift from in-phase to anti-phase, coherence remained non-zero in the sway-referenced condition, decreasing to approximately 0.4. In the fixed and foam conditions, coherence decreased to near zero during the shift, meaning that cophase is undefined during the shift. The direction of the shift from in-phase to anti-phase is known only during sway-referencing.

Discussion

The present experiment demonstrated the simultaneous coexistence of in-phase and anti-phase relationships between the leg and trunk angles during quiet stance. The relationship was generally in-phase for frequencies below 1Hz and anti-phase for frequencies above 1Hz. Altering the support surface characteristics with foam had only minor effects. For the fixed and foam surface conditions, the shift between in-phase and anti-phase as a function of frequency was abrupt and was accompanied by coherence near zero, indicating a weak relationship between the two segment angles at the transition frequency. Changing the sensory/mechanical condition to sway-referencing had a more dramatic effect. Coherence remained non-zero at the transition and the change in cophase was more gradual. Cophase increased with increasing frequency, indicating an increasing phase lead of the trunk angle with respect to the leg angle. Considering that the postural task was relatively simple, unperturbed stance on a fixed surface, the results suggest that the simultaneous coexistence of two postural synergies is due partially to the mechanical characteristics of a multi-link pendulum.

These results question the prevailing notions of how coordinative patterns predominate to maintain upright stance. Horak and Nashner (1986) concluded that hip and ankle strategies were implemented as centrally controlled programs that are selected depending upon task requirements. Bardy et al. (1999, 2002) argued that transitions between postural states are based upon the inherent stability of the patterns. McCollum and Leen (1989)

showed that the upright body could behave as a single-link or double-link pendulum, but offered no explanation as to how each mode could predominate. We argue that the ankle and hip strategies are not extremes along a continuum of mixed strategies to maintain upright stance. Instead, quiet stance can be viewed similarly to the proposal of Alexandrov et al. (2001a, 2001b, 2004) for perturbed stance. Multiple, co-existing strategies are simultaneously present during upright stance, with varying amounts of power, depending upon biomechanical, environmental and task constraints. This view has a number of implications. First, it unifies the relationship between quiet and perturbed stance. Quiet stance has typically been viewed as a more passive form of upright stance control than perturbed stance. Passive characteristics of the neuro-musculoskeletal system (e.g., passive stiffness) keep the segments aligned, allowing tonic activity of ankle extensors to maintain an upright position during quiet, unperturbed stance. In contrast, perturbed stance engages reflexive activity and compensatory strategies from musculature throughout the body. The presence of an anti-phase relationship during quiet stance questions whether the “passive” control of quiet upright stance is an adequate characterization. Both quiet and perturbed stances invoke a common form of control, quiet being a more subtle version of perturbed.

Second, the idea that a single postural mode is adopted to maintain upright stance is questionable. The contrasting views of earlier cited studies are relevant here. Alexandrov et al. (2001a, 2001b, 2004) showed that up to

three modes simultaneously co-exist during a voluntary trunk-bending task and in response to platform perturbations. Conversely, Bardy et al. (1999, 2002) argued for transitions between ankle and hip strategies as the characteristics of a voluntarily-tracked visual stimulus were varied. The term "transition" implies that one state is initially adopted and then disappears as a different state becomes stable. However, we question whether the peak-picking method of analysis used by Bardy et al. (1999, 2002) fully characterizes the behavioral modes. Peak-picking essentially acts as a filter and characterizes the mode that is most closely aligned with the visual stimulus, ignoring significant power at other frequencies. We speculate that if all power in the voluntary task were analyzed, as in Alexandrov et al. (2001a, 2001b, 2004), the presence of phase relationships other than the one identified by peak-picking would emerge. The upright body does not behave like a limit cycle, even when oscillatory stimuli are imposed (cf. Jeka et al. 1998). Upright stance control is essentially a stable, fixed point influenced by noise, with simultaneous co-existing modes, in both the quiet and perturbed state.

Finally, even though body mechanics alone can account for two different patterns as a function of frequency, a solely mechanical explanation cannot explain the coordinative changes corresponding to different types of perturbations, such as an increase in the amplitude of a support surface perturbation. For example, a mechanical view would predict an approximately linear response: larger amplitude perturbations would be

matched by larger amplitudes of the ankle pattern, rather than the well-documented predominance of a hip strategy with increasing perturbation amplitude (Horak & Macpherson 1996). Therefore, it is likely that the central selection of a motor program combines with mechanics in the expression of these synergies.

Conclusion

The coexistence of in-phase and anti-phase body sway during quiet, unperturbed stance implies that the mechanical characteristics of a multilink inverted pendulum play a significant role in defining the coordinative patterns between the trunk and legs. This modifies the views that these coordinative patterns represent two extremes of a continuum of mixed strategies (Horak & Macpherson 1996) or two states that are individually expressed based on their stability (Bardy et al. 1999, 2002). Instead, the ankle and hip strategies may be viewed as “simultaneously co-existing excitable modes”, both always present, but one which may predominate depending upon the characteristics of the available sensory information, task or perturbation.

Footnote

1. Alexandrov et al. [1] did not consider the non-inverted form of their model. However, the eigenfrequencies in this case can be computed as $f_i = 1/(2\pi\sqrt{\lambda_i})$, where the λ_i are the eigenvalues given in [1].

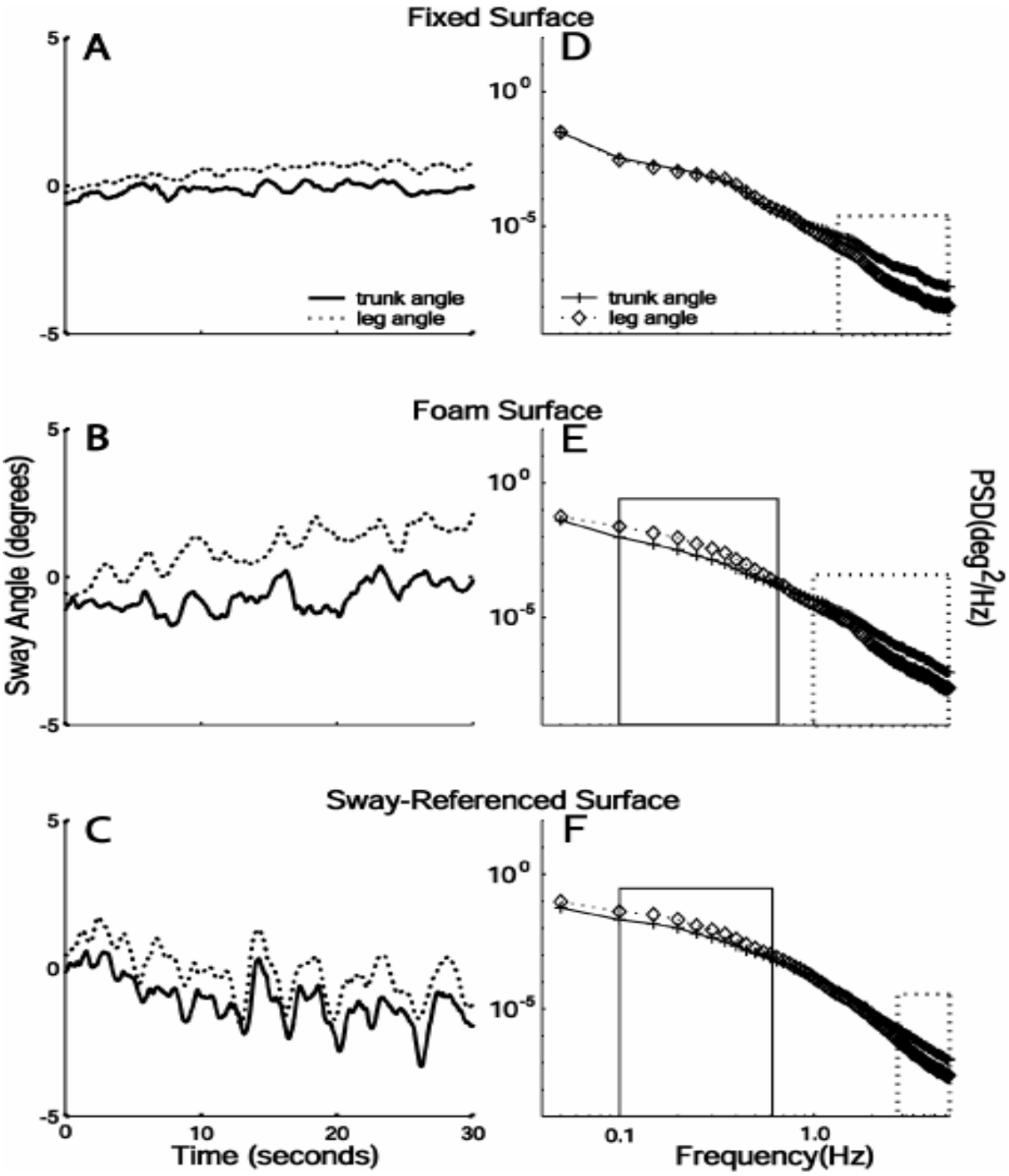

Figure 1. Exemplar time series plots of trunk and leg segment angular displacements for fixed (A), foam (B), and sway-referenced (C) surfaces. Comparisons of mean trunk and leg power spectral densities, averaged across subjects, for fixed (D), foam (E), and sway-referenced (F) surfaces.

The frequency range enclosed within the solid rectangles identifies frequencies where leg power was significantly greater than trunk power while the frequency range enclosed within the dotted rectangle identifies frequencies where trunk power was greater.

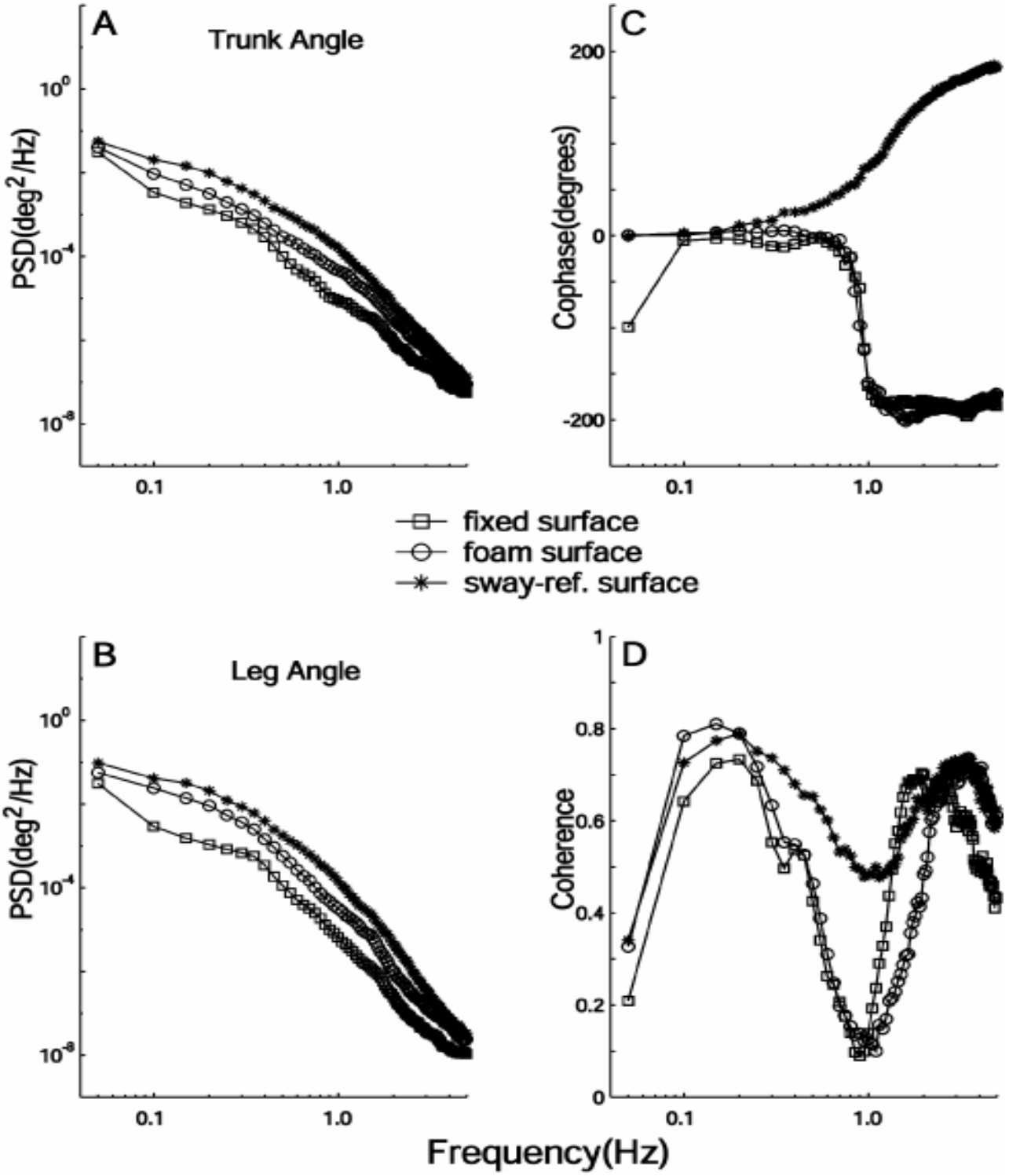

Figure 2. Mean Spectral measures of sway in the three conditions. (A) Trunk PSD (B) Leg PSD. (C) Cophase. (D) Coherence.

Chapter 6

The role of vestibular and somatosensory systems in intersegmental control of upright stance.

Creath R, Kiemel T, Horak F, Jeka J,

J Vestib Res. 2008;18(1):39-49..

Introduction

Human postural control is often approximated as having two essential modes of control: a single-joint, inverted pendulum “ankle strategy” and a two-joint double-pendulum “hip strategy” (McCollum & Leen 1989, Horak & Macpherson 1996, Horak & Nashner 1986). As their names imply, the ankle and hip strategies are characterized by rotation primarily about the ankle and hip, respectively. During quiet stance and small perturbations, the nervous system is thought to employ primarily the single-joint ankle strategy, with active control of CoM motion derived primarily from ankle torque (Horak & Kuo 2000, Horak & Nashner 1986, Runge et al. 1998, Winter et al. 1998). With larger support surface translations, the hip strategy, in which CoM motion derives primarily from hip torque, is “recruited”. The generally accepted idea is that these basic patterns are centrally selected from a set of motor programs, arising from high-level neural strategies and implemented by complex sensorimotor control processes to most effectively counteract the physical characteristics of the perturbation (Horak & Nashner 1986, Horak et al. 1990).

Recent experimental and theoretical work, however, has questioned the distinction between these two modes of control. The current thinking is that both patterns are present to varying degrees all the time. For example, a re-analysis of body kinematics during support surface translations showed that both ankle- and hip strategies were observed at all translation frequencies (Park et al. 2004, Runge et al. 1998). Theoretical work from Alexandrov et al. (2001a&b) has also shown the co-existence of multiple patterns. They derived ankle, hip and knee eigenmovements from the mechanical properties of the body, where each eigenmovement is named after the joint that contributes most to the movement. The three patterns emerged as solutions to a three-joint model which co-exist with varying amounts of power during tasks such as voluntary bending, but that the ankle and hip eigenmovements constitute the biomechanical bases for the ankle and hip strategies described by Horak and Nashner (1986). Even during quiet, unperturbed stance, in-phase and anti-phase coordination patterns have been shown to co-exist (Creath et al. 2005, Zhang et al. 2007). At frequencies below 1 Hz, the trunk-leg segments clearly show an in-phase pattern. However above 1 Hz, an abrupt shift to an anti-phase strategy is observed. Such results unify the artificial distinction between quiet and perturbed stance, reflecting excitable modes or flexible synergies that predominate depending upon the task. Moreover, co-existing patterns discount the need for a selection process between pre-programmed patterns

depending upon perturbation, environmental constraint or pathology (Horak & Kuo 2000, Horak & Nashner 1986, Kuo 1995).

A recent study has shown that the co-existing in-phase and anti-phase trunk-leg patterns during quiet stance respond differently to different types of sensory information (Zhang et al. 2007). Changes in coherence due to additional sensory information were observed at frequencies below 1 Hz where the in-phase pattern predominates, but no discernable effect was observed above 1 Hz, where the anti-phase pattern predominates. The sensitivity of the in-phase pattern to sensory changes potentially reflects a greater degree of neural control than the anti-phase pattern, whose underlying basis may be primarily due to the biomechanics of the human body approximated as a double pendulum (McCollum & Leen 1989).

The role of the vestibular sensory system in coordination of the ankle and hip postural strategies is not well understood. Previous studies of patients with bilateral vestibular loss responding to discrete surface translations showed normal ankle strategy patterns but inability to use the hip strategy to balance across a narrow beam although vestibular loss subjects could add hip torque to ankle torque to recover equilibrium in response to large translations while standing on a large, firm surface (Horak et al. 1990, Runge et al. 1998). Studies have also suggested that light fingertip touch on a stable surface may substitute as a vertical reference for patients with bilateral vestibular loss to reduce postural sway (Lackner et al. 1999, Horak et al. 2002, Creath et al 2002). Here, we used spectral methods to investigate

intersegmental dynamics during continuous translations of various frequencies between individuals with bilateral vestibular loss (BVL) and healthy controls. Our intent was to investigate how intersegmental dynamics adjust to platform perturbations of different frequencies in the presence or absence of vestibular information, and in the presence or absence of additional somatosensory information supplied by light touch fingertip contact (Jeka & Lackner 1994).

Methods

Subjects

The experimental protocol was approved by the Institutional Review Boards of the Oregon Health Sciences University and the University of Maryland and was performed in accordance with the 1964 Helsinki Declaration. All subjects gave their informed consent prior to participation in this study.

Five bilaterally deficient vestibular subjects, two females and three males (age=54.8 ±8.9 years), and five healthy control subjects matched by age and gender participated in the study. Vestibular function was assessed by a combination of methods to determine the degree of deficit, as shown in Table 1. Dynamic otolith function was determined from the modulation component of horizontal eye movements recorded during off-vertical axis rotations (OVAR) (Haslwanter et al. 2000). Static otolith function was determined by measuring the peak-to-peak amplitude of counter-rolling eye

movements during left and right slow-roll tilts (OC) (Miller 1970). Horizontal semicircular canal function (HVOR) was determined by fitting an exponential function, $A^* \exp(-t/T_c)$, to the slow-component velocity of HVOR eye movements for constant velocity rotations about an earth-vertical axis (Honrubia et al. 1982). DC gain of the HVOR relative to acceleration was estimated from the product of the time constant, T_c, and the gain constant. The gain constant was determined by dividing the response amplitude, A, by the velocity of rotation. Pitch and yaw VOR gain were derived in a similar manner (Peterka et al. 1990).

Apparatus

Subjects were instructed to stand on a variable pitch platform that rotated $\pm 1.2^{O}$ in the A-P direction, as shown in Figure 1. Subjects stood in a standard parallel stance with their ankles directly above the platform axis of rotation. In the touch condition, subjects maintained contact with a touch plate with their right index fingertip. The touch plate consisted of a circular aluminum disk that was mounted on top of a 97.8 cm pedestal. Force sensors mounted between the disk and pedestal determined touch forces in the anterior-posterior, medial-lateral, and vertical directions. The pedestal stood on a supportive metal structure that straddled the platform in order to isolate the touch plate from platform vibrations. The center of the touch plate was adjusted so that it was directly in front of the subject's right shoulder. The distance between the subject and the touch plate was adjusted so that the

subject could reach the touch plate with their right index finger in a comfortable manner. Subjects wore a safety harness that was secured to a movable ceiling mount by a connecting strap. The connecting strap was adjusted to allow subjects to lower their body approximately 30 cm before becoming taut. The platform rotation signal was sampled at 120 Hz.

Kinematic data was recorded using a Motion Analysis data acquisition system (Motion Analysis Crop., Santa Rosa, CA) at a sampling rate of 30 Hz. Markers were located on the right side of the subjects' bodies as shown in Figure 1. The trunk segment was defined as the distance between the acromium process (shoulder) and the head of the greater trochanter (hip) while the leg segment was defined as the distance between the head of the greater trochanter and the lateral malleolus (ankle). Additionally, reference markers were placed on the pedestal and a stationary position on the non-rotating part of the platform. To quantify measurement noise, we computed the power spectral density (PSD) of the stationary platform marker using the same method applied to markers placed on the body (see below). The PSD of measurement noise was about 0.02 mm^2/Hz, which was substantially less than the PSDs of hip and shoulder displacements up to about 3 Hz.

Measures

The study of posture is a complex problem partly because the human body consists of many segments that have been shown to be active during quiet stance (e.g. Gage et al. 2004, Hsu et al. 2006). In the present

experiment, we chose to study trunk and leg segments as a continuation of previous work which explored the manner in which these segments respond to changes in sensory information (Creath et al. 2005, Zhang et al. 2007). Trunk segment angular displacement was defined as the angle formed by the shoulder, the hip, and vertical. Leg segment angular displacement was defined as the angle formed by the hip, the ankle, and vertical. Angular displacements were measured in the sagittal plane. Positive angles refer to forward movements from upright vertical.

Procedures

The platform rotation stimulus consisted of a single sinusoidal waveform at five frequencies: 0.01, 0.03, 0.10, 0.20, and 0.40 Hz. Two sensory conditions were employed: (1) Light (non-supportive) touch. Subjects were instructed to maintain contact of the center of the touch plate with their right index fingertip. An auditory alarm sounded when touch force exceeded 1 Newton; (2) No touch. Subjects were instructed to hold their right index finger in a stationary position in space, slightly above the point they believed to be the center of the touch plate.

Subjects were instructed to stand facing a visual target. Before the light touch trials, subjects were instructed to place their right index finger at the center of the touch bar. Before the no touch trials, subjects were instructed to place their finger directly above the center of the touch bar without making contact. This hand position mimicked the arm position and any

biomechanical effects due to changes in the COM during light touch trials. After positioning the finger, but prior to the start of each trial, subjects were instructed to close their eyes. Trials were initiated with the movement of the support surface.

All trials were 100 seconds in duration. All subjects completed two, randomized 10-trial blocks, consisting of 5 frequency conditions x 2 sensory conditions. Subjects rested a minimum of 100 second between trails, but were allowed more rest if they desired. The total experiment lasted approximately 1.5 hours.

All of the control subjects and three of the BVL subjects completed all trials without falling. The remaining two BVL subjects fell close to the end of the trials (t=90 seconds or later) on the .4 Hz platform condition. BVL subjects did not repeat trials in which they lost equilibrium. Data recorded before a subject lost equilibrium was included in the analysis.

Analysis

A linear systems spectral analysis was performed on each trial by calculating the Fourier transforms of the platform and the subjects' leg and trunk angles after subtracting the mean angle. Fourier transfer functions describing the response of the leg and trunk angles to platform movement were calculated as the Fourier transform of the response divided by the Fourier transform of the input at the driving frequency. Since the platform motion is deterministic, this calculation is consistent with the definition of the

transfer function in terms of the power spectra. Within-subject gain and phase were calculated as the absolute value and the argument of the average transfer function across trials for each subject. Group averages for gain and phase were calculated as the arithmetic and circular means respectively. The circular mean of phase ϕ in radians is the argument of the mean of $\exp(i\phi)$. A positive phase indicates that body sway led the platform movement.

One-sided power spectral densities (PSDs) and cross spectral density (CSD) were computed for the leg and trunk segment angles using Welch's method with 100-second Hanning windows.

Velocity PSDs were calculated by multiplying the position PSD by $(2\pi f)^2$, where f is frequency. Velocity variability was calculated as the square root of the integral from .01-3.0 Hz of the velocity PSD after subtracting the power at each of the five driving frequencies. Within-subject velocity variability was calculated for each trial, and then averaged. Group means were calculated as the arithmetic mean of the within-subject averages.

Additionally we calculated cophase and magnitude squared coherence from the complex coherence, $P_{xy} \Big/ \sqrt{P_{xx} P_{yy}}$, where P_{xy} is the CSD between the trunk and legs, and P_{xx} and P_{yy} are the respective PSDs of the trunk and legs. Within-subject averages for complex coherence were calculated as the arithmetic mean across trials while group averages were calculated as the arithmetic mean across subjects. Cophase was calculated as the argument of the group average of the complex coherence using the trunk as the reference (positive is legs leading trunk) and magnitude squared coherence

was calculated as the absolute value squared of the group average of the complex coherence.

Statistical Analysis

Values for gain, phase, and variability were assessed using a group (2) x frequency (5) x condition (2) x segment (2) repeated-measures ANOVA with condition, frequency and segment as the repeated measures. The Greenhouse-Geiser correction for non-spherical data was applied. For all testing, $p<.05$ resulted in rejection of the null hypothesis.

In order to address the low statistical power associated with the small number of subjects, nonparametric pairwise comparisons for gain, phase and variability were made using the Wilcoxon Rank-Sum test. Multiplicity of testing for the five platform stimulus conditions was addressed by applying a Bonferroni correction.

Differences in magnitude squared coherence were tested for statistical significance using paired (touch condition) and unpaired (group) T tests on the Fisher's z-transformed coherence values at each frequency step. Multiplicity of testing for the 300 frequency steps was addressed by controlling the false discovery rate (Benjamini & Hochberg 1995).

Differences in cophase and complex coherence were tested for significance using paired (touch condition) and unpaired (group) F tests at each frequency step based on the assumption that the complex values of the transfer function were bivariate normally distributed in the complex plane

(Jeka et al. 2006). Cophase was tested using the argument of the complex coherence. Multiplicity of testing (cophase tested at 300 frequency steps) was addressed by controlling the false discovery rate (Benjamini & Hochberg 1995).

Results

Representative BVL and control subjects

Figure 2 compares the trunk segment, platform, and leg segment time series of a healthy control subject (black) with a BVL subject (gray) standing on the oscillating platform. The left plots show the no-touch condition and the right plots show the light-touch condition. For illustrative purposes, only the .01 Hz and the .4 Hz platform conditions are shown.

Figures 2A-B show how both the BVL and control subjects display similar sway characteristics for the .01 Hz platform condition. Both subjects show similar trunk/leg sway without light touch and an attenuation of trunk/leg sway with light touch. Comparing these results to the .4 Hz platform condition in Figures 2C-D, the trunk/leg segments of both subjects contain motion at the platform frequency of .4 Hz, but the amplitude of the BVL subject is larger than that of the control subject. When compared to the .01 Hz platform condition, the BVL subject showed an increase in both trunk and leg sway, but the increase in trunk sway was noticeably greater than the increase in leg sway. When light touch was added, both subjects show an attenuation of

body sway, although the BVL subject does not appear to use light touch as effectively at the higher platform frequency.

Light touch

All BVL and control subjects were able to control fingertip contact force below the 1 N threshold for all platform stimulus-frequency conditions. The average (standard deviation) of the contact force across all platform conditions was .503 (.167) N for BVL subjects (range .327 to .721 N) and .401 (.166) N for control subjects (range .252 to .599 N).

Gain, phase, and velocity variability

Figure 3 shows the group data for gain, phase and velocity variability. The primary result was that BVL subjects displayed dramatic deficits in trunk control that were not observed in control subjects which can be seen in Figure 3A&B as a significant, 4-way group x condition x frequency x segment interaction (p=.0097).

Gain

A significant group x segment effect was observed for gain (p=.023). BVL (gray) and control (black) subjects showed similar trunk gains for the no-touch condition (Figure 3A) at the lowest platform frequency (.01 Hz), but as the platform frequency increased, BVL trunk gains increased dramatically for the four highest platform frequencies (.03, .1, .2, and .4 Hz) compared to

control subjects (Bonferroni corrected p=.045). In fact, for the three highest platform frequencies, trunk gains for all of the BVL subjects were greater than all of the control subjects. There were no significant group differences in leg gain for the no-touch condition (Figure 3B). For the light touch condition (solid lines) there were no significant group differences in trunk or leg gain at any of the platform frequencies.

A significant group x condition effect for gain was also observed (p=.018). With the addition of light touch, BVL subjects showed a decrease in trunk gain (Figure 3A) at the four highest platform frequencies (.03, .1, .2, and .4 Hz) (p=.010), whereas light touch caused a somewhat smaller decrease in trunk gain for control subjects at the 4 lowest platform frequencies (.01, .03, .1, and .2 Hz) (p=.010). Light touch also caused a reduction in leg gain (Figure 3B) for the BVL subjects at the three highest platform frequencies (.1, .2 and .4 Hz) (p=.010), while the control subjects displayed a decrease in leg gain at the four lower platform frequencies (.01, .03, .1, and .2 Hz) (p=.010).

A significant group x frequency effect for gain (p=.024) can also be seen in Figure 3A&B. Differences were found to occur only for the no-touch condition. BVL subjects displayed an increase in trunk gain with increasing platform frequency for the four lowest platform frequencies (Figure 3A, .01, .03, .1 and .2 Hz) (p=.008). In contrast, control subjects showed decreasing trunk gains with increasing platform frequency for the three highest platform frequencies (p=.008). Leg gains for BVL subjects (Figure 3B) increased for the three lowest platform frequencies (p=.008), then decreased for the two

highest frequencies (.2 and .4 Hz, p=.010). Control subjects showed decreasing leg gains with increasing platform frequency for the four highest platform frequencies (p=.008).

Phase

Differences in phase were observed between trunk and leg segments relative to the platform (p=.0002). Trunk segment phase, shown in Figure 3C, led the platform at lower frequencies and lagged the platform at frequencies above .1 Hz. By comparison, leg segment phases, shown in Figure 3D, were not significantly different from zero. Additionally, there were no significant differences in phase for either segment based on group although there was a significant condition x segment interaction (p=.0133) that can be seen in Figure 3C that shows slightly less negative phase angles for the light touch condition above .1 Hz.

Velocity Variability

While gain and phase characterize the postural response at the platform driving frequency, velocity variability reflects changes in body sway at all frequencies other than the driving frequency. There was a significant 4-way group x frequency x condition x segment interaction (p=.0052) as shown in Figure 3E&F.

Figure 3E shows how BVL subjects displayed a dramatic increase in trunk variability for the no touch condition at the two highest platform

frequencies (.2 and .4 Hz) (p=.045), a result that was not observed in control subjects. BVL leg variability, Figure 3F, showed a smaller, but significant increase at the highest platform frequency (p=.045). By comparison, notice that velocity variability for the control subjects did not appear significantly different for either the trunk or the legs for all platform frequencies and touch conditions.

Trunk-leg cophase and coherence

Figure 4A-C shows the cophase, magnitude squared coherence, and complex coherence that describe the dynamic relationship between trunk and leg segments averaged across all platform frequencies. BVL and control subjects showed a similar in-phase coordinative relationship between the trunk and leg segments for frequencies below ~.8 Hz and an anti-phase relationship for frequencies above ~1.1 Hz (Figure 4A). Note that the anti-phase relationship may be represented by either positive or negative 180 degrees.

The magnitude squared coherence in Figure 4B varied across the frequency spectrum and showed no significant condition differences. The only significant group difference occurred for the no touch condition between 2-3 Hz (compare gray and black dashed lines).

Figure 4A (shaded region) shows that there are two possible paths from the in-phase pattern to the anti-phase pattern that occur at ~1 Hz. At the transition between in-phase and anti-phase, BVL subjects appear to adopt a

legs-leading-trunk coordinative relationship (i.e. cophase goes from 0 to +180 degrees), while control subjects appear to do the opposite. In Figure 4C we show the complex form of the coherence corresponding to the frequency range defined by the shaded region shown in Figure 4A, illustrating how the coordinative relationship between the trunk and legs changes in the complex plane. Complex coherence values that lie along the positive real axis represent the in-phase relationship between trunk and legs while values that lie along the negative real axis represent the anti-phase relationship. Likewise, complex coherence values with imaginary parts that are greater than 0 represent a "legs-leading" coordinative relationship (the trunk was used as the reference in the calculation of complex coherence) while complex coherence values with imaginary parts that are less than 0 represent a "trunk-leading" coordinative patterns. Complex coherence for BVL subjects in the no-touch condition (gray dashed line) were above the real axis (i.e. the imaginary part is greater than 0) indicating that the legs are leading the trunk while shifting from in-phase to anti-phase. For the light touch condition (gray solid line), the trajectory appears to have a positive imaginary part, but in fact the group values were not statistically different from 0. A frequency-by-frequency analysis of individual values showed that three of the BVL subjects displayed a "legs-leading" coordinative relationship while the remaining two did not. In the case of the control subjects, neither condition was significantly above or below the real axis indicating that control subjects displayed neither

a “legs-leading” nor a “trunk-leading” relationship between in-phase and anti-phase coordinative patterns.

Discussion

Trunk and leg segment dynamics and their coordination during continuous surface rotations showed a number of trunk-specific and frequency-specific effects due to the loss of vestibular information.

Vestibular loss affects control of the trunk

With a rotating support surface, several important differences emerge between BVLs and controls that demonstrate the influence of vestibular information on postural control. The most striking difference was the control of the trunk. Trunk gain for control subjects showed a slight decrease with increasing platform frequency in the no-touch condition while BVL subjects showed a large increase in trunk gain for the same condition. Unlike trunk gains, leg gains for all platform conditions appeared similar in the present results, suggesting that vestibular information plays more of a role in controlling trunk sway than leg sway. Furthermore, vestibular information seemed to have a less significant effect on leg segment gains than information derived from the platform, suggesting that control of the legs is affected by somatosensory information from the support surface to a much greater degree than other forms of sensory input.

These results are consistent with the conclusions of studies that have linked trunk control to vestibular sensory information (Buchanan & Horak 2001-2002, Horak & Hlavacka 2001). Horak and Hlavacka (2001) found that body sway induced by 3 sec galvanic pulses caused greater increases in trunk sway than in center of mass sway. Buchanan and Horak (2001-2002) found that although BVL and control subjects behaved in a similar manner at low frequencies of platform translations by riding the sinusoidally oscillating platform, their postural strategies differed at higher frequencies. The present results similarly show that as the frequency of surface rotation increased, healthy subjects oriented their trunks in a stationary position in space while their legs moved with the platform underneath them, whereas, BVLs continued to follow the platform with both the trunk and legs, often resulting in a fall or temporary loss of stability. Such results suggest that healthy subjects use vestibular information to improve control of the trunk in space at higher frequencies, while somatosensory information from the platform is used to control the legs. BVL trunk sway was far more variable, presumably because platform somatosensory information alone was less effective for trunk control at the higher rates of velocity/acceleration.

In addition to larger gains, postural sway velocity variability increased at the highest two platform frequencies in BVLs with no touch, whereas controls showed no differences. Postural sway velocity variability measures sway power at frequencies other than the driving frequency, which is interpreted as a measure of overall postural stability (i.e., higher variability =

less stability). Loss of vestibular information clearly affects not just the response to the driving stimulus, but overall postural stability as well, primarily at higher frequencies. Semicircular canals effectively convey angular velocity information to the CNS over a broad range of frequencies (Fernandez & Goldberg 1971, Goldberg & Fernandez 1971a&b, Miles & Braitman 1980). Consequently, deficits in BVLs are observed primarily at frequencies in which vestibular information is useful for minimizing body sway.

The addition of light touch fingertip contact caused a large reduction in trunk sway for BVL subjects while the decrease for control subjects was significant, but less pronounced. Previous studies (Creath et al. 2002, Horak et al. 2002, Lackner et al. 1999) have demonstrated that light touch information can act as a substitute for sensory information in subjects with vestibular deficits. Results of the present study suggest that the benefit from light touch is primarily in trunk control. While both trunk and leg segment gains were reduced with the addition of light touch for both groups, the reduction was most dramatic for the trunk in BVLs who displayed large increases in trunk gain with increasing platform frequency.

Similar findings were observed for velocity variability with the addition of light touch in BVL subjects, which showed reductions at the two highest platform frequencies for the trunk and at the highest platform frequency for the legs. An important difference however, is that light touch had no apparent effect on velocity variability in the trunk and leg segments in controls. With a fully intact vestibular system, the benefit of light touch was observed as a

reduction in gain, but not velocity variability, at the lower platform driving frequencies, while with vestibular loss, benefits of light touch are apparent at higher platform driving frequencies as a reduction in both gain and velocity variability.

Intersegmental dynamics is affected by vestibular loss

The trunk-leg intersegmental coordinative relationship was in-phase for frequencies below ~1 Hz and anti-phase for frequencies above ~1 Hz for all touch and platform conditions in all subjects, similar to previous studies (Creath et al. 2005, Zhang et al. 2007). However, differences between the two groups occurred at the shift between in-phase and anti-phase behavior. While control subjects displayed no tendency for one segment to lead the other, the shift between the in-phase and anti-phase patterns showed a legs-leading-trunk relationship for BVL subjects for the no touch condition. When compared to the control subjects, it appears that BVL subjects are receiving all of their sensory information from the support surface, which relegates the trunk to follow the platform-driving signal via the legs. The presence of vestibular information in the control subjects has the effect of eliminating the "legs-leading" relationship perhaps because the postural control system is able to determine that the signal driving the legs and the vestibular system are one in the same and treats the stimulus as a single, synchronized signal. For the light touch condition, three of the BVL subjects displayed the "legs-leading" relationship while the remaining two appeared similar to the control

subjects, consistent with varying abilities to compensate for their vestibular loss with remaining sensory information (Buchanan & Horak 2001-2002). Not only do BVL subjects become more reliant than controls upon proprioceptive information from the support surface, but this increased proprioceptive dependence shifts the coordinative strategy to one in which the legs could be interpreted as “driving” the coordinative relationship.

The heavy reliance on proprioceptive information through the support surface may explain why BVL subjects are extremely sensitive to changes in the support surface (Horak et al. 1990). BVLs compensate for support surface translations similarly to healthy individuals when the feet are in contact with the full length of the support surface. However, on a surface that is shorter than the length of the feet, vestibular patients lose equilibrium almost immediately after a perturbation, rather than changing to a "hip strategy" as observed with healthy subjects (Horak et al. 1990). Such observations are not confined to the laboratory. Vestibular loss patients commonly relate no difficulty walking on hard support surfaces, but report discomfort maintaining normal equilibrium on compliant surfaces (e.g., grass, sandy beach) that disrupt the interpretation of somatosensory information at the feet, severely hampering their range of functional mobility.

These results are consistent with the up- and down-channeling hypothesis of Mergner and colleagues which postulates that vestibular information is transmitted down to lower body segments where it is fused with ascending somatosensory information, resulting in a transformation of

sensory coordinates that enables one to accurately estimate body position in space (Mergner et al. 1997, Mergner & Rosemeier 1998).

The present results indicate that segments close to the sensor are influenced more strongly than more distal segments. Loss of vestibular information led to deficits in trunk control but had less effect on the legs. Light touch led to more precise control of the trunk, but also had less effect on the legs. Measurable trunk gains during platform rotation indicate that somatosensory information from the platform drove the trunk motion more effectively than vestibular or light touch information drove the leg motion. Alternatively, because the platform stimulus is not purely sensory, trunk gain due to platform movement may be the result of mechanical trunk-leg coupling as well.

Conclusion

This study illustrates that the effect of vestibular loss or the addition of light touch cannot be viewed relative to single segments in isolation. The trunk and legs are biomechanically coupled and the vestibular system and light touch influences all body segments through such coupling. The larger variability observed in the trunk due to loss of vestibular function is due not only to the proximity of the trunk to the vestibular sensor but as well to its massive size relative to other segments. Joint interactions lead to segment variability that may originate from distal forces. For example, flexion at the hip may result primarily from ankle plantarflexion combined with gravitational

forces acting on the trunk (Zajac 1993). Hip motion during upright stance is necessary to stabilize the upper body segments due to forces from more distal joints and the fact that muscles in the lower limbs act at more than one joint (Kuo 1995, Zajac 1993). From this perspective, it is the effect of vestibular loss on intersegmental dynamics that we find most interesting. The sensitivity of BVL subjects to the properties of the support surface clearly emerges from their “legs-leading” intersegmental coordination strategy (see Figure 4C), resulting in the disruption of trunk segment control through interaction torques and overall loss of balance stability.

Table 1 Characteristics of the Vestibular Deficient Subjects

(Data provided by R.J. Peterka)

Subject	BVL1	BVL2	BVL3	BVL4	BVL5	Normal
Gender	m	m	f	f	m	n/a
Age	70	47	54	53	50	n/a
Duration of Loss (months)	22	60	49	27	24	n/a
Cause of Loss	ototoxic	ototoxic	idiopathic	ototoxic	ototoxic	n/a
HVOR Sensitivity[a] (sec)	0.029	0.396	0.0	0.193	1.37[b]	>6.0
Pitch VOR Gain	0.029	0.11	0.0431	0.07	b	>0.4
Yaw VOR Gain	0.061	0.14	0.04	0.22	0.45	>0.43
OVAR Amplitude (deg/s) (dynamic otolith)	3.75	5.21	1.98	1.69	b	>3.52
Ocular Counter-rolling (deg) (static otolith)	2.65	5.05	1.29	3.29	b	>9 deg

a HVOR sensitivity calculated from 100 deg/s velocity step stimulus. Equal to the area under slow phase eye velocity exponential decay curve.

b HVOR sensitivity for BLV5 was calculated (product of VOR gain constant and time constant, Gc*Tc) from values derived from sum of sines stimulus.

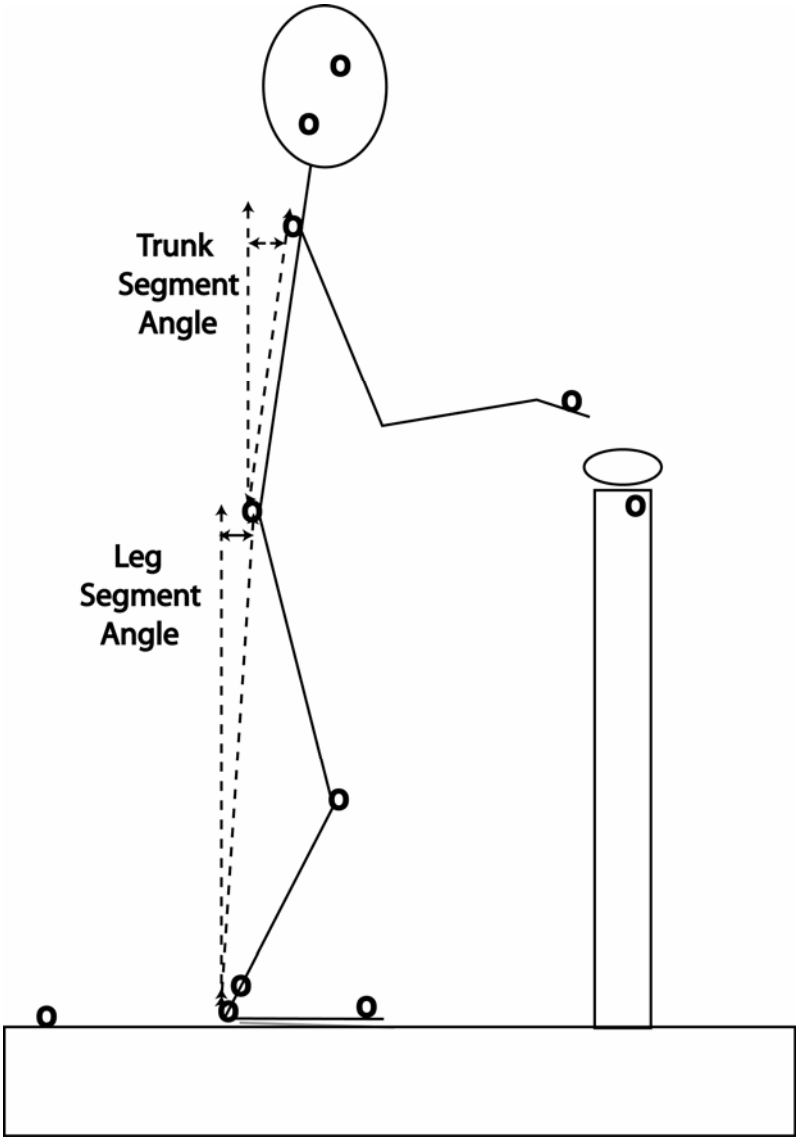

Figure 1 Sagittal view of a subject in a side-by-side stance on the force platform with their right index finger positioned above touch surface. Trunk and leg segment displacements were defined as the angular displacement with vertical. "o" designates placement of kinematic markers.

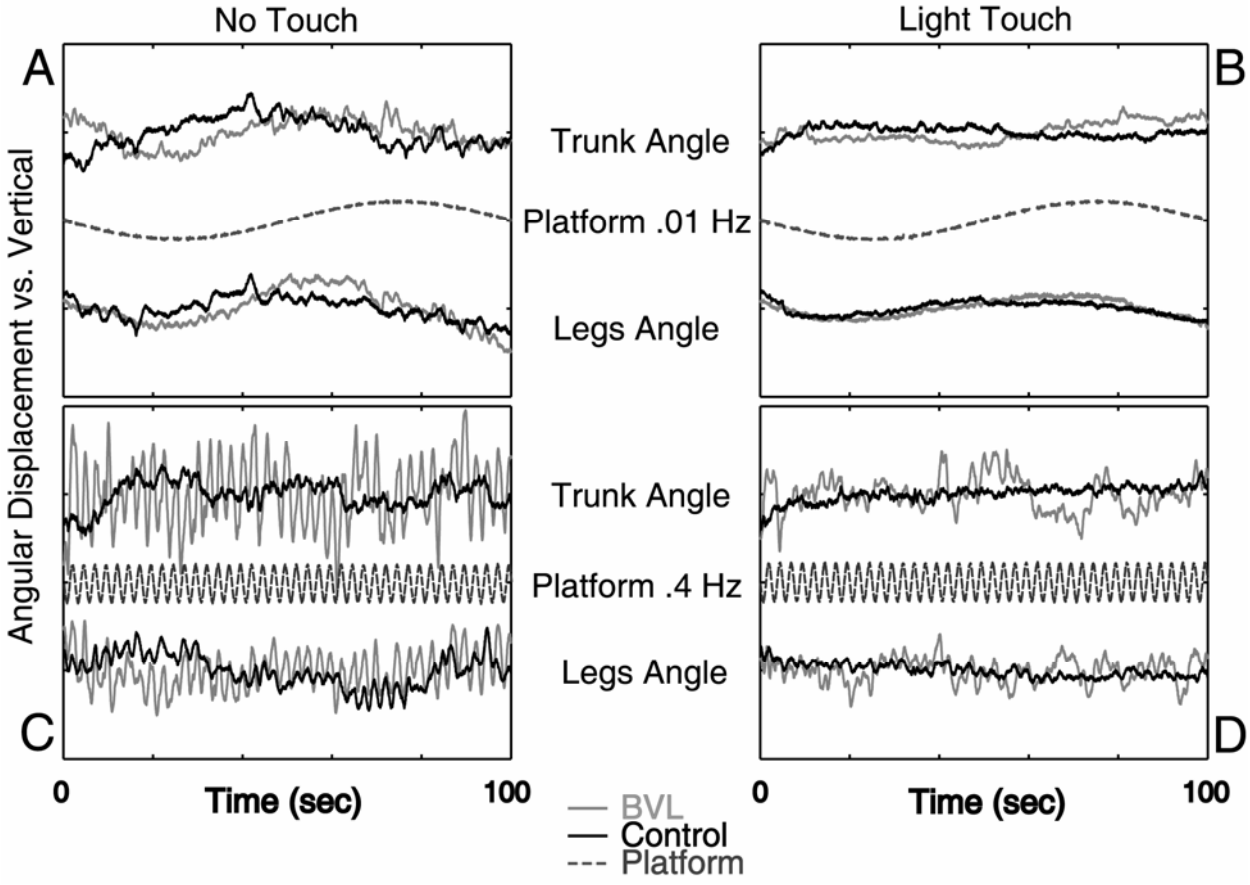

Figure 2 Exemplar time series for a BVL subject (gray) and their age/gender matched control (black). A and C show trunk segment, leg segment, and platform trajectories for the no-touch condition for the .01 Hz (A) and .4 Hz (C) platform conditions while B and D show the light touch condition. The platform amplitude was ±1.2 degrees in the A-P direction.

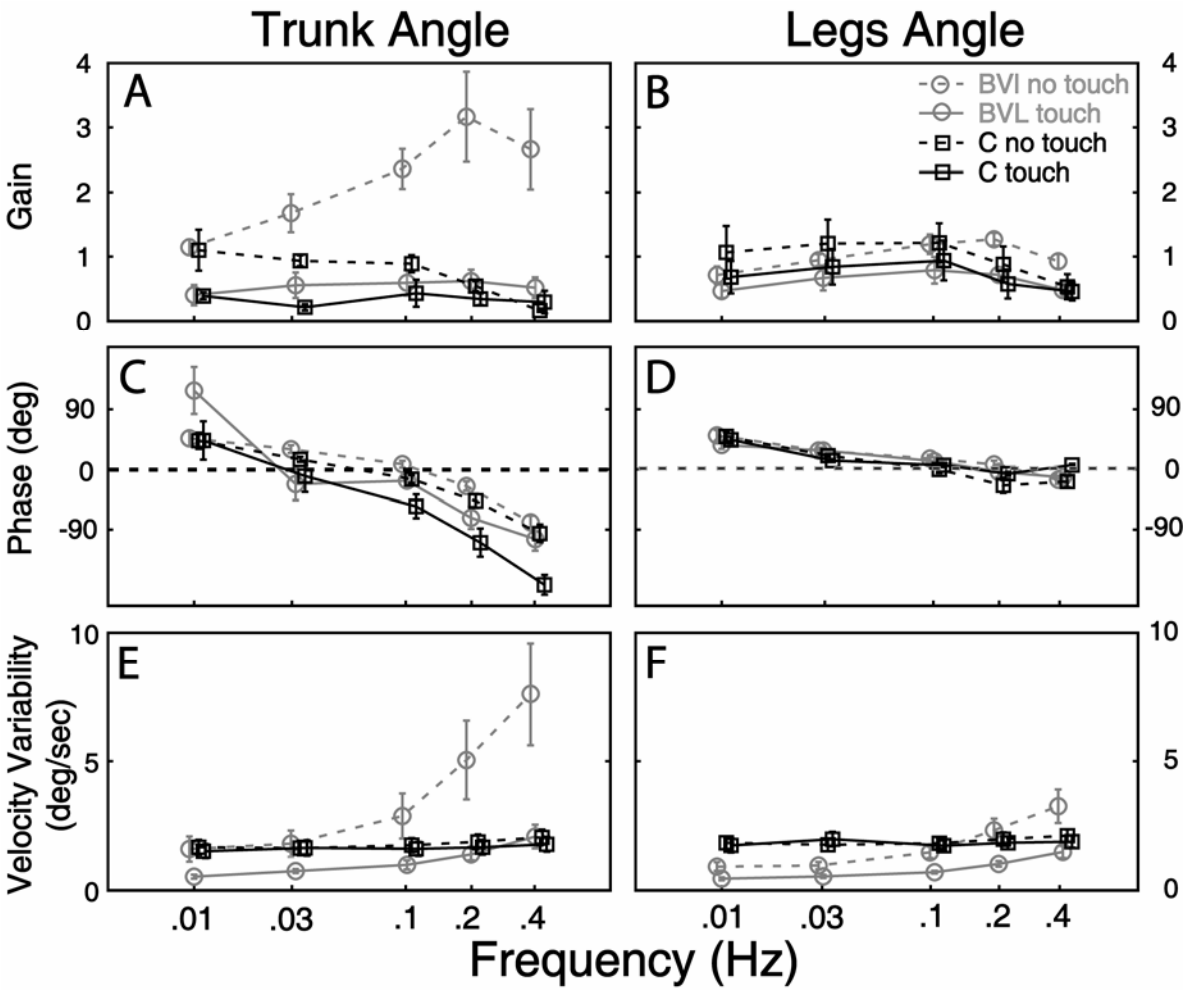

Figure 3 Trunk and leg segment averages for gain (A&B), phase (C&D), and velocity variability (E&F) for BVL (gray) and control subjects (black). Error bars = standard error (all plots).

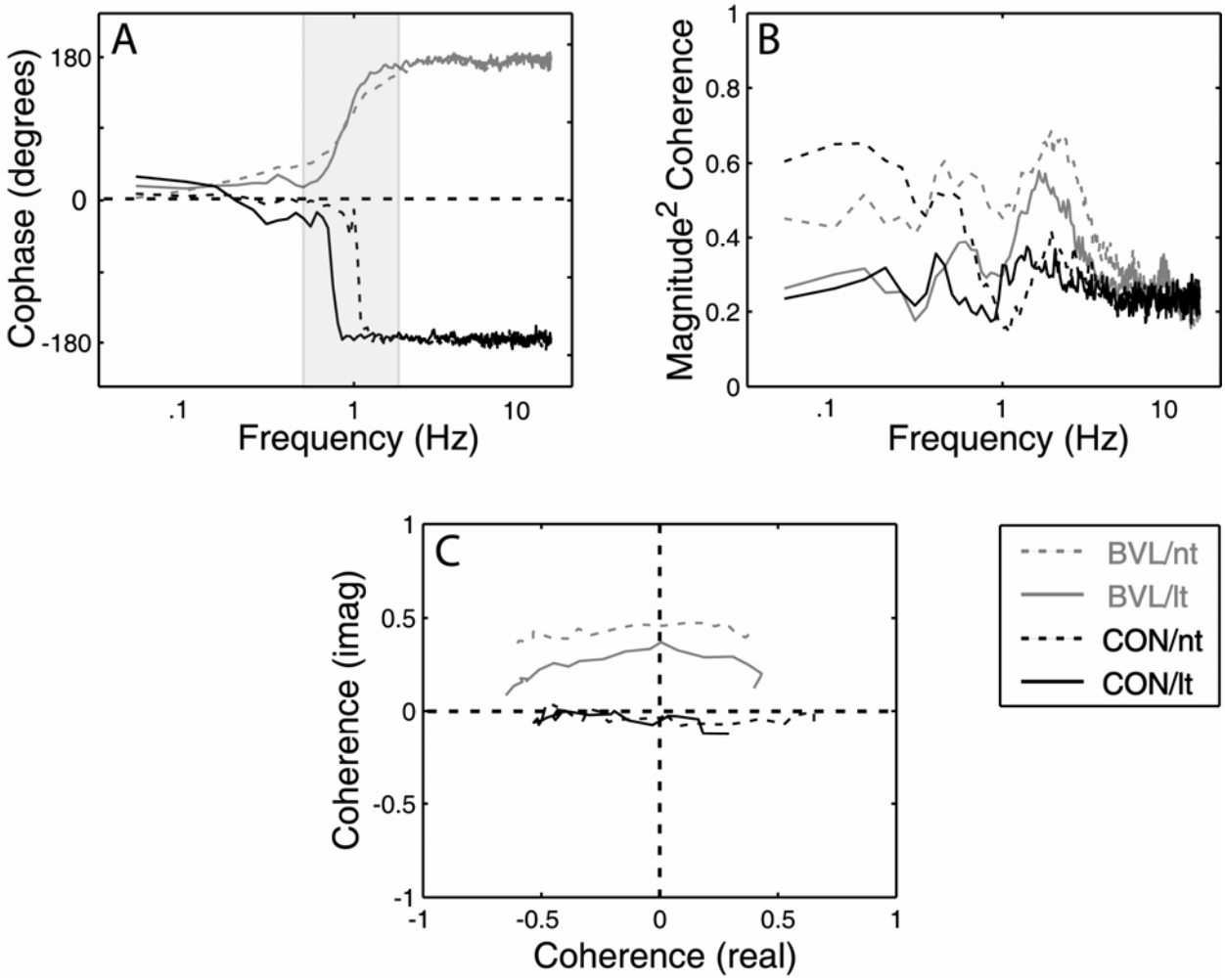

Figure 4 Cophase (A), magnitude squared coherence (B), and complex coherence (C) between trunk and leg segments for BVL (gray) and control subjects (black). Shaded region in A corresponds to comparisons shown in C.

Part III. Experimental proposal

Chapter 7

Recent experimental developments

The focus of this proposal is to understand sensory-related changes in two-segment dynamics on a sway-referenced support surface. The proposed experimental methods will utilize moving visual and support surface stimuli, with and without a sway-referenced support surface. Recent experimental developments have suggested that several important questions should be addressed. In this chapter I review the results of recent experiments that provide relevant insight into the motivation behind this proposal.

Experiment 1: Active and Passive Neuromuscular Contributions to Postural Control during Sway-Referencing

The first study looked at sway-referencing 15 healthy subjects (8m/7f) for two visual conditions, eyes open and eyes closed, and four platform conditions. The purpose of the experiment was to understand the coupling between body sway and movement of the support surface and to understand the coordinative relationship between the trunk and leg segments during sway-referencing.

The visual scene for the eyes open condition was a geometric grid consisting of vertical and horizontal lines. The four platform conditions were: 1) Fixed (stationary) surface; 2) Sway-referenced (SR) surface to subject's

hip (see Figure 1); 3) 10-frequency sum-of-sines (SOS) AP platform rotations; 4) Combined sum-of-sines and sway-referenced platform rotations (SR+SOS). The SOS platform stimulus consisted of 10 sinusoids of various frequencies between .024 and 2.96 Hz. The frequencies were determined from a sequence of prime numbers divided by 125. Amplitudes were determined by taking the inverse of the frequency and multiplying by .025. The purpose of this approach was to minimize harmonic effects in the resulting body sway of subjects. Two trials of 260s were conducted for each condition for a total of 6 trails (eyes open) and 8 trials (eyes closed). Measures included trunk and leg segment angular displacements, transfer function, power spectral density, and complex coherence.

Figure 2 shows power spectral density (PSD) plots of both visual conditions for trunk and leg segments. Spectral power decreases with increasing frequency for all visual and platform conditions. Subjects entrained their body sway to the driving stimulus as can be seen by the visible peaks in the PSD for the SOS conditions. Peaks are visible at low frequencies for the SR+SOS condition, but not for higher frequencies, suggesting that entrainment of trunk and leg segments to the driving stimulus was less pronounced for this condition.

The transfer function was determined in order to see more clearly the effects of the driving stimulus at each of the SOS frequencies. Figure 3 shows gain and phase values for the SOS and SR+SOS conditions. In general, gain showed an increase from the lowest SOS frequencies to a

maximum point in the range of .584-.904 Hz (6^{th} and 7^{th} SOS frequencies) after which it decreased for both segments. The addition of SR to SOS caused a decrease in leg gain, but not trunk gain for both visual conditions. Adding vision caused a decrease in trunk and leg gains for the SOS condition, but not for the SR+SOS condition.

Figure 4 shows the complex coherence between trunk and leg segments. The complex form of the coherence illustrates how the coordinative relationship between the trunk and legs changes in the complex plane. Complex coherence values that lie along the positive real axis represent the in-phase relationship between trunk and legs while values that lie along the negative real axis represent the anti-phase relationship. Likewise, complex coherence values with imaginary parts that are greater than 0 represent a "legs-leading" coordinative relationship (the trunk was used as the reference in the calculation of complex coherence) while complex coherence values with imaginary parts that are less than 0 represent a "trunk-leading" coordinative patterns. The real part of the complex coherence showed no differences due to visual or platform condition, but the imaginary part did showed a legs-leading–trunk coordinative relationship between the trunk and leg segments for all moving platform conditions.

A unique aspect of this study was the combination of a sway-referenced support surface while incorporating a 10-frequency driving stimulus. Sway-referencing is believed to cause an increase in body sway by eliminating or degrading proprioceptive information that is normally obtained

through ankle flexion due to body sway. The unexpected result was the small drop in gain that occurred when SR was added to SOS (compare SR and SR+SOS gains in Figure 2). If SR was effective at eliminating proprioception, then the expected gain drop would have been larger. A possible explanation is that the mechanical component of sway due to contact with support surface contributed to the higher than expected gains or that sway-referencing is less effective at reducing proprioception than previously thought.

The legs-leading-trunk relationship seen in Figure 4 suggests that subjects are relying on platform information which is then up-channeled to the trunk causing the trunk to lag behind the legs. While this explanation makes sense for the SOS and SR+SOS conditions, it does not for the SR condition since removing proprioception would make the up-channeling of support surface information less effective. This result should be compared to the results of Chapter 6 which showed that subjects with bilateral vestibular displayed a legs-leading-trunk coordinative relationship when standing on a support surface that rotated sinusoidally in the AP direction. Lacking vestibular information, the vestibular loss subjects were only able to obtain information from the support surface making trunk position dependent on information transmitted from the platform via the leg segment. Consideration should be given to the possibility that the platform motion is driving the leg-leading pattern, but given that the subjects of the present experiment had available vestibular information and that the pattern was observed during

sway-referencing, adopting a legs-leading strategy when available proprioceptive information has decreased is counterintuitive.

Experiment 2: Sway-referencing vision

The second study consisted of a sway-referenced visual scene. This experiment tested three healthy subjects, one male and two female between the ages of 20 and 21. The purpose of this experiment was to see if sway-referencing using a sensory modality that provided only a neural (visual SR), but not a neuro-mechanical stimulus (support surface SR) affected posture in an effort to understand how trunk and leg segment sway behaves for the two components.

Subjects stood on a fixed support surface within a visual virtual reality environment consisting of three rear-projection screens (front, left, and right screens). The visual scene consisted of a random array of white triangles projected onto a dark background with the subject approximately 1.5 meters from the front screen and equidistant from the side screens. The area on the front screen that corresponded to the subjects' central field vision was without triangles (see Figure 5). A computer-controlled system was used to produce a moving visual scene commonly referred to in the postural control literature as the "moving room paradigm" (Oie et al., 2005). The computer-controlled system was used to produce three moving visual scenes: 1) Stationary; 2) 10-frequency SOS; 3) Sway-referenced (SR) to subject's hip so that the visual scene moved in proportion to the subject's sway; 4) Combined

SR+SOS. The SOS stimulus was as described in experiment 1 above. Trial length was 260 seconds.

Figure 6 shows PSD plots for trunk and leg segments for all four visual conditions. The distribution of spectral power shows a pattern similar to that seen for support-surface sway-referencing in experiment 1, i.e. the power decreases with increasing frequency. Unlike the support-surface experiment, peaks due to the driving stimulus are not visible in the power spectra.

The transfer function can be seen in Figure 7. Gains for the trunk and legs show an increase with increasing platform frequency to a maximum value of .4 corresponding to an SOS frequency of .3 Hz after which they decrease. Trunk and leg gains appear to be similar for the 4 lowest frequencies. At higher frequencies the SR+SOS condition has lower leg gains at all frequencies except for .344 Hz. Phase angles show no segment or conditions differences.

Figure 8 shows cophase, and magnitude squared coherence between trunk and leg segments. Cophase (upper left plot) shows an in-phase coordinative relationship between the segments until approximately 1 Hz where it switches to anti-phase (-180 degrees). Note that the transition to anti-phase results in all conditions switching to -180 degrees. Magnitude squared coherence (MSC) shows values of approximately .5 indicating a moderate in-phase correlation between the segments. At a frequency of approximately 1 Hz, the MSC drops to about .1 after which it increases to .5 indicating a moderate anti-phase correlation pattern between segments.

The transition from in-phase to anti-phase cannot be assessed from the cophase alone. It is necessary to consider the MSC at the transition frequency. If the MSC is zero, then the transition is undefined. The nonzero values shown for MSC at the transition frequency indicate that the coordinative relationship at the transition frequency is defined as trunk-leading-legs.

The lack of any condition or segment differences in the PSDs is not surprising given the small number of test subjects. Differences in gain at the higher SOS frequencies show a frequency related vision effect for both segments. This result should be compared to the support-surface experiment (exp. 1 above) which showed condition differences in gain at lower frequencies, but none at higher frequencies. Cophase and MSC show a trunk-leading intersegmental relationship. Again referring to the support surface experiment, the results for these two experiments suggest that the source of sensory information plays a role in determining which segment leads the other. In the case of the support surface, sensory information originates from the support surface and is transmitted to the subject's leg segment while in this experiment visual information affects the trunk.

Experiment 3: Measuring Loop Gains during Human Balance Control (Elahi et al. 2006)

In an experiment by Elahi et al., (2006) the authors presented a feedback control system consisting of a single input-single output (SISO),

closed-loop model. The purpose of this model was to illustrate the functions of the plant, defined as muscle and body dynamics (see boxes A_1 and A_2 in Figure 9), and feedback within a closed-loop system (see boxes labeled B in Figure 9). Following the method of Fitzpatrick et al., (1996), Fourier transfer functions were determined which represented subsets of the closed-loop process that illustrated the function of the plant by mapping the visual driving stimulus to EMG muscle activity and the visual driving stimulus to trunk and leg segment sway displacement angles. Next, dividing the vision-to-sway angle transfer function by the vision-to-EMG transfer function they were able to obtain the open-loop transfer function, EMG to sway angle for the plant.

EMG and sway angle displacement measurements were taken on 18 subjects while standing quietly in a visual virtual reality environment that displayed a 10-frequency sum-of-sines driving stimulus. Transfer functions were determined as described above and the open loop transfer function of the plant was determined. Figure 10 shows an exemplar transfer function for visual scene to EMG (top), visual scene to sway angle (middle), and EMG to sway angle for the soleus muscle. Similar results were presented for other muscle-sway relationships.

The authors came to three important conclusions. First, the experimental evidence was consistent with a linear plant. Second, the results agreed with those of Fitzpatrick et al., (1996) for a non-mechanical sensory perturbation (Fitzpatrick used a galvanic vestibular perturbation), and third,

phase differences between trunk and leg segments suggested that a single-joint model was inadequate for assessing posture.

Figure 1

Experimental Apparatus:

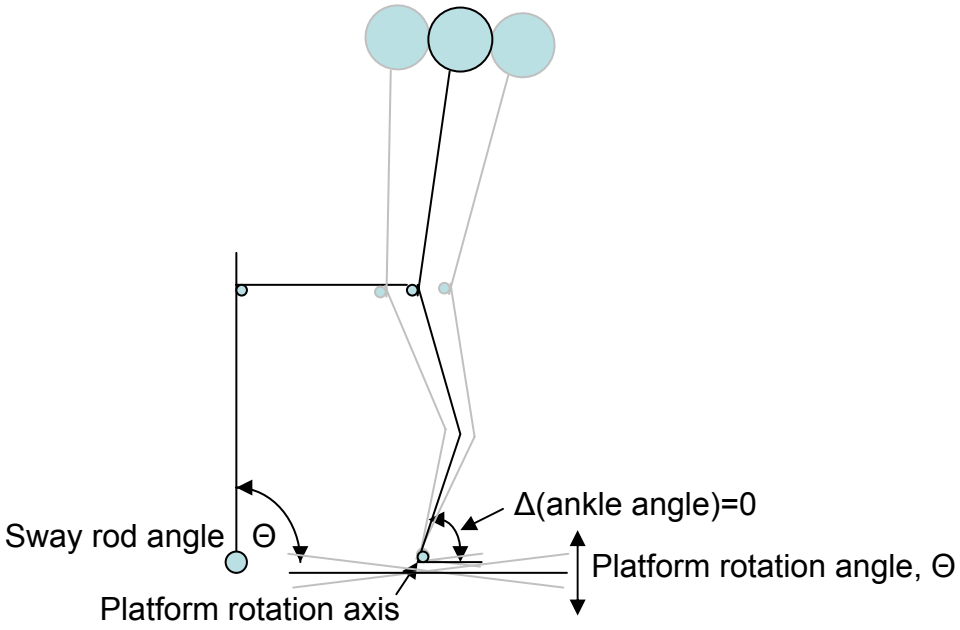

Figure 2

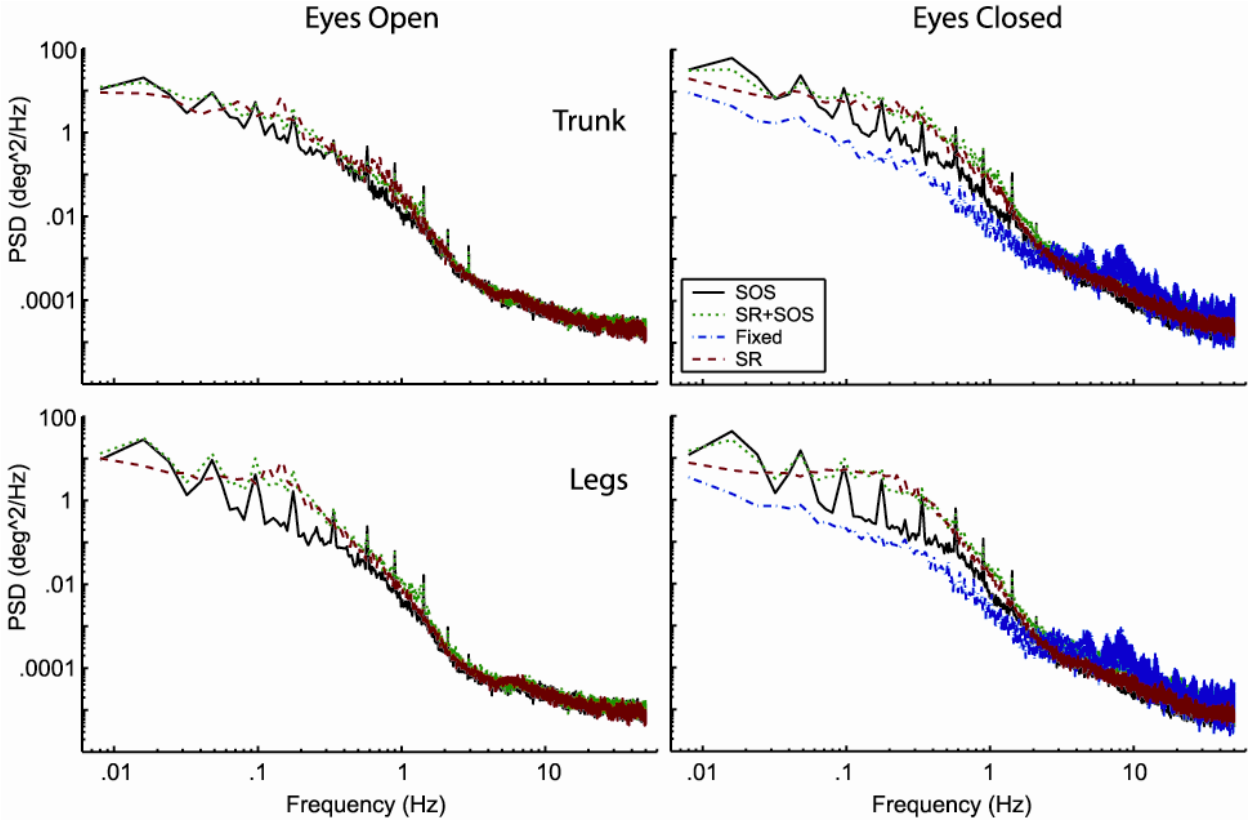

Figure 2 shows power spectral density plots for trunk (top) and legs (bottom) for the eyes open (left) and eyes closed (right) sensory conditions.

Figure 3

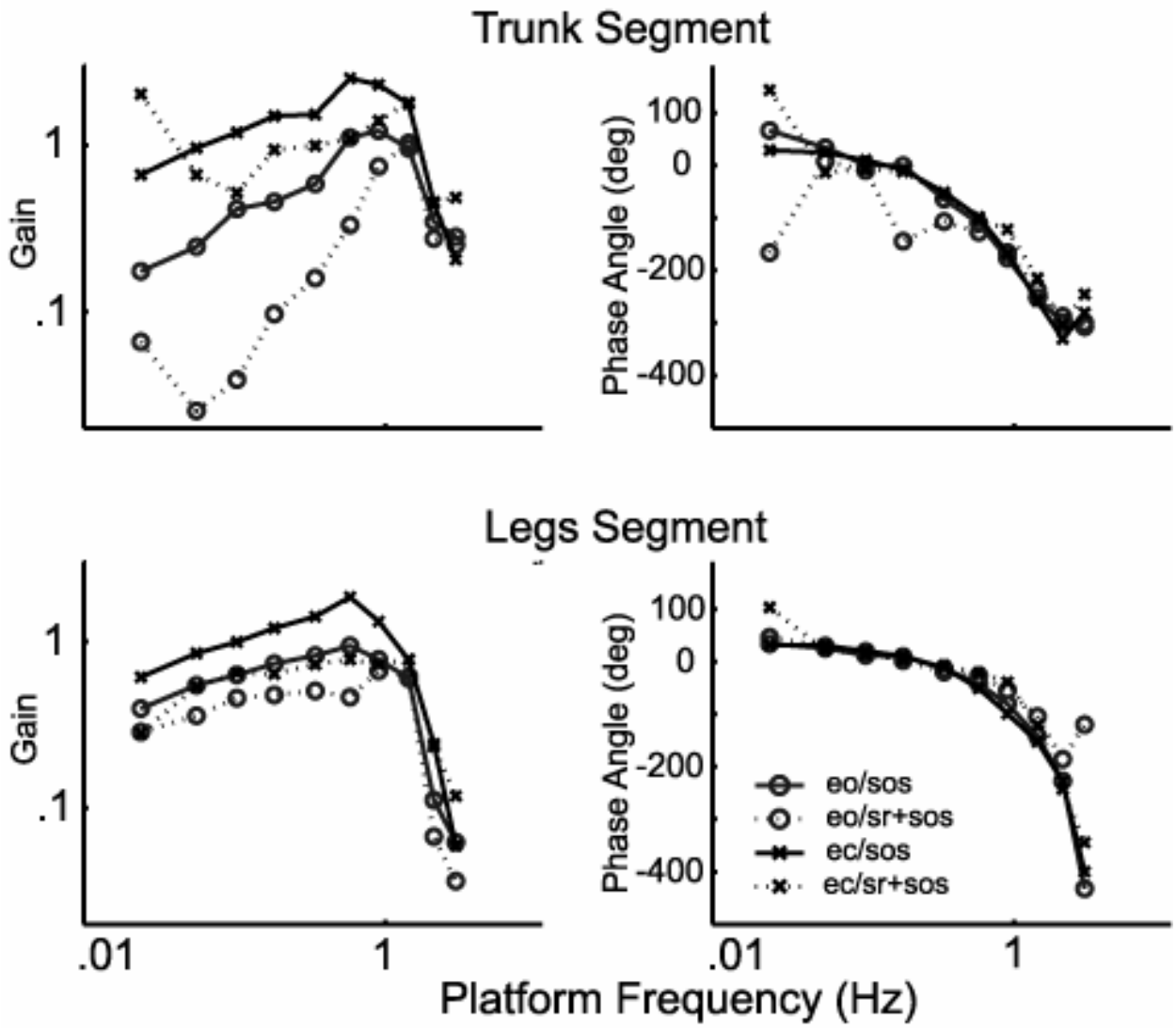

Figure 3 shows gain and phase plots for trunk and leg segments for two visual conditions, eyes open and eyes closed, and two platform conditions, sum-of-sines (SOS) platform rotations and combined sway-referencing and sum-of-sines (SR+SOS) platform rotations.

Figure 4A

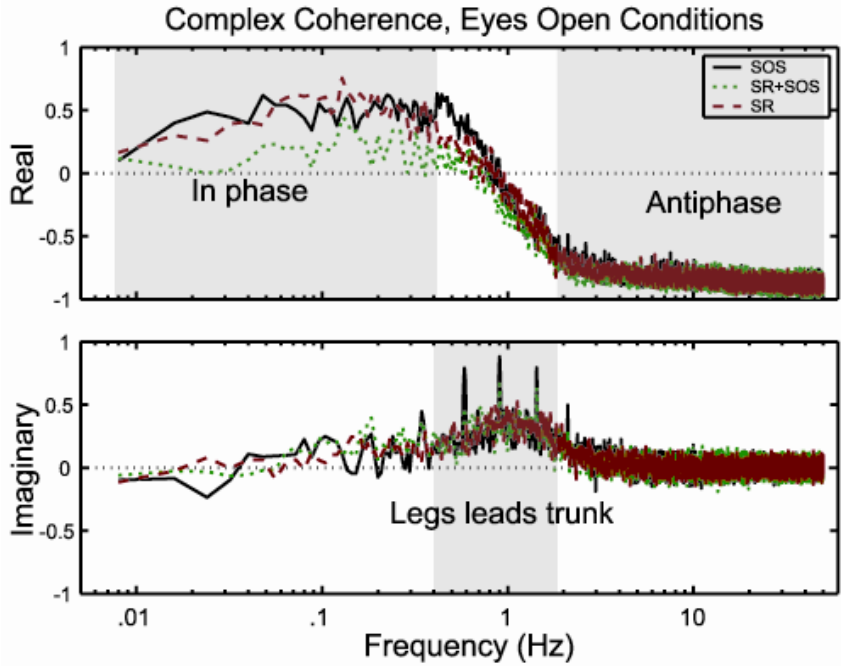

Figure 4B

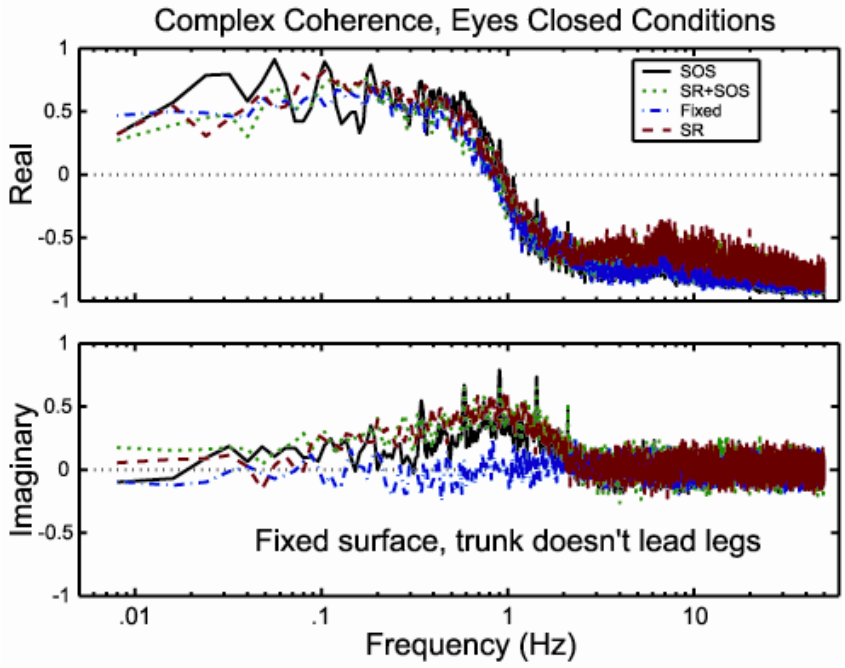

Figure 4 shows the real and imaginary parts of the complex coherence for the eyes open (A) and eyes closed (B) conditions.

Figure 5

Figure 5 Visual virtual reality environment during a sway-referencing experiment.

Figure 6

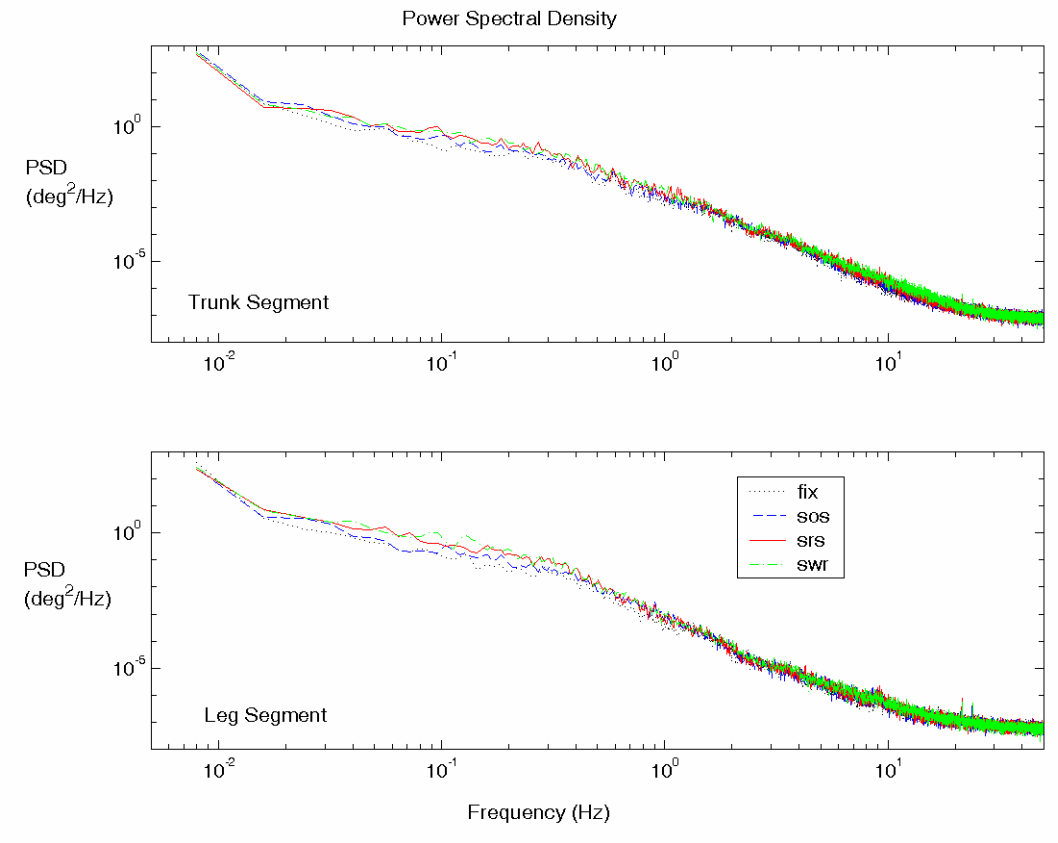

Figure 6 Power spectral density plots for trunk and leg segments for the visual sway-referencing experiment. The four sensory conditions were stationary visual display (fix), sum-of-sines driving stimulus (SOS), combined sway-referencing with sum-of-sines (SRS), and sway-referenced (SWR).

Figure 7

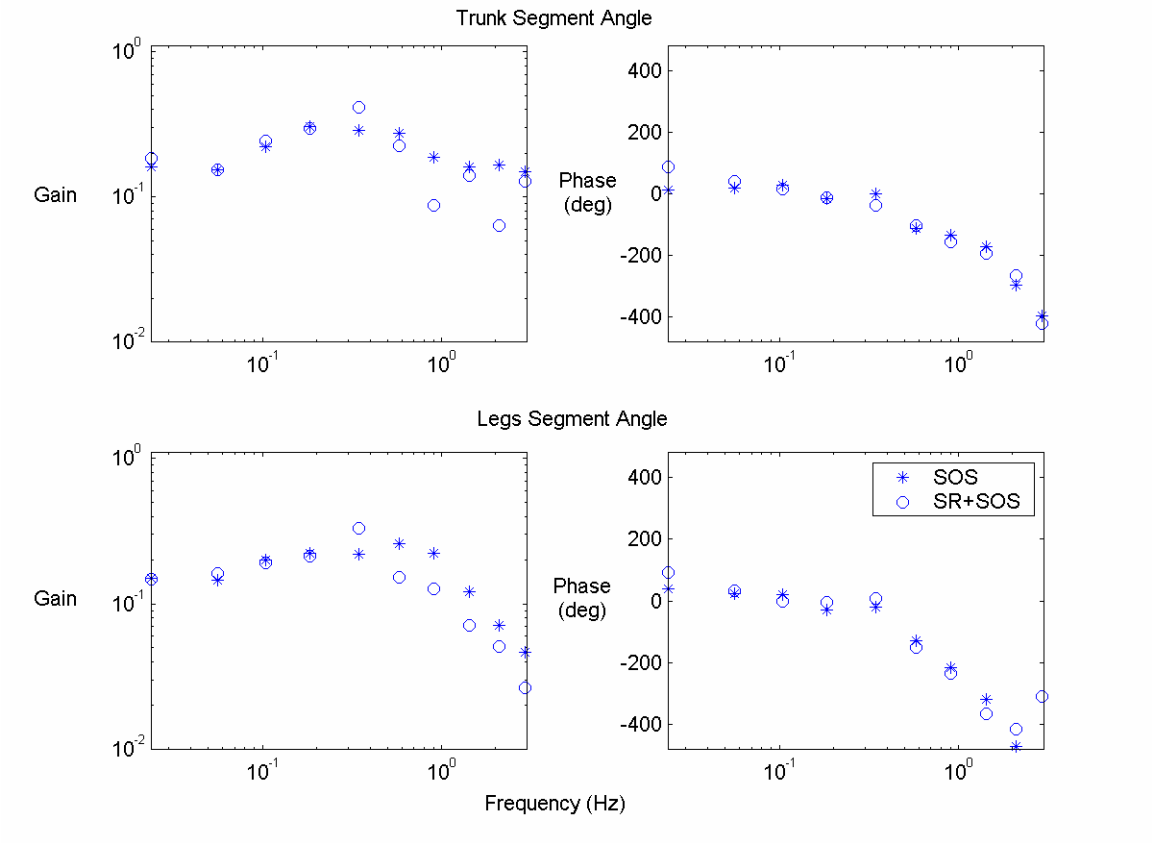

Figure 7 Gain and phase plots for trunk (top) and leg (bottom) segments for the visual sway-referencing experiment

Figure 8

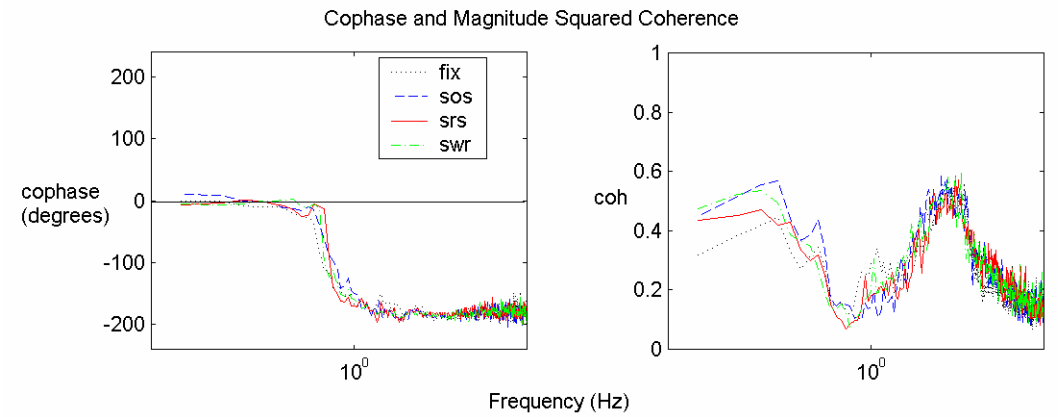

Figure 8 Cophase and magnitude squared coherence between trunk and leg segments. The four sensory conditions were stationary visual display (fix), sum-of-sines driving stimulus (SOS), combined sway-referencing with sum-of-sines (SRS), and sway-referenced (SWR).

Figure 9

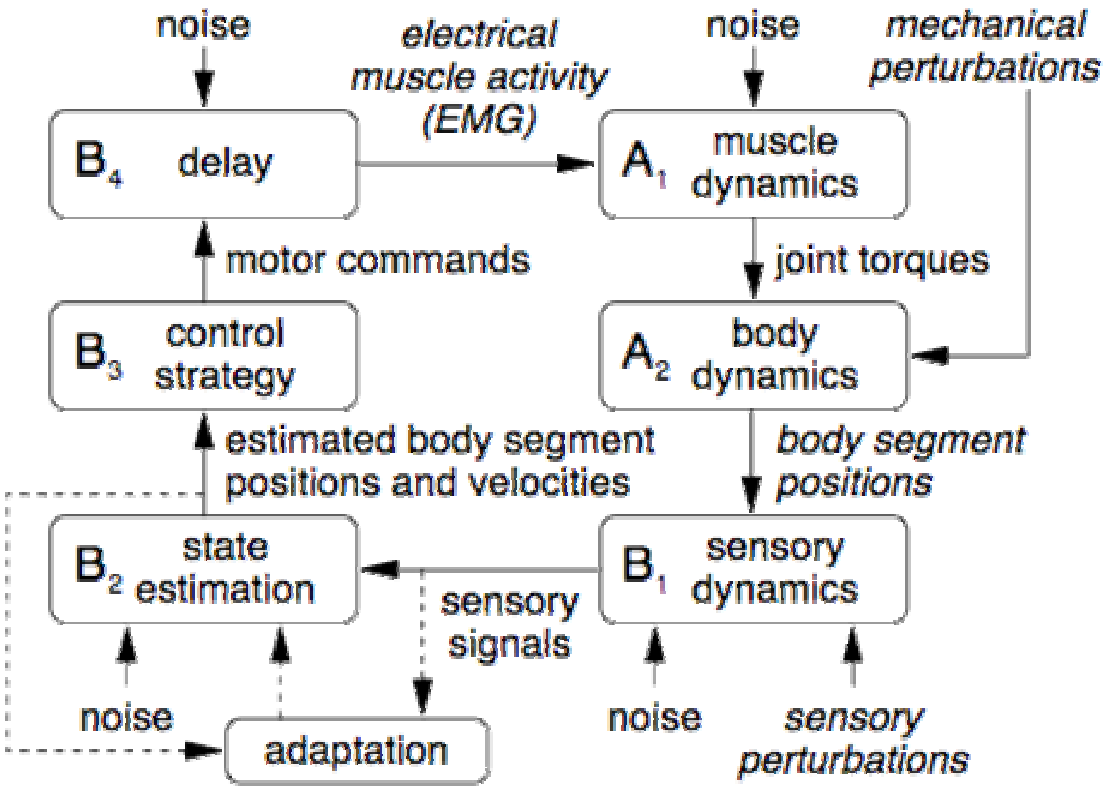

Figure 9 Closed-loop feedback control system described by Elahi et al., (2006). The plant is designated by blocks labeled A while the feedback loop is designated by blocks labeled B.

Figure10

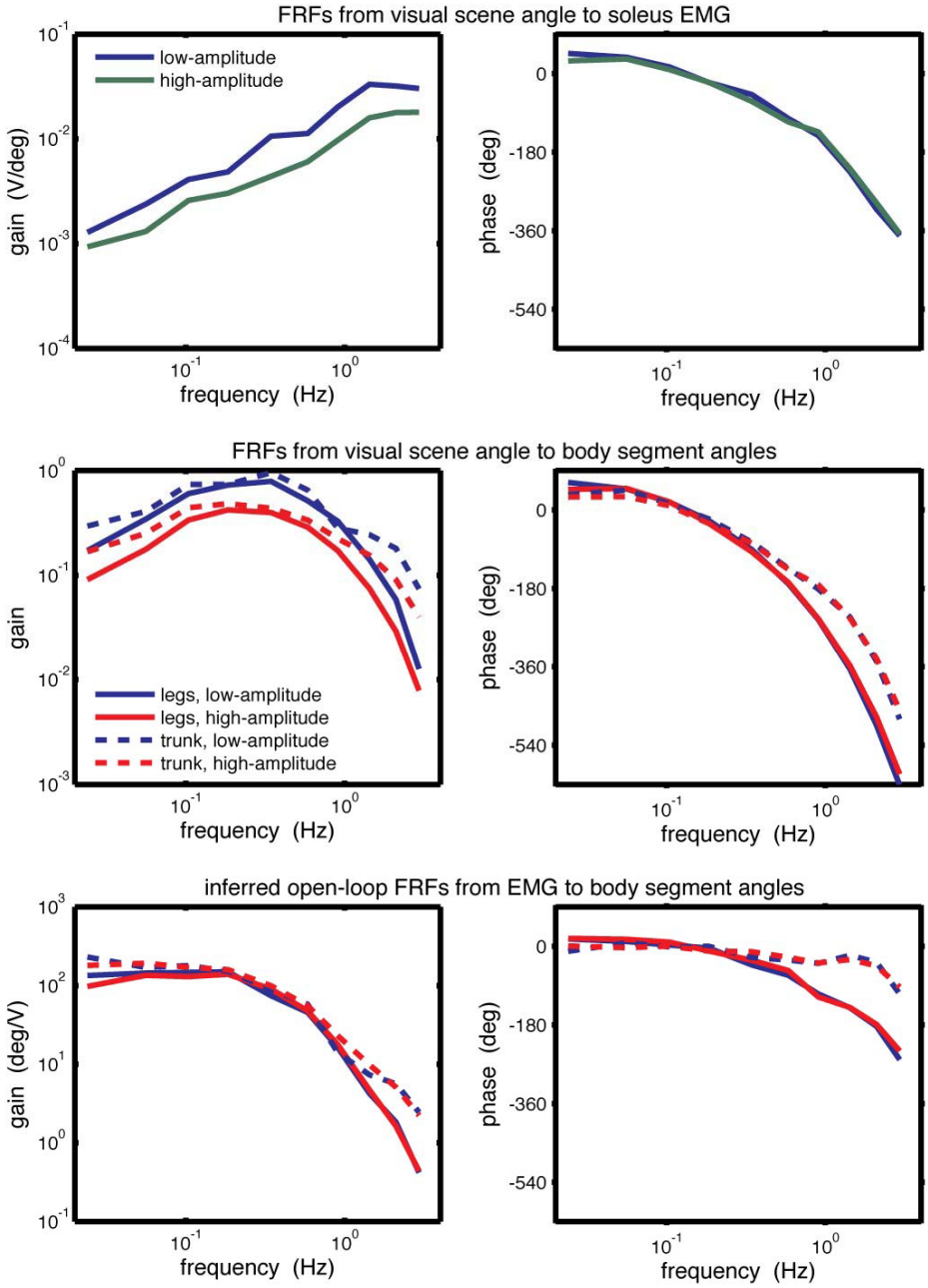

Figure 10 Exemplar plots showing the gain and phase of vision-EMG (top), vision –sway (middle), and EMG-angle (bottom) transfer functions for trunk and leg segments.

Chapter 8

Proposed Experiment

Introduction

Experimental results discussed in previous chapters suggest that determining whether a different postural strategy has been adopted in response to a change in sensory information is not straightforward. For example, the experiment in Chapter 6 compared trunk and leg segment sway between vestibular loss subjects and healthy controls while standing on a platform that rotated sinusoidally in the AP direction. We interpreted the increase in trunk gain for the vestibular deficient subjects as evidence that vestibular information is used to selectively control the trunk. However, similar gains between subject groups for the leg segment suggested that vestibular information was not used in the leg-segment control strategy. It's likely that evidence of a definitive leg control strategy was inconclusive due to the small number of vestibular subjects.

Evidence of vestibular influence affecting leg segment control can be seen in a study by Allum et al., (1994). In this study the authors compared vestibular deficient subjects with healthy controls using two different types of platform perturbations, rotations and translations. EMG results showed similar patterns for both groups, but the vestibular subjects showed greatly increased EMG activity in muscles that control the trunk and reduced activity

in muscles of the legs, a result that enabled the authors to claim 100% accuracy in predicting vestibular loss when the platform was rotated, but only 80% when the platform was translated.

The discrepancy between the results of Allum et al., (1994) and the results of Chapter 6 suggest that there is a change in leg-segment control in the absence of vestibular information, but that it's likely very small and therefore difficult to characterize. The problem that emerges is that the EMG results of Allum et al., (1994) provide evidence of a change in control strategy, but fail to characterize it.

Using EMG to understand control strategies

In an effort to understand the relationship between muscle activity and postural control, Fitzpatrick et al., (1996) devised an effective analytical approach that allowed them to separate muscle activity from reflex activity.

First, the authors assumed a simple feedback control model that consisted of a plant (muscles and load) and reflexes (feedback) (See Figure 1A).

Next, in order to observe each component in this closed-loop model, it was necessary to "break" the loop which they did by inserting two probes. The mechanical probe used to isolate the plant consisted of random forces applied by motor-spring apparatus (see Figure 2) attached to the subject's waist which pulled on the subject in order to produce a mechanical perturbation. The reflex probe consisted of galvanic stimulation to the

vestibular nerve via the mastoid processes. Inserting the probes into the otherwise closed-loop system produced two closed-loop transfer functions that consisted of perturbation-to-EMG for the reflex loop, and stimulus-to-angle for the plant loop (see Figure 1 B&C).

Finally, the perturbation-to-EMG transfer function was divided by the perturbation-to-angle closed-loop transfer function to yield the angle-reflexes-EMG open-loop transfer function, and the stimulus-to-angle transfer function was divided by the stimulus-to-EMG closed-loop transfer function to yield the EMG-plant-angle open-loop transfer function.

The experimental protocol applied the analysis to three sensory conditions for the mechanical (spring-motor) and vestibular (galvanic) perturbations, respectively (6 conditions total): 1) eyes open on a fixed surface; 2) eyes closed on a fixed surface; 3) compliant surface (platform rotation around subject's ankle joints, eyes open assumed).

The results for the reflex loop showed an increase in gain with increasing frequency while the plant loop showed a decrease in gain with increasing frequency (Figure 3A&B). Phases increased with increasing frequency for the reflex loop and decreased with increasing frequency for the plant loop (Figure 3A&B). Closed-loop gains were approximately 1 while their related phase angles showed a slight decrease (lag) from approximately 0 degrees at .25 Hz to approximately -180 degrees at 5 Hz (Figure 3C).

The inclusion of EMG in this proposal will make it possible to discern whether the plant changes with changing sensory information. This will

indicate whether sway-referencing imposes changes in the neural component of posture control or whether the observed changes in sway are the result of a change in the plant.

Two-segment analysis of posture

In another experiment by Elahi et al., (2006), which was reviewed in the previous chapter, the authors used a similar approach to isolate the open-loop transfer function of the plant. Using a visual rather than vestibular sensory perturbation, they found their results in agreement with those presented by Fitzpatrick et al., (1996). An important distinction of the Elahi et al., (2006) experiment is that the authors chose to analyze trunk and leg segment sway angles instead of center of mass sway. Their findings suggested that phase differences between trunk and leg sway angles at frequencies above 1 Hz made single-joint models inadequate for studying posture.

Further evidence supporting using a two-segment model can be found in Chapter 5 (Creath et al., 2005). To reiterate the findings of that study, the relationship between trunk and leg sway showed an in-phase relationship for frequencies below ~1 Hz and an anti-phase relationship for frequencies above ~1Hz during quiet stance. The importance of this finding is that it suggests a continuum of sway behavior between quiet stance, considered to be dominated by the ankle strategy, and the hip strategy described by Horak and Nashner (1986) for stronger mechanical perturbations. Using a two-

segment model will demonstrate how trunk and leg segment dynamics change when stimulated by neural (vision) and neuro-mechanical (platform) perturbations.

Single vs. multiple inputs

In the discussion section of their study, Fitzpatrick et al., (1996) offer insightful criticism of several possible limiting factors in their analysis. One such point the authors make is that if the system behavior is linear, then uncorrelated mechanical and sensory perturbations could be applied simultaneously. As the experiment was presented, it consisted of two single input-single output (SISO) systems. The reasons for not attempting multiple inputs were because the protocol was easier for subjects and because they felt that potential nonlinearities existed if the two stimuli had any degree of correlation. They further stated that since reflex behavior was determined separately from plant function that it was not likely that vestibulofugal drive interacted with sway-related reflex pathways, justifying the use of separate experiments for the reflex pathway and the plant. But, even when standing quietly we interact with the environment using multiple sensory inputs, and the manner in which multiple inputs affect intersegmental dynamics with the addition of sway-referencing is unknown. This proposal will address the way in which simultaneous multiple inputs affect posture during sway-referencing.

Summary of experimental goals

The purpose of this proposal is to characterize sensory-related changes in two-segment dynamics during quiet stance on a sway-referenced support surface. The experiments referenced in the introduction of this chapter suggest two specific goals.

First, by recording EMG from multiple muscles supporting trunk and leg movement, and determining the appropriate open-loop transfer functions, changes in the plant will be characterized in an effort to determine the neural and neuromechanical effects that occur when the support surface is sway-referenced.

Second, using a two-segment analysis, changes in trunk and leg segment dynamics will be characterized when stimulated by simultaneous neural and neuromechanical driving stimuli during sway-referencing.

Experimental design

Institutional Review Board

The protocol for this experiment has been approved by the Institutional Review Board of the University of Maryland, College Park. All subjects will be informed of their rights as test subjects and will provide written consent before participating.

Subjects

Subjects for this experiment will be recruited from the University of Maryland community. Subjects will be primarily, but not limited to students. Efforts will be made to ensure a diverse subject population in regard to gender and ethnic background.

Statistical power calculations from previous work has suggested a minimum of 14 subjects is needed to demonstrate condition differences in the pilot studies described in Chapter 7. The proposed protocol combines new elements that were not tested simultaneously for which the power calculations may be inadequate. Therefore I propose testing a minimum of 20 subjects.

Apparatus

The apparatus to be used for this experiment consists of a 60cm(width) x 40cm(length) moving platform situated within a visual virtual reality environment.

The platform was constructed such that rotation occurs in the AP direction about an axis that is collinear with the subject's ankles. Platform movement is driven by a computer-actuated servomotor system (Compumotor, Parker Hannifin Corp., Rohnert Park, CA). Rotation using this system can be achieved by three means: 1) Predetermined driving signal of any desired waveform (e.g. sinusoid). The signal is generated as a text file which is read by a custom designed software program using LabView (National Instruments Corp., Austin, TX). The text signal is translated into a

voltage signal which drives the servomotor system; 2) Sway-referenced to the subject's body sway. This method utilizes a rigid hip rod attached to the subject's hip (see Figure 1, Chapter 7). Angular displacement of the subject's hip causes the rod to rotate an equivalent displacement. The resulting signal is used to drive the servomotor system in lieu of a predetermined driving signal; 3) Combined predetermined and sway-referenced driving signals. Custom circuitry allows for the two separate voltages to be summed together producing a combined signal which is then used to drive the servomotor system. The system is calibrated by adjusting voltage gain and offset in the custom circuitry in order to platform rotation that is proportional to hip rod angular displacement.

The visual virtual reality environment was constructed by FakeSpace (Marshalltown, Iowa) and consists of three rigid, translucent screens 10'(width) x 8'(height) (see Figure 5, Chapter 7). Illumination occurs from projectors located behind each screen which project images generated by a cluster of three networked computers. The computers work synchronously to produce a three dimensional virtual environment which is projected onto the screens. The image is calibrated such that the subject, standing 1.5 meters from the front screen, is at the center of the virtual environment. From the subject's perspective, each screen displays a two dimensional image of what the subject would see if they were contained in a cube. The three screens show the images that would appear to the left, right, and in front of the subject.

Safety equipment consists of a ceiling-mounted harness capable of supporting a subject's body weight that is adjusted to allow for normal body sway before the support straps become taught. Additionally, a platform system shutdown-switch located directly adjacent to the rotating platform which can be activated to immediately stop platform movement.

Data Collection

Data will be collected using an Optotrak system (Northern Digital, Waterloo, Ontario, Canada). Subject markers will be placed on the left side of the subject's body at the ankle, knee, hip, shoulder, and head (see Figure 1, Chapter 7). Platform markers will be placed on the moving and stationary parts of the platform. Collection frequencies will be 1000 Hz. Additionally, visual and platform driving stimulus signals will be collected.

Measures

Kinematics

Trunk segment angular displacement was defined as the angle formed by the shoulder, the hip, and vertical. Leg segment angular displacement was defined as the angle formed by the hip, the ankle, and vertical. Positive angles refer to forward movements from upright vertical.

EMG

EMG will used to measure muscle activity. Electrodes will be placed on the soleus, rectus abdominus, gastrocnemious, rectus femoris, tibialis anterior, biceps femoris, erector spinae using techniques described by Konrad (2005). The raw EMG signal will be collected at 1200 Hz.

EMG normalization

Measuring EMG during quiet stance is difficult for two reasons. First, quiet stance produces relatively low amounts of EMG activity and as a result, it is difficult to distinguish small changes in signal strength from noise and second, due to differences in skin conductance between subjects, the broad variance in EMG activity levels between subjects makes comparisons difficult. In order to address these issues I will employ a method to normalize each subjects EMG.

The goal of normalization is to find the maximum degree of muscle activity for a specific task, in this case quiet stance, to use as a scale in order to observe changes in muscle activity that occur during the execution of the task. If successful at determining the maximum degree of muscle activity, then the normalized activity will be between values of zero and one (normalized units of muscle activity). A subject's normalized activity can then be compared between muscles which may display different levels of activity, as well as between subjects whose skin conductance is dissimilar.

In order to find the maximum degree of muscle activity for quiet stance it is necessary to have subjects contract their postural muscles close to their limits of postural stability. Starting from an upright vertical position, subjects will lean backwards (the same approach will be employed for forward lean) with assistance from the investigator. The investigator will assist by placing their hands on or near the subject's shoulders, supporting some, but not all of the subject's body weight. Assistance is necessary for two reasons. The first reason is for safety. Although most healthy subjects probably wouldn't have trouble with a self-directed leaning task, patient populations might. It is important that this method can be applied to the entire testing population so all levels of postural stability should be considered. The second reason is that by assisting the subject, the investigator will be able to help the subject control their momentum closer to their limit of stability. Once at their maximum level of lean, the investigator will withdraw assistive support allowing the subject to remain unassisted in a stationary position for 5 seconds in order to record EMG levels for all muscles in that position. The average signal obtained for 5 seconds in the stationary positions will be used in the normalization calculations.

Procedures

The platform and visual driving stimuli will consist of a 1 degree (peak-to-peak), 60.5sec/period (.25 sec time step) pseudorandom ternary sequence (PRTS) as described by Peterka (2002). Although previous experiments

have emphasized using a 10-frequency sum-of-sines driving signal as a probe, frequency selection for simultaneous visual and platform drives would prove difficult for drives that need to be uncorrelated which can be accomplished easily by having an appropriate time lag between the two signals.

The PRTS has the benefit of producing power across the frequency spectrum. Platform and visual conditions will be as follows: 1) Fixed platform with visual PRTS; 2) Sway-referenced platform with visual PRTS; 3) PRTS platform with visual PRTS; 4) Combined sway-referenced and PRTS platform with visual PRTS.

All trials will be 242 seconds (4 x PRTS period) in duration. All subjects completed three randomized 4-trial blocks with rest periods between blocks. The total experiment will last approximately 3.5 hours. Subjects will be instructed to stand as quietly as possible with eyes open before the start of a trial.

Analysis

Kinematic Analysis

A linear systems spectral analysis will be performed on each trial by calculating the Fourier transforms of the platform, the visual driving signal and the subjects' leg and trunk angles after subtracting the mean angle. Fourier transfer functions describing the response of the leg and trunk angles to platform and visual scene movement will be calculated as the Fourier

transform of the response divided by the Fourier transform of the input at the driving frequency. Within-subject gain and phase will be calculated as the absolute value and the argument of the average transfer function across trials for each subject. Group averages will be calculated as the arithmetic and circular means respectively. A positive phase indicates that sway leads platform movement.

Power spectral densities (PSDs) and cross spectral density (CSD) will be computed for the leg and trunk angles using Welch's method with an appropriate size Hanning window using a 50% overlap.

Additionally, cophase and magnitude squared coherence will be calculated from the complex coherence, $P_{xy} \Big/ \sqrt{P_{xx} P_{yy}}$, where P_{xy} is the CSD between the trunk and legs, and P_{xx} and P_{yy} are the respective PSDs of the trunk and legs. Cophase for each subject will be calculated as the argument of the across-trials average of the complex coherence using the trunk as the reference (positive is legs leading trunk). Magnitude squared coherence for each subject will be calculated as the absolute value squared of the across trials average of the complex coherence. Group averages will be calculated as the arithmetic mean of the Cophase and magnitude squared coherence, respectively.

EMG analysis

Raw EMG data will be rectified, but not filtered. The normalized EMG signal will be calculated by dividing the raw data by the average EMG signal

determined using the normalization method described above. Stimulus-to-EMG and stimulus-to-segment sway angle Fourier transfer functions will be calculated for visual and platform stimuli. Transfer functions will be averaged across trial for each subject. The open-loop transfer function for EMG-to-sway will be determined by dividing the stimulus-to-segment transfer function by the stimulus-to-EMG transfer function. Group means will be determined by calculating the arithmetic mean across subjects.

Statistical Analysis

Statistical significance for differences in PSDs will be determined using a frequency-by-frequency comparison consisting of paired T-tests. Multiplicity of testing will be controlled by employing the false discovery method (Benjamini & Hochberg, 1995).

Values for gain and phase will be assessed using a condition (4) x segment (2) x frequency (to be determined) repeated-measures ANOVA with condition, segment and frequency as the repeated measures, averaged across the five platform frequencies to test for statistical significance. For all testing, $p<.05$ will result in rejection of the null hypothesis.

Condition differences in cophase will be tested for statistical significance using frequency-by-frequency paired T-tests. Condition differences in magnitude squared coherence will be tested for significance using frequency-by-frequency paired T-tests on the Fisher's z-transformed coherence values.

Multiplicity of testing will be controlled by employing the false discovery method (Benjamini & Hochberg, 1995).

Figure 1

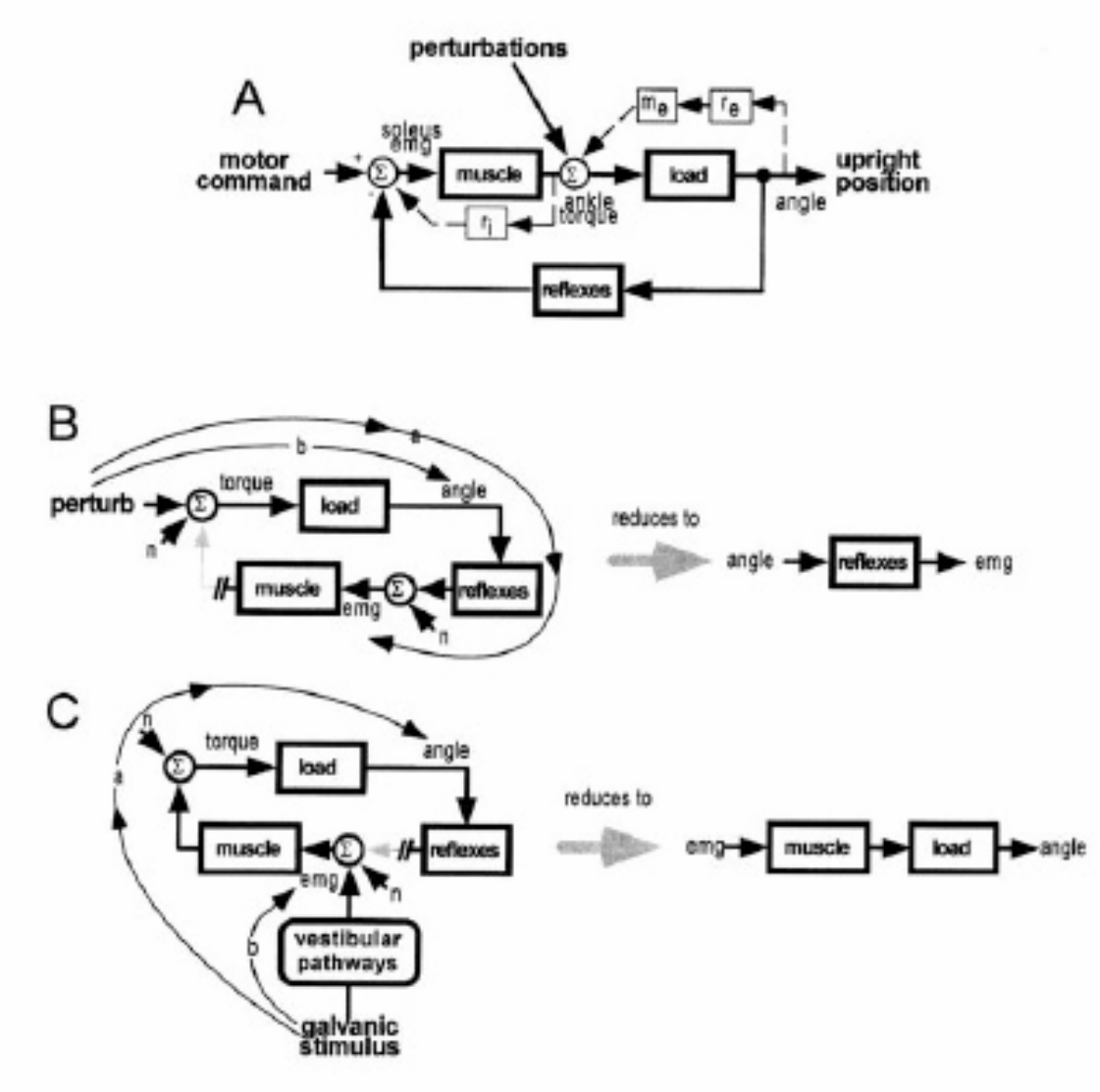

Figure 1A shows the closed-loop feedback control model described by Fitzpatrick et al., (1996). 1B shows the perturbation-to-EMG and perturbation-to-angle pathways used to determine the open-loop reflex pathway transfer function. 1C shows the stimulus-to-angle and stimulus-to-EMG pathways used to determine the open-loop reflex plant transfer function.

Figure 2

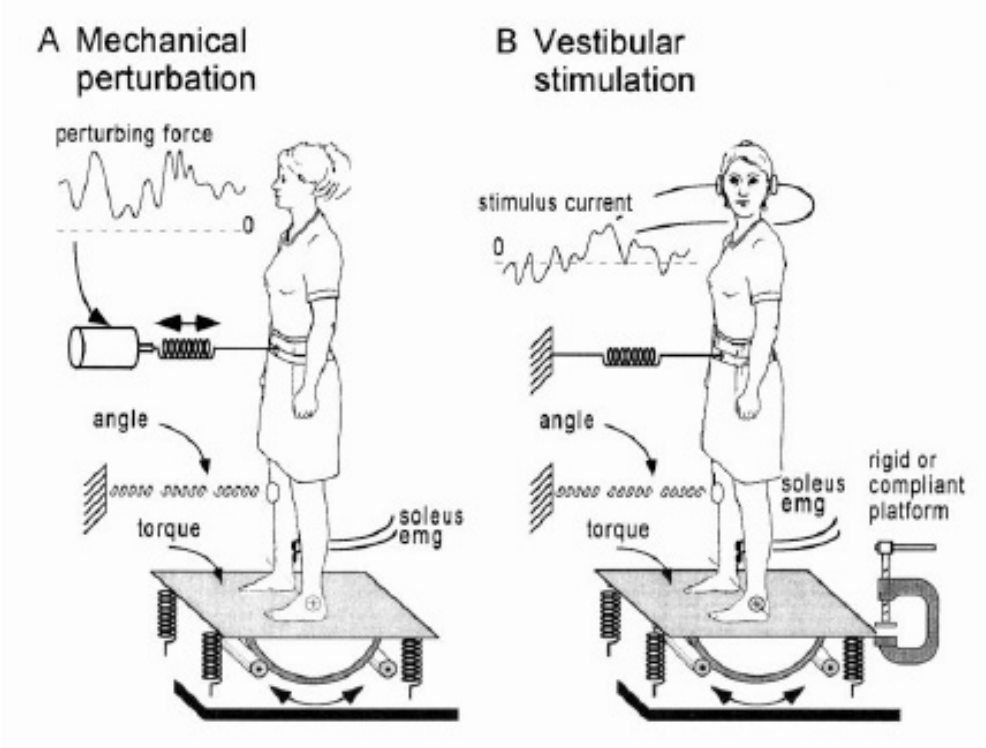

Figure 2 shows the apparatus set-up for the mechanical (A) and vestibular (B) perturbation experiments.

Figure 3

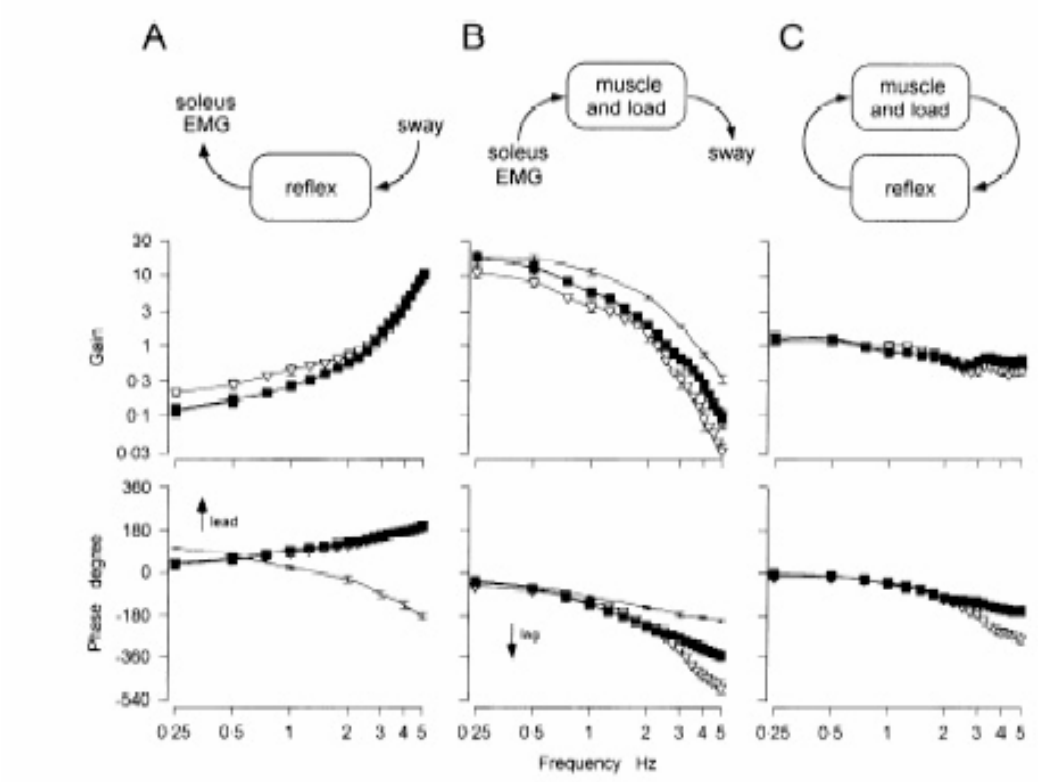

Figure 3 shows gain and phase for the reflex transfer function (A), the plant transfer function (B), and the closed-loop transfer function (C).

Figure 4 PRTS for 1 degree amplitude peak-to-peak

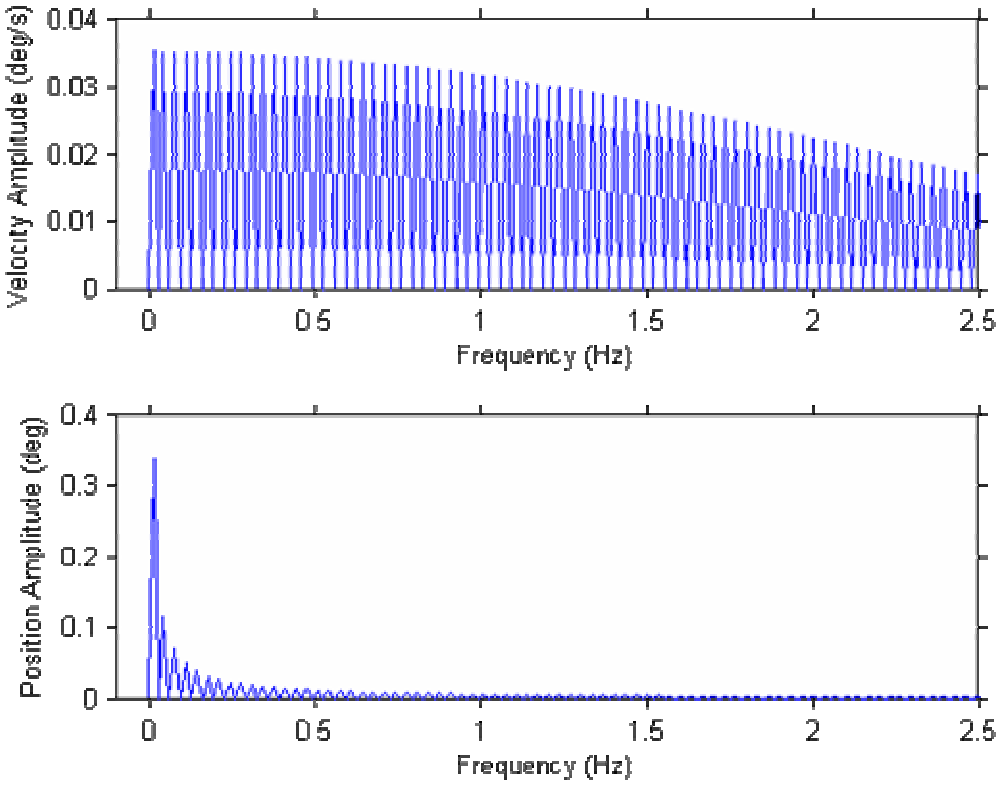

Chapter 9

Different support surface: different control system

Introduction

In its simplest form, the human postural control system can be described as a closed-loop control system consisting of a plant (i.e. body segments and musculotendon actuators) and feedback (Kiemel et al., 2008) (see Figure 1). Efforts to understand the relationship between feedback and plant are complicated by the fact that the corrective forces generated during standing posture contain both active and passive components which result from the neural activation of muscle due to feedback and the viscoelastic properties of musculotendinous tissue respectively. When applied to an everyday task such as standing in a stationary position, separating the plant and feedback becomes a difficult, if not impossible task. As postural corrections are made, changes in muscle activation alter the magnitude of the active component. Similarly, changes may occur in the passive component which are dependent on neural activity, but do not require it. The problem then becomes to separate the plant and feedback components of the closed, sensorimotor loop so that the characteristics of each component can be identified. Conceptually, it should be possible to “open the loop” by eliminating sensory feedback, but maintaining upright bipedal stance is not possible in the absence of sensory information.

A clever approach to opening the loop for postural control was demonstrated by Fitzpatrick et al. (1996) who used frequency-domain system identification to estimate the open loop transfer functions that described both the plant and feedback. They accomplished this for the plant by estimating two closed-loop transfer functions between a sensory perturbation and: 1) sway angle (defined as the angular displacement of the lower leg vs vertical); and 2) the EMG signal from the soleus. Dividing the closed-loop sway angle transfer function by the closed-loop EMG transfer function mathematically cancels the feedback portion of the control loop, leaving the "inferred" opened-loop transfer function from EMG to sway angle which defines the transfer function of the plant. (Fitzpatrick et al., 1996). Here we apply this same method to identify: 1) properties of a two-segment plant during upright standing; and 2) how an experimental manipulation such as sway-referencing changes the properties of that plant.

Understanding the plant is not trivial. Fitzpatrick et al. (1996), like many, used a simplified representation for posture by measuring the angular displacement of the lower leg under the assumption that the perturbations they imposed were small enough that they would not elicit a hip strategy (Horak and Nashner, 1986). Their approach reflects the common view that a single-joint model rotating about the ankle approximates upright stance unless a large perturbation elicits an anti-phase coordinative relationship between the trunk and legs (i.e., a hip strategy) (Horak and Nashner, 1986).

However, the human body is multi-segmented and recent studies have shown that even during quiet stance, a single-joint model is inadequate.

For example, Creath et al (2005) showed that in-phase (ankle) and anti-phase (hip) sway patterns between trunk and leg segments coexist during quiet stance. Trunk/leg coordination was in-phase at frequencies below ~1 Hz and anti-phase for frequencies above ~1 Hz. In fact, these two patterns have been shown to co-exist even during perturbations (Scholz et al., 2007). Moreover, the prevalence of these patterns is influenced by available sensory information. In the Creath et al (2005) study, subjects showed an abrupt transition from in-phase to anti-phase trunk/leg coordination for fixed and foam surface conditions at approximately 1 Hz, but for the sway-referenced condition a gradual change from in-phase to anti-phase was observed. Zhang et al. (2007) showed that the frequency at which the in-phase to anti-phase shift occurred decreased with the addition of vision or light touch contact. More recently, Creath et al. (2008) demonstrated that subjects with bilateral vestibular loss (BVL) standing on a moving platform showed large increases in trunk gain with increasing platform frequency compared to control subjects, as well as a legs-leading coordinative relationship between trunk and leg segments not seen in controls. Thus, the current thinking is that the in-phase (ankle) and anti-phase (hip) patterns co-exist during upright stance, but the relative prevalence of the two patterns is modulated by perturbation, available sensory information, and task constraints.

In the current experiment a closed-loop system identification method, the joint input-output method (Fitzpatrick et al., 1996, van der Kooij et al., 2005), is used to understand trunk/leg intersegmental dynamics during sway-referencing. We seek to identify plant characteristics when proprioceptive information from the support surface is disrupted through sway-referencing or through deterministic platform motion using a visual stimulus as a probe. Because sway-referencing enjoys widespread use as a clinical and research tool (e.g. EquiTest, NeuroCom International Inc.), a better understanding of how changes in support surface characteristics affect the plant will enhance clinical and research applications.

Methods

Subjects

The experimental protocol was approved by the Institutional Review Boards of the University of Maryland and was performed in accordance with the 1964 Helsinki Declaration. All subjects gave their informed consent prior to participation in this study.

Eighteen healthy subjects, nine females and nine males (age=22.8 ±3.9 years) participated in the experiment. Subjects had no known neurological or musculoskeletal deficiencies.

Apparatus

Subjects were instructed to stand on a variable pitch platform that rotated about an axis perpendicular to the sagittal plane, as shown in Figure 2. Subjects stood in a standard parallel stance with their ankles aligned along the platform axis of rotation. Feet were placed slightly less than shoulder width apart. Platform rotation was controlled by a computer actuated servomotor system that either: 1. remained fixed in a stationary position; 2. rotated in the sagittal plane driven by a specified signal; 3. rotated in direct proportion to the subject's A-P body sway (sway-referenced) via a rigid rod attached to the subject's hip. The hip rod was connected to a potentiometer that interfaced with the platform control computer. The sway-reference function was calibrated so that an angular deflection of the hip rod produced an equivalent angular rotation of the platform.

The platform was located within a three-screen (front, left and right), rear projection virtual reality cave (Fakespace Systems, Mechdyne Corp.) such that the subject's eyes were approximately 1.1 meters from the front screen and equidistant from the side screens. Screens were 305 x 244 cm (w x h).

Motion of the visual scene

CAVELib software (VRCO) was used to generate the visual scene which consisted of 500 white 1.52 x 1.52 x 2.16 cm right triangles on a black background with random positions and orientations. The triangles were

projected onto the three screens (front, left, and right) with a 30 cm circular region excluded on the front screen directly in front of the subject's eyes (see Figure 2). The virtual position of the visual display rotated about an axis through the subject's ankles, assuming a fixed perspective point at the average position of the subject's eyes.

The visual scene angle consisted of a 10-frequency sum-of-sines function with frequencies based on prime numbers which had the form

$$v(t) = \sum_{j=1}^{10} (-1)_j A_j \sin(2\pi f_j t), \qquad A_j = A/f_j, \text{ if } j \leq 8 \text{ or } A_j = A/f_j, \text{ if } j > 8,$$

where t is time. The frequencies were (3, 7, 13, 23, 43, 73, 113, 179, 263, 367)/125. The frequencies were chosen such that the visual motion repeated every 125 seconds. Choosing frequencies based on prime numbers helped avoid low-order harmonics. Amplitudes were scaled inversely with frequency so that each sinusoid had the same peak velocity. The exception to this was that the ninth and tenth frequencies had the same amplitude as the eighth frequency in order to improve sway responses.

Platform motion

The support surface consisted of a platform that rotated about an axis perpendicular to the sagittal plane that was co-linear with the subject's ankles. Platform rotation was controlled by a computer-controlled servomotor system that accepted input signals from one of two sources. One input source was a potentiometer located at the base of a rigid rod that was attached to the subject's hip via a rigid horizontal rod affixed to a neoprene belt around the

subject's hips. The hip-rod potentiometer was calibrated using a custom built circuit such that angular changes in a subject's body sway produced equivalent angular rotations of the platform for the sway-referenced (SR) platform condition. The second input source used to control platform rotation consisted of a LabVIEW (National Instruments) based control program which produced the 10-frequency sum-of-sines (SOS) from a text file. For the combined SOS+SR platform condition, the two input signals, SOS and SR, were summed using custom built circuitry.

Platform performance

In order to assess the effectiveness of the platform control system, the FRF from driving signal to platform rotation angle was calculated for the SOS condition, averaging across subject (4 SOS trials/subject). Subject data was used to assess the effects of subject-platform interaction encountered during the experiment. Ideal platform operation would be defined as a gain of 1 and phase of 0 degrees across all 10 stimulus frequencies. The platform gain was within 1% of ideal up to .344 Hz (.99 ±.01, standard deviation), after which it gradually decreased to .85 ±.03 at 1.432 Hz then increased slightly to ~.90 ± .11 for the two highest platform frequencies. Phase was within 1% of ideal up to .184 Hz (2.9 ± .8 degrees) then decreased gradually to -26.1 ±4.5 degrees at 2.936 Hz.

Coherence between visual and platform stimuli

The simultaneous use of two similar stimulus signals (visual and platform) raises the concern that sway responses to one stimulus will be affected by the other. Nonzero complex coherence between the two signals means the effects of the neural probe (in this case the visual stimulus) may show a sway response that originated from the platform stimulus. Three methods were employed to address the issue. First, the phase of the visual signal was reversed for every other frequency compared to the platform signal. Second, the two signals were offset by 45 seconds. Third, the sign for half of the platform trials was reversed (the order of reversal was randomized within trial blocks) which served to reverse the complex coherence between the visual and platform signals such that the average complex coherence between the two signals for all trials was zero. The reasoning behind this approach is the assumption that the sway responses to the individual stimuli are approximately linear.

Kinematics

Body kinematics were measured using an OptoTrak (Northern Digital, Inc.) system with a sampling rate of 60 Hz. Small, infrared markers were placed on the subject's right side at the ankle (lateral malleolus), hip (head of the greater trochanter), knee (lateral condyle), and shoulder (acromion). Additional markers were placed on the moving part of the platform to detect platform rotation and on the stationary part of the platform as a reference.

EMG

Muscle activity was measured using a Noraxon Zerowire surface EMG system. Pairs of Ag/AgCl electrodes (Ambu Blue Sensor M) with circular, wet-gel measuring areas (15 mm diameter) were arranged parallel to the muscle fibers with an inter-electrode distance of approximately 2 cm. The EMG signal was band-pass filtered between 10Hz-1Khz by built-in filters. The signal was collected at 2160 Hz sampling rate. Muscle activity was collected from soleus, tibialis anterior, medial gastrocnemius, rectus femoris, biceps femoris, rectus abdominus, and erector spinae muscles of the lumbar spine on the right side of the subject's body.

Procedures

The 10-frequency sum-of sines visual signal was used in all experimental trials. The four platform conditions were: 1. Fixed support surface (FIX); 2. Platform rotations in the sagittal plane using the 10-frequency sum-of-sines (SOS); 3. Sway-referenced to the subject's hip (SR); 4. Combined SOS and SR (SOS+SR) where the platform motion was determined by the combined signal from sway-referencing and the 10-frequency sum-of-sines.

All trials were 250 seconds in duration. Trials were randomized within 4 blocks of 4 trials each (4 trials for each condition for a total of 16 trials). In the event that a subject lost their balance the trial was repeated. Subjects were

instructed to stand facing the front screen and look directly into the circular area that was devoid of triangles.

Prior to the start of data collection, subjects performed practice trials for the SR condition. They were not told the how the platform would move, only to expect movement. The reason for this was to minimize the “surprise effect” displayed by subjects, as well as to minimize falls. An assistant was positioned slightly behind the subject’s left side to assist if they lost balance, but out of their visual range.

Analysis

Kinematics

Trunk segment angular displacement was defined as the angle formed by the shoulder, the hip, and vertical. Leg segment angular displacement was defined as the angle formed by the hip, the ankle, and vertical. Angular displacements were measured in the sagittal plane. Positive angles refer to forward movements from upright vertical.

EMG

Data for the EMG signals for the seven recorded muscles were band-pass filtered (10-1000 Hz) and full-wave rectified after subtracting the mean. The rectified signals were normalized by dividing by their root-mean-square values computed across all trials for each subject.

Spectral analysis

Power spectral density (PSD) and cross spectral density (CSD) were computed using Welch's method using a 125 second window with a 50% overlap.

The closed-loop frequency response function (FRF) is $H_{xy}(f) = P_{xy}(f) / P_{xx}(f)$. Gain and phase are the absolute value and argument of $H_{xy}(f)$ respectively. The mean FRF across subjects was defined as $\overline{H}_{xy}(f) = \overline{C}_{xy}(f)\sqrt{\overline{P}_{yy}(f) / \overline{P}_{xx}(f)}$, where $\overline{C}_{xy}(f)$ is the mean complex coherence and $\overline{P}_{xx}(f)$ and $\overline{P}_{yy}(f)$ are the geometric mean PSDs. This definition of $\overline{H}_{xy}(f)$, which reduces to $P_{xy}(f) / P_{xx}(f)$ in the case of a single subject, has an advantage if the output signal is the normalized EMG (Kiemel et al., 2008).

Weighted EMG signals

Weighted EMG signals were calculated for the muscles associated with ankle movement (soleus, medial gastrocnemius, tibialis anterior), hip movement (rectus femoris, biceps femoris, rectus abdominus, erector spinae), as well as all muscles (ankle and hip muscles). The weighted EMG signal for each muscle group was calculated as $u(t) = w_1 u_1(t) + w_2 u_2(t) + w_3 u_3(t) + ... + w_n u_n(t)$, where the weights w_n were adjusted to maximize the average coherence between the visual scene angle $v(t)$ and the weighted EMG signal $u(t)$ subject to the constraint that posterior

muscle weights were positive, anterior muscle weights were negative, and $\sum|w_n|=1$. Average coherence was computed by averaging complex coherence C_{vu} across the four conditions and then averaging coherence $|C_{vu}|^2$ across the ten stimulus frequencies. The Matlab constrained optimization function FMINCON was used to maximize coherence. For each subject $u(t)$ was normalized by dividing by the geometric mean of the response amplitude across conditions and stimulus frequencies where response amplitude is the product of the gain $\overline{H}_{vu}(f)$ and the stimulus amplitude (Kiemel et al., 2008).

Identification of the plant frequency response function

The FRF of the plant was identified using the joint input-output method described by van der Kooij et al. (2005). The plant was assumed to be linear and having a single input, the weighted EMG signal, and two outputs, trunk and leg segment angles (SIMO).

Closed-loop FRFs were determined for the visual stimulus to EMG signal, $H_{vu}(f)$, and the visual stimulus to trunk and leg segment angles, $H_{v\Theta}(f)$. The inferred open loop FRF from EMG signal to segment angle $P_{u\Theta}(f)$ was determined by dividing $\overline{H}_{v\Theta}(f)/\overline{H}_{vu}(f)$. Mean closed-loop FRFs were calculated across subjects.

Intersegmental dynamics

The dynamic relationship between leg and trunk segments was characterized by comparing the ratios of the FRFs, $P_{u\Theta,legs}(f)/P_{u\Theta,trunk}(f)$, which within condition reduces to $\overline{H}_{v\Theta,legs}(f)/\overline{H}_{v\Theta,trunk}(f)$. The gain ratio and phase angle difference were calculated as the absolute value and argument of the $\overline{H}_{v\Theta,legs}(f)/\overline{H}_{v\Theta,trunk}(f)$ ratio respectively. Using this method, differences between segments occur when the gain ratio deviates from 1 or the phase difference from 0.

Additionally, cophase and complex coherence, $P_{xy}\Big/\sqrt{P_{xx}P_{yy}}$ were calculated, where P_{xy} is the CSD between the trunk and legs, and P_{xx} and P_{yy} are the respective PSDs of the trunk and legs. Within-subject averages for complex coherence were calculated as the arithmetic mean across trials while group averages were calculated as the arithmetic mean across subjects. Cophase was calculated as the argument of the group average of the complex coherence. Complex coherence was calculated using the trunk as the reference (positive is legs leading trunk).

Statistical Analysis

The experimental design was 4 (platform conditions) x 10 (visual stimulus frequencies). Confidence intervals (95%) were calculated for gain and phase to compare inferred FRFs between conditions using the percentile-t method with 4000 bootstrap resamples and 400 nested bootstrap resamples for variance estimation (Zoubir and Boashash, 1998). Condition differences

were calculated by similar bootstrap methods by comparing the ratios of the FRFs between conditions (4 conditions produced 6 comparisons). Differences between conditions were considered significant if the gain ratio was more than the 95% confidence interval from 1 or the phase angle difference was more than the 95% confidence interval from zero degrees.

Similarly, differences in segment dynamics between conditions were determined using the same number of resamples for gain ratio and phase angle difference.

Differences in cophase and complex coherence were tested for significance using paired F tests at each frequency step based on the assumption that the complex values of the transfer function were bivariate normally distributed in the complex plane (Jeka et al., 2006). Similarly, cophase was tested using the argument of the complex coherence. Multiplicity of testing (cophase tested at 625 frequency steps) was addressed by controlling the false discovery rate (Benjamini & Hochberg, 1995). In order to characterize the coordinative relationship between segments, the 95% confidence region of the complex coherence was determined for the transition frequencies between in-phase and anti-phase modes.

Results

Exemplar trial

In order to perform the joint input-output method of system identification, three components are necessary. Figure 3 shows an exemplar

trial for the sway-referenced platform condition. The top graph, Figure 3A, shows the displacement angle for the 10-frequency sum-of-sines visual stimulus which was presented to subjects on every trial regardless of platform condition (see Methods). The second graph, Figure 3B, shows the weighted EMG signal which was used as the proxy for the muscle activations. Note that the signal displays both positive and negative voltage changes. The weighted signal is composed of signals from 7 muscles associated with ankle and hip flexion. Anterior muscles were assigned negative values and posterior muscles were assigned positive values to reflect their respective A-P directional bias for controlling movement. The weighted signal appears to favor positive voltage changes indicating that the posterior muscles (soleus, medial gastrocnemius, biceps femoris, and erector spinae) played the dominant role in controlling posture.

The two bottom graphs, Figures 3C&D show the angular displacements of the leg and trunk segments with respect to vertical. Visual comparison of the leg segment (3C) with the weighted EMG signal (3B) indicates a high degree of correlation, suggesting that the weighted EMG signal is weighted more heavily in favor of ankle muscles.

SIMO

The plant was defined as having a single input, EMG, and multiple outputs, trunk and leg segment sway. An important assumption of this experiment is that the EMG signal acts as a proxy for the motor command,

providing a single input to the plant. EMG signals composed of subsets of the all-muscle weighted EMG signal should possess similar characteristics. Figure 4 A&B compares the FRFs of weighted ankle and hip muscles EMG responses to the visual stimulus. The gain ratios are constant and the phase differences are zero degrees to a first approximation across frequency indicating that ankle and hip EMG signals are similar. The two sway-referenced conditions show greater gain ratios than the FIX and SOS conditions while the phase difference shows a condition effect at the higher stimulus frequencies, primarily between FIX and the moving platform conditions (SOS, SR, and SR+SOS). Condition differences appear to affect the relative magnitude of the ankle/hip FRFs, but the gain ratios remain constant within condition and the phase difference remains approximately zero degrees across frequency indicating that to a first approximation the plant is single input.

A second assumption is that the SIMO plant is capable of multiple outputs. Figure 4 C&D shows the gain ratios and phase differences for the plant (legs/trunk) FRFs. At the lower stimulus frequencies the gain ratios for the two sway-referenced conditions are slightly greater than FIX and SOS which decrease at the three highest stimulus frequencies. Phase differences are approximately constant, although the sway-referenced conditions display a slight phase lead of legs over trunk. At higher frequencies, the phase difference shows a decrease with increasing frequency for the SOS and FIX conditions (note that SR and SR+SOS are not significantly different from zero

at higher frequencies). Within-condition variations across frequency in the leg/trunk plant FRF ratios show the existence of multiple intersegmental relationships between trunk and leg segments indicating that the plant output can not be described by a single variable. Therefore, to a first approximation the plant has multiple outputs.

EMG signals

The weighted EMG signal consists of contributions from all 7 recorded muscles. Figure 5 shows the rectified, band-pass filtered (10 Hz-1KHz) EMG signals of the recorded muscles for the trial shown in Figure 3 (sway-referenced platform condition). Visual inspection of the data shows several distinct characteristics. First, muscles A and C (soleus & m. gastrocnemius) show continuous activation throughout the duration of the trial while muscles B, D, and E (tibialis, r. femoris & b. femoris) display activity in short bursts separated by periods of inactivation. The last two muscles, F and G (r. abdominus & e. spinae) show activity at a low, but continuous level.

The rectified signals for each muscle were normalized by dividing by their root-mean-square values computed across all trials for each subject. Weighted EMG signals were calculated for the muscles associated with ankle movement (soleus, m. gastrocnemius, tibialis), hip movement (r. femoris, b. femoris, r. abdominus, e. spinae), as well as all muscles. Weights were adjusted to maximize the average coherence between the visual scene angle and the weighted EMG signal.

The muscle weights can be seen to the right of their corresponding graphs. Note that the posterior muscles (A, C, E & G) show positive values while the anterior muscles (B, D, &F) show negative values. The weighted muscle signals for r. abdominus, m. gastrocnemius and soleus, provided the greatest contribution to the weighted muscle signal (Figure 5H).

Leg segment

Figure 6 A&B show the gains and phases of the closed-loop FRFs from the visual stimulus to EMG. Gain increases with increasing frequency from about 1 for the FIX condition to about 100 for the SR+SOS condition while the phases decrease from about 90 degrees at the lowest frequency to -360 degrees at the highest. Gain differences occur between conditions with the fixed condition always less than the other three conditions. The two sway-referenced conditions, SR and SR+SOS, are always greater than FIX and SOS, but are not different from each other. Gain for the SOS condition is closer to the FIX condition at lower frequencies, but closer to SR and SR+SOS at higher frequencies. Despite this, the SOS gain is significantly different from the other three at all frequencies. Phase differences occur between all of the conditions except the two sway-referenced conditions, SR and SR+SOS. Unlike the gain differences which showed a well-defined, almost parallel hierarchy, the phase differences are very small relative to the phase range across frequency and vary from leading to lagging with no apparent pattern.

Figure 6 C&D show the gains and phase angles of the closed-loop FRFs from the visual stimulus to leg segment sway angle. Gains show an increase with increasing frequency from a value of approximately .1 to about 1 at .3 Hz, and then decrease to their lowest values of approximately .01 at the highest stimulus frequency. Phase angles decrease with increasing frequency from about 60 degrees to about -540 degrees at the highest stimulus frequency. Gain differences occur between conditions following a similar pattern to those observed in 6 A&B, i.e. FIX has the lowest value at all frequencies, the two sway-referenced conditions, SR and SR+SOS, are always the highest, but not significantly different from each other, and SOS lies in between, closer to FIX at lower stimulus frequencies, but closer to SR and SR+SOS at higher frequencies. It should be noted that the SOS is not significantly different from the two sway-referenced conditions at the .584 and .904 stimulus frequencies. Phase differences in 6D at lower stimulus frequencies, .584 Hz and below, show similarities to the phases in 6B in that there are slight differences, but no apparent pattern of differences. Above .584 Hz the FIX condition shows a significantly greater phase lag than the other three conditions while the SOS condition shows a slightly greater phase lag than the SR+SOS condition in the .904 to 2.104 Hz range.

Figure 6 E&F show the gains and phase angles for the inferred open-loop FRF from EMG to leg segment sway angle. Gains are approximately .1 for the first three stimulus frequencies, then decrease with increasing frequency to approximately .0001 at the highest frequency. Phases are

approximately 0 degrees at the lowest stimulus frequency and decrease with increasing frequency to a range of -135 to -200 degrees at the highest frequency. Unlike the gain differences in 6 A&C, gain differences for the inferred open-loop FRF are virtually non-existent. Small differences occur between SR and fixed at .344 and 2.104 Hz, between SR+SOS and FIX at .584 Hz, and between SOS and SR+SOS at 2.104 and 2.936 Hz without any apparent pattern. On the other hand, significant phase differences occur between the FIX condition and all other conditions from .344 to 2.936 Hz with the FIX condition always showing a greater lag than the other three (there are no significant differences below .344 Hz). Additional differences occur between SOS and SR+SOS at 1.432 and 2.104 Hz, and between SR and SOS at .344 and 2.104 Hz. In either case there doesn't appear to be any apparent pattern of a phase lead or lag.

Trunk segment

Since the plant is defined as having a single input, the stimulus-to-EMG FRF for the trunk shown in Figure 7 A&B is the same as that shown for the legs in Figure 6 A&B. Please refer to the previous section for a description.

Figure 7 C&D show the gains and phase angles of the closed-loop FRFs from the visual stimulus to trunk segment sway angle. Similar to leg segment gains, trunk gains show an increase with increasing frequency from a value of approximately .1 to about 1 at .3 Hz, and then decrease to their

lowest values of approximately .01 at the highest stimulus frequency. Phases decrease with increasing frequency from about 60 degrees to about -400 degrees at the highest stimulus frequency. A notable difference between leg and trunk FRFs is that the three highest frequencies show much greater variance than for the trunk FRFs than for the leg FRFs. In Figure 7C, FIX gain is significantly less than the other three, but only below 1 Hz. Significant differences between conditions for phase occur infrequently with no systematic pattern.

Figure 7 E&F show the gains and phase angles for the inferred open-loop FRF from EMG to trunk segment sway angle. Gains are approximately .1 for the first three stimulus frequencies, then decrease with increasing frequency to approximately .0001 at the highest frequency. Phases are approximately 0 degrees at the lowest stimulus frequency and appear to remain at, or slightly less than 0 degrees with increasing stimulus frequency. Both gain and phase show increased variance at the higher stimulus frequencies.

It's apparent from the results shown in Figures 6 and 7 that significant differences exist, but they are difficult to visualize because the differences between conditions are often much smaller than the range of values across the stimulus frequency spectrum. In order to address this issue, bootstrap methods were applied (see Methods Section) to ratios of FRFs ($FRF_{conditon1} / FRF_{condition2}$) in order to determine significant condition differences. Inter-condition differences comparing legs (Figure 8) and trunk (Figure 9)

were considered significant if the 95% confidence intervals did not overlap with 1 for the gain ratios, or with 0 degrees for the phase differences (only significant differences are shown).

Figure 8 shows significant between-condition differences for the leg segment FRFs in Figure 6. Figure 8 A&B and Figure 9 A&B are the significant between-condition differences for the stimulus-to-EMG FRF. Figure 8C, the visual stimulus to leg sway FRF, shows significant gain ratio differences between all conditions except SR+SOS and SR across all frequencies. On the other hand, in Figure 8E, the plant FRF, shows only a few differences at the higher stimulus frequencies. Likewise for phase difference, Figures 8D and 8F both show significant condition differences at the higher stimulus frequencies, but 8F, the phase difference for the plant, doesn't show any differences below .344 Hz. Additionally, differences in the visual stimulus-to-sway FRFs, 8C&D, occur for most of the comparisons while differences in the plant FRFs, 8E&F occur almost exclusively for comparisons between the FIX and sway-referenced conditions.

Making a similar comparison for the trunk, Figure 9C shows differences in gain ratio for frequencies below 2.104 Hz primarily between the FIX and all other conditions, while in Figure 9E the differences extend to higher frequencies and occur primarily between sway-referencing and all others. Phase differences in Figure 9D occur at only a few frequencies without any apparent pattern, while the plant shows significant differences

between .056 and .184 Hz primarily between the sway-referenced conditions and all others.

Intersegmental dynamics

Further exploration of Figure 4 C&D demonstrates how the coordinative relationship between legs and trunk changes with condition. The gain ratios shown in Figure 4C are approximately 1 and phase angle differences are approximately zero degrees (4D) at the lowest stimulus frequency. As frequency increases two distinct segmental interactions appear. SR and SR+SOS increase to values slightly above 1 while the fixed and SOS conditions remain at 1 up to stimulus frequency of .584 Hz where the gain ratios converge. Above .584 Hz the gain ratios for all four conditions diverge. At the three highest stimulus frequencies, overlap of the confidence intervals for the two sway-referenced conditions prevents distinguishing differences. Note that confidence intervals that extend to the lower border of the graph in Figure 4C represent values of the FRFs that are not significantly different from zero.

Phase differences (Figure 4D) are approximately 0 degrees at the lowest stimulus frequency. As frequency increases, the phase differences for the two sway-referenced conditions increased slightly compared to the fixed and SOS conditions indicating a slight phase lead of the legs over the trunk. The phase differences converged at .344 Hz. Above .584 Hz the fixed condition showed a decrease compared to the other conditions. Similar to

gain ratio, overlap of confidence intervals prevent distinguishing differences between conditions. Confidence intervals that range ±180 degrees indicate that the FRF isn't significantly different from zero.

In a manner similar to that shown in Figures 8 and 9, condition differences were assessed by performing bootstrap calculations (see Methods Section) on the ratio of the conditions, $(FRF_{legs} / FRF_{trunk})_{condition1} / (FRF_{legs} / FRF_{trunk})_{condition2}$ in order to determine significance. Figure 10 C&D shows $gainratio_{condition1} / gainratio_{condition2}$ and $phasedifference_{condition1} - phasedifference_{condition2}$ respectively. Inter-condition differences were considered significant if the confidence intervals didn't overlap with 1 for the gain ratios, or with 0 degrees for the phase angle differences (only significant differences are shown).

Figure 10C shows significant between-condition gain ratio differences for all condition comparisons except FIX vs. SOS (exception at 1.432 Hz discussed below). Figure 10D shows significant between-condition differences in phase difference between all conditions except SR+SOS vs. SR (exception at .584 Hz discussed below). No differences occur at the lowest stimulus frequency.

An interesting contrast exists for 10C and 10D. In the case of 10C, the FIX vs. SOS comparison was represented only at 1.432 Hz, but shows significant phase angle differences (10D) across a wide range of stimulus frequencies from .184 to 2.104 Hz. On the other hand, the opposite appears to be true for the SR vs SR+SOS comparison. This comparison (10C) shows

significant gain ratio differences from .184 to .344 Hz, but is represented by a single phase angle difference (10D) at .584 Hz.

Figure 11 shows the cophase (11A) and the complex coherence (11B) between trunk and leg segments for the four platform conditions. Subjects displayed in-phase behavior between trunk and leg segments at lower platform frequencies and anti-phase behavior above ~1 Hz. Note that ±180 degrees are anti-phase behavior. For the frequency range in between .2 and ~1 Hz the transition from in-phase to anti-phase shows several condition-specific differences. The FIX condition (blue) appears to deviate slightly from 0 degrees up to a frequency of .5 Hz after which it shifts to anti-phase following a negative pathway. At first the shift is abrupt at .6 Hz and then continues more gradually to 1 Hz. The SOS condition (red) also deviates slightly around 0 degrees to .5 Hz before shifting positively towards anti-phase. The shift is less sudden than for the FIX condition, but the slope describing the shift appears more linear, occurring between .5 and .9 Hz. SR (green) and SR+SOS (black) conditions show similar behavior, increasing in a gradual manner starting at .2 Hz up to +180 degrees.

Peaks at frequencies corresponding to the stimulus frequencies appear in both phase modes as well as the inter-modal transition range. Note that a phase shift, positive or negative, occurs at these frequencies while the neighboring frequencies show that the underlying intersegmental coordinative relationship (in-phase, anti-phase, or inter-modal transition) is not affected.

Figure 11B shows the complex coherence calculations for the data points at the frequencies designated by asterisks (*) in 11A. Two data points were selected for each condition by determining the points immediately before and after 90 degrees (i.e. crossing the imaginary axis in the complex plane) as the phase went from in-phase (0 degrees) to anti-phase (±180 degrees). The average of the two data points (+) as well as the 95% confidence region (area enclosed by ellipse) were calculated for each condition.

Complex coherence values that lie along the positive real axis represent the in-phase relationship between trunk and legs while values that lie along the negative real axis represent the anti-phase relationship. Likewise, complex coherence values with imaginary parts that are greater than 0 represent a “legs-leading” coordinative relationship (the trunk was used as the reference in the calculation of complex coherence) while complex coherence values with imaginary parts that are less than 0 represent a “trunk-leading” coordinative patterns.

The 95% confidence regions of the complex coherence (Figure 11B) at the phase mode transition for the sway-referenced conditions (SR & SR+SOS) lie above the real axis indicating a legs-leading coordinative relationship. SOS lies slightly above the real axis and FIX slightly below, but the confidence regions for both include the origin indicating neither a leading nor lagging relationship at the transition.

Discussion

In this experiment, closed-loop system identification (van der Kooij 2005, Fitzpatrick 1996) was used to determine whether changes occurred in the plant when the support surface was sway-referenced. The results show that the plant was different in response to changes in support surface conditions suggesting that the control strategy adopted by the postural control system depends on support surface dynamics.

SIMO

The justification for using a single plant input is based on the results shown in Figure 4 A&B. Gain ratios for the visual stimulus-to-EMG FRF of the weighted ankle-muscle to weighted hip-muscle signals are approximately constant across frequency and the phase difference is approximately zero degrees. This suggests that either the ankle or hip signals, or the weighted all-muscle signal could adequately serve as the single plant input proxy for the motor command, a result that is in agreement with Kiemel at al. (2008). However, a condition effect was noted where the two sway-referenced conditions displayed higher gain ratios at the lower stimulus frequencies than the non-sway-references conditions. This change was unexpected because an increase in ankle muscle activity would suggest an increase in ankle flexion rather than a decrease which is the case during sway-referencing (i.e. ideal sway-referencing would eliminate changes in ankle angle). The increase in ankle muscle activity may be the result of an increase in active

stiffness implemented to compensate for the effective decrease in passive stiffness that occurs as changes in ankle angle decrease during sway-referencing. The differences in gain ratio suggest that ankle and hip muscle EMG may be the same signal, but are scaled differently as a result of sway-referencing. This may indicate the single input approximation is valid, but limits its use to within-condition comparisons.

The leg/trunk FRF ratios shown in Figure 4 C&D varied with frequency in a manner similar to Kiemel et al. (2008) for the FIX condition. The frequency-dependent differences gain ratio and phase difference indicates that the plant output cannot be described by a single variable. Consistent with the results of Kiemel et al. (2008), the plant meets the assumption of multiple outputs.

A condition effect was evident at the lower stimulus frequencies which showed an increase in the gain ratios for the two sway-referenced conditions compared to the non-sway-referenced conditions. The relevance of the condition effect in a multiple output plant is unknown.

Plant identification

Similar to the methods employed by Kiemel et al. (2008), plant dynamics were determined by calculating the open loop transfer functions from a single, weighted EMG signal to trunk and leg segments. For the plant (ref. Figures 6 E&F, 7 E&F) to remain unchanged, the gains and phases for all four conditions would have to be equal across frequency. The plant FRFs

appear qualitatively similar, but show deviations across conditions. The between-condition comparisons shown in Figures 8 & 9 highlight the significant differences. The leg segment gain ratios show virtually no change in response to different sensory conditions (8E) while the phase differences show significant differences at the higher stimulus frequencies (8F), primarily between the FIX condition and the moving-platform conditions. The phase differences appear in the frequency range where the trunk and leg segments display anti-phase behavior (Zhang et al. 2007, Creath et al. 2005). In comparison, trunk segment gain ratios (9E) and phase differences (9F) show sensitivity to the sway-referenced conditions with the frequency range for the phase differences in the lower frequency range where trunk and legs display in-phase behavior (Zhang et al. 2007, Creath et al. 2005).

Differences in gain and phase indicate that differences in the plant primarily affect the trunk. Differences in the legs component, which shows differences in phase that are limited to higher frequencies, may be the effect of increases in trunk movement.

Intersegmental dynamics

The results discussed above regarding the trunk and leg components of the plant demonstrated that the plant was different in response to changing support surface conditions. The question remains as to how these changes can be characterized. The physical characteristics of the plant are defined by the musculoskeletal system. Since the physical dimensions of trunk and leg

segments are fixed (assuming no knee or trunk flexion), a likely source of change lies in the coordinative relationship between the segments.

Figure 4 C&D shows the gain ratios and phase differences of the open-loop, legs/trunk FRFs. Subjects showed an increase in gain ratio and a "legs-leading" phase difference for the sway-referenced conditions at lower stimulus frequencies indicating that leg sway increased more than trunk say. Remember that although leg sway increases with sway-referencing (Figure 6C), the gain of the legs component of the plant does not change (6E). This suggests that the increase in leg sway due to sway-referencing is due to decreased sensory feedback. On the other hand, the trunk shows increased sway (Figure 7E), and although its increase in sway is less than that of the legs, its change in open loop gain (Figure 7E) suggests that an alternative postural strategy is implemented that serves to stabilize the trunk. The current results differ from previous studies using a moving support surface (Buchanan and Horak, 2002; Creath et al., 2008) in that both of the referenced studies concluded that healthy control subjects stabilize their trunks in response to any support surface movement at higher movement frequencies rather than just when sway-referenced.

Figure 11 shows the phase relationship and the complex coherence between trunk and legs. These measures illustrate the frequency-specific changes that occur between the trunk and legs, but utilize techniques that don't distinguish between changes that are due to the plant or feedback. Subjects show in-phase behavior between segments at lower frequencies

and anti-phase behavior at higher frequencies. The current results differ from Creath et al. (2005) in that the transition frequency between phase modes for the FIX condition occurs at a lower frequency. Creath et al. (2005) tested subjects with eyes closed whereas the current experiment tested with eyes open. The decrease in transition frequency for the FIX condition between Creath et al. (2005) and the current experiment is similar to that seen in Zhang et al. (2005) with the addition of vision. For the sway-referenced conditions, the current experiment shows a shift to +180 degrees following a gradual path similar to Creath et al. (2005). The frequency range of the transition is similar for both studies from approximately .2 Hz to 3 Hz. A notable difference between Zhang et al. (2007) and the current experiment occurred regarding the decrease in the transition frequency. Zhang et al. (2007) noted the decrease with the addition of visual sensory information whereas the current experiment showed a decrease in the transition frequency as a result of removing sensory information by sway-referencing. It's possible that sway-referencing causes a change in the trunk-legs relationship that overrides the effects of vision or that .2 Hz represents the lowest attainable frequency for the phase mode transition.

It should be noted that the frequency range of the phase mode transition in the current experiment is difficult to determine for two reasons (ref. Figure 11). First, peaks at the stimulus frequencies show shifts in the phase from what appears to be a continuous transition pathway, and second, the appearance of noise due to differences in window size used for the

calculation. Creath et al. (2005) used a 20 second window and averages over more windows whereas the current experiment uses a 125 second window and averages over fewer windows in order to preserve the frequency resolution of the lowest stimulus frequency (.024 Hz).

In Figure 11A, the sway-referenced conditions displayed a gradual transition from in-phase to anti-phase for the phase mode transition suggesting that a “legs-leading” coordinative relationship is adopted between the segments (trunk is the reference). Figure 11B shows the complex coherence between segments where “+” is the complex coherence and the ellipses represent the 95% confidence regions for the average of the two data points designated by “*” in Figure 11A. The data points selected straddled the imaginary axis, i.e. the threshold between in-phase and anti-phase, in order to see the coordinative relationship between segments during the phase mode transition. Complex coherence values that lie along the positive real axis represent the in-phase relationship between trunk and legs while values that lie along the negative real axis represent the anti-phase relationship. Likewise, complex coherence values with imaginary parts that are greater than 0 represent a legs-leading coordinative relationship while complex coherence values with imaginary parts that are less than 0 represent a trunk-leading coordinative patterns. The average complex coherence and confidence regions for the two sway-referenced conditions lie above the real axis indicating a legs-leading relationship, similar to the result of Creath et al. (2005). The average complex coherence for the SOS condition lies slightly

above the real axis while the average for the FIX condition lies slightly below. In both cases the confidence regions include the origin indicating that the complex coherence for these conditions isn't significantly different from the origin at the transition. The SOS result is in agreement with the results of Creath et al. (2008) where healthy control subjects exhibited similar behavior while the FIX result is in agreement with Creath et al. (2005).

Factors affecting the "legs-leading" relationship

During sway-referencing, test subjects appear to exert greater effort in maintaining upright posture compared to standing on a firm surface. One possible explanation is presented in the work of Edwards (2007) whose computational study examined the combined passive stiffness requirements necessary for quiet standing using a three joint model. Relevant to this study, the results of the study showed that a decrease in stiffness in one joint required a compensatory increase at other joints in order to maintain stability. Under ideal conditions, sway-referencing works by rotating the support surface in direct proportion to body sway, eliminating (or attenuating) support surface information due to changes in ankle angle. Since stiffness depends on displacement, eliminating changes in ankle angle effectively removes the contribution of passive ankle stiffness in maintaining stable posture. According to the results of Edwards (2007), by eliminating changes in ankle angle, reduced passive stiffness at the ankle would require an increase in

active stiffness at the hip, directly affecting the trunk-legs coordinative relationship.

Quasi-linearity and posture

The results of this experiment rely heavily on the assumption that the postural control system behaves in an approximately linear manner. Quasi-linear models of posture effectively describe posture because movement during postural studies is usually limited to a narrow range of motion with an average position close to upright vertical (Kearney and Hunter, 1990). The condition-related differences observed in the current experiment suggest that sway-referencing affects intrinsic stiffness or damping at the ankle joints by greatly reducing the change in ankle angle.

Nonlinear stiffness

The assumption of linearity discussed above meets the criteria outlined by Kearney and Hunter (1990) for several of the factors affecting joint dynamics (e.g. ankle torque) with a notable exception, stiffness. In a more recent study, nonlinear changes in intrinsic stiffness were determined for ankle joint displacements which showed a five-fold decrease (67±8% to 13±2% normalized to mgh) for displacements of .2 and 1.6 degrees respectively (Loram et al. 2007a&b), representing values well within the physiological range of ankle rotation during standing posture. Although in the current experiment ankle rotation was significantly reduced by sway-

referencing, the nonlinear changes in stiffness described by Loram et al. (2007a&b) likely affected stiffness at the hip. If the previously described results of Edwards (2007) are considered in which the decreased stiffness in one joint resulted in a compensatory increase in stiffness at others, the effect of nonlinear stiffness may be enhanced by the increased stiffness at the hip.

Another effect described by Loram et al. (2007a&b) equated decreases in intrinsic stiffness to decreases in the response time the postural system needs to respond to a loss of balance. In the case of sway-referencing, the decrease in response time occurs as a result of decreased intrinsic ankle stiffness. As a consequence, the increase in sway may be the result of changing the biomechanical system time constant.

Conclusions

Sway-referencing is believed to cause an increase in body sway compared to standing on a fixed surface by reducing sensory information obtained through feedback from the support surface. The results of the current experiment demonstrate that sway-referencing the support surface also causes differences in the plant that serve to enhance plant stability under different support surface conditions.

Figure 1

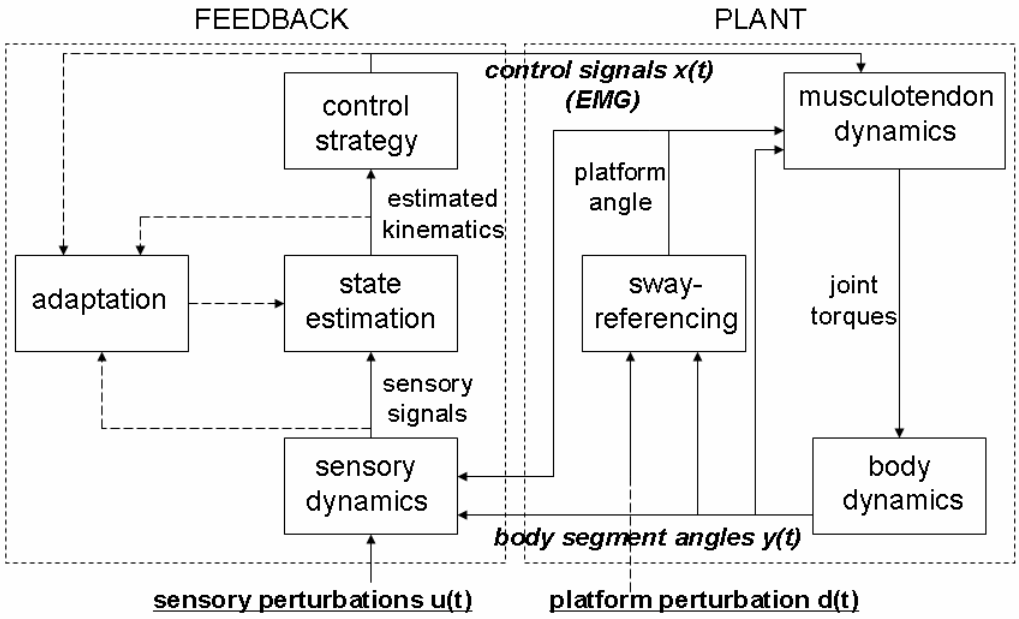

Figure 1. Closed-loop control model showing plant (A) and feedback (B) components.

Figure 2

Figure 2. Virtual reality “cave” with sway-referencing platform.

Figure 3

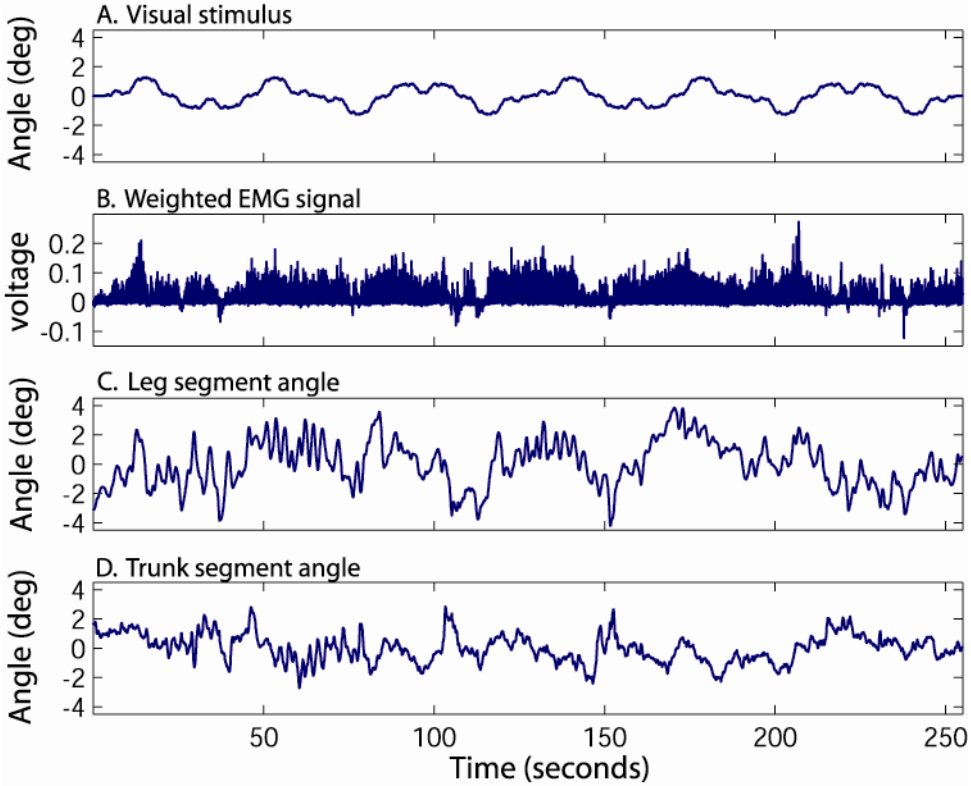

Figure 3. Exemplar graph showing time series of the visual stimulus signal, weighted EMG signal, and leg and trunk segment angles for 1 trial for the sway-referenced condition.

Figure 4

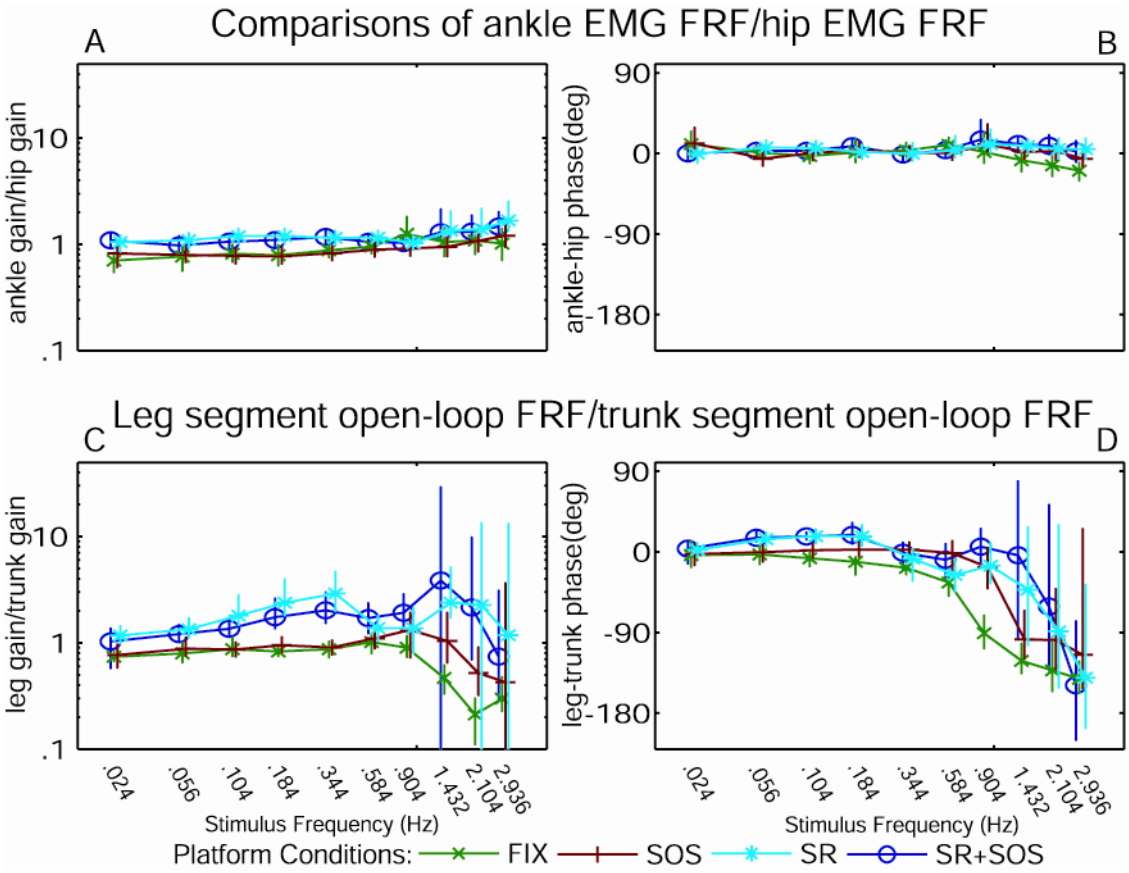

Figure 4 A&B. Gain ratio and phase angle difference of FRF(ankle muscle EMG)/FRF(hip muscle EMG), and (C&D) open-loop FRF(leg segment)/FRF(trunk segment) showing the segmental relationship between legs and trunk for the four platform conditions. Error bars are 95% confidence intervals.

Figure 5

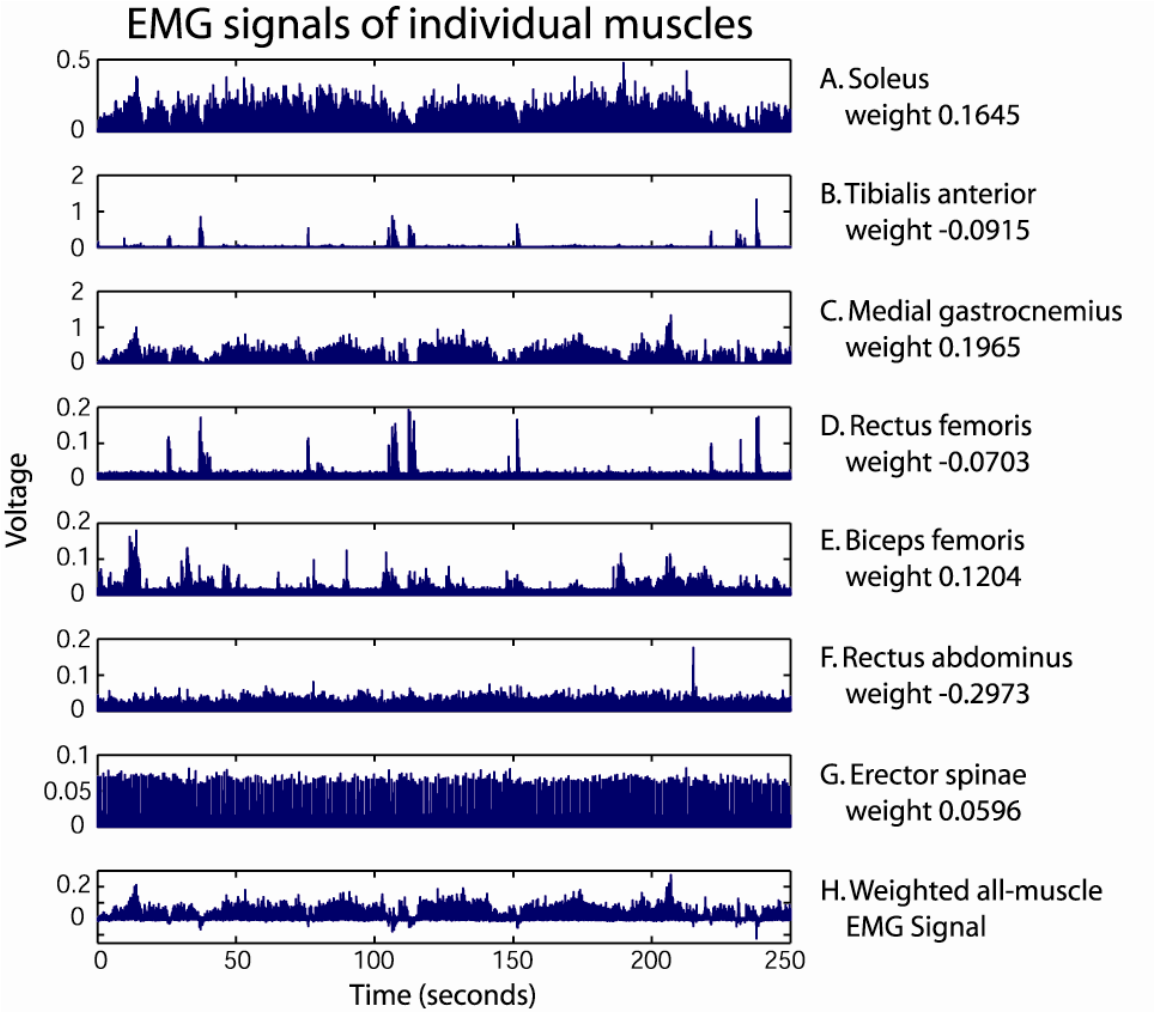

Figure 5. Rectified EMG (A-G) and weighted EMG (H) for all 7 muscles for the same sway-referencing trial shown in Figure 3.

Figure 6

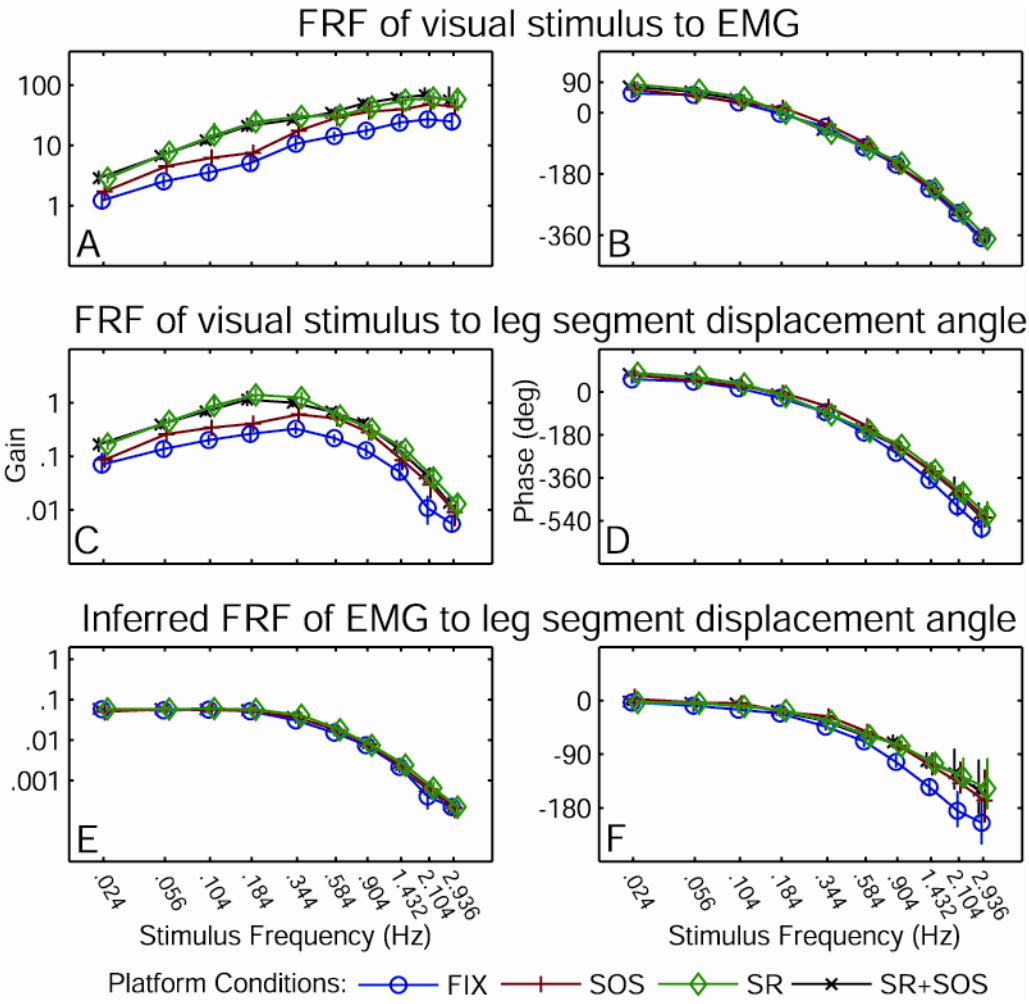

Figure 6. FRFs of visual stimulus to EMG, visual stimulus to leg segment sway angle, and inferred EMG to leg segment sway angle for the four platform conditions. Error bars are 95% confidence intervals.

Figure 7

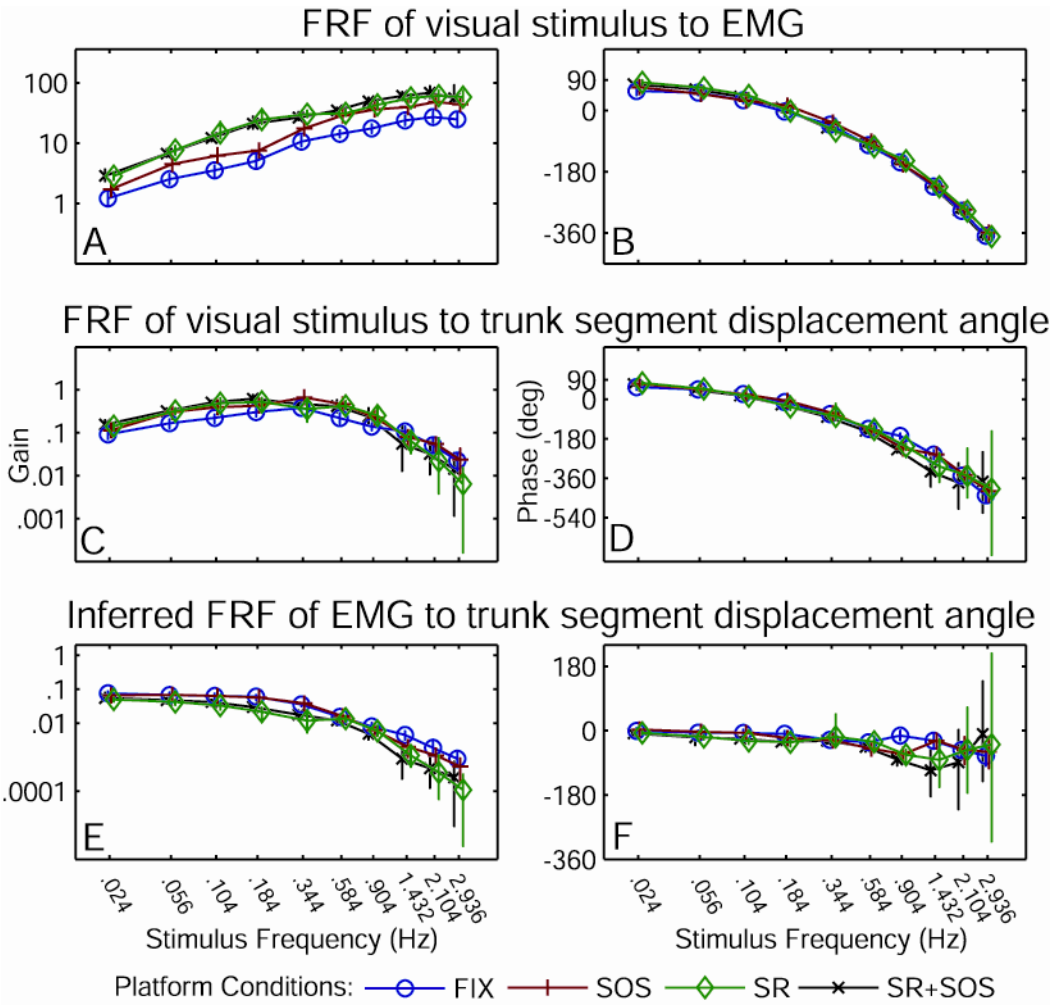

Figure 7. FRFs of visual stimulus to EMG, visual stimulus to trunk segment sway angle, and inferred EMG to trunk segment sway angle for the four platform conditions. Error bars are 95% confidence intervals.

Figure 8

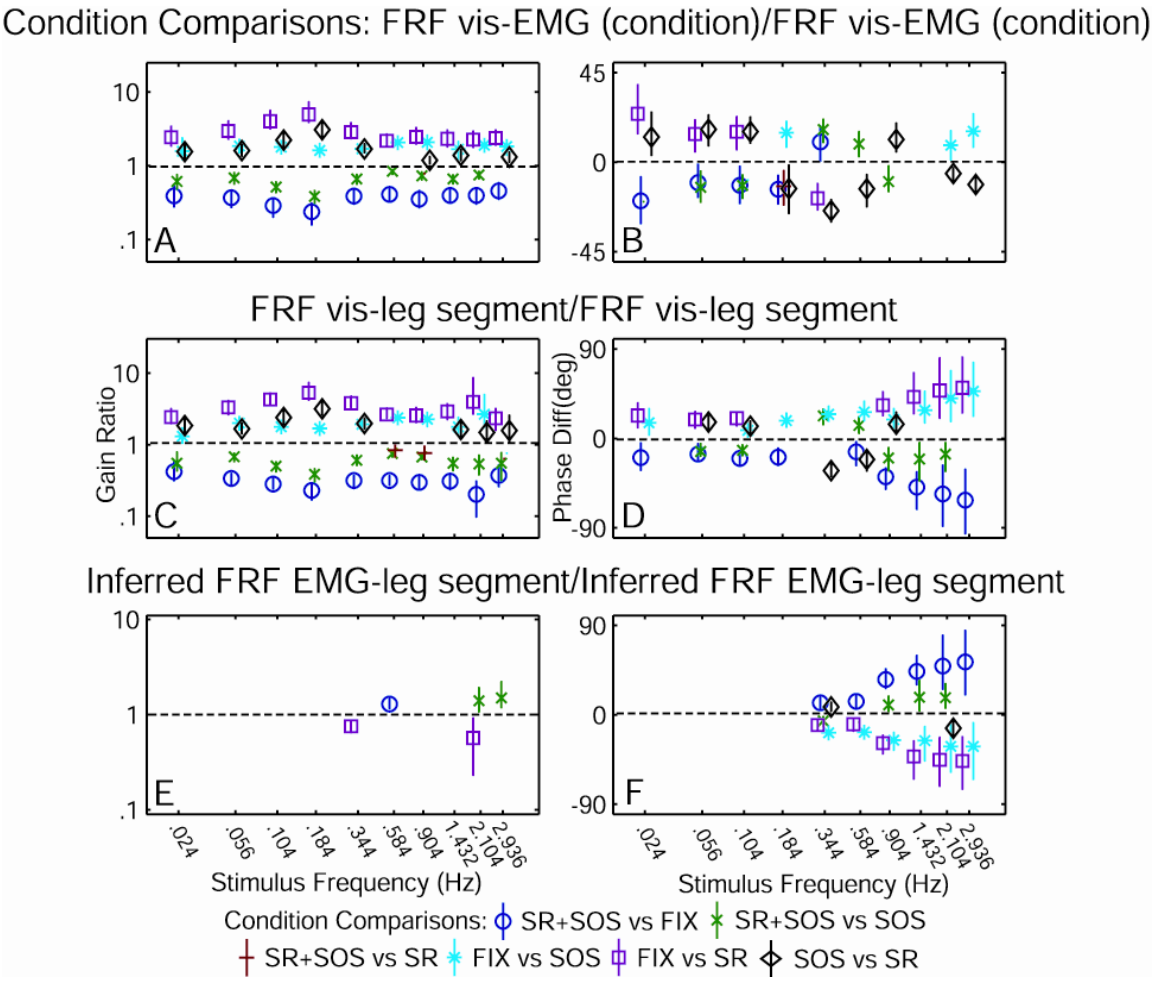

Figure 8. Ratios of FRF(condition1)/FRF(condition2) showing significant differences for the leg segment between conditions. Only significant differences are shown.

Figure 9

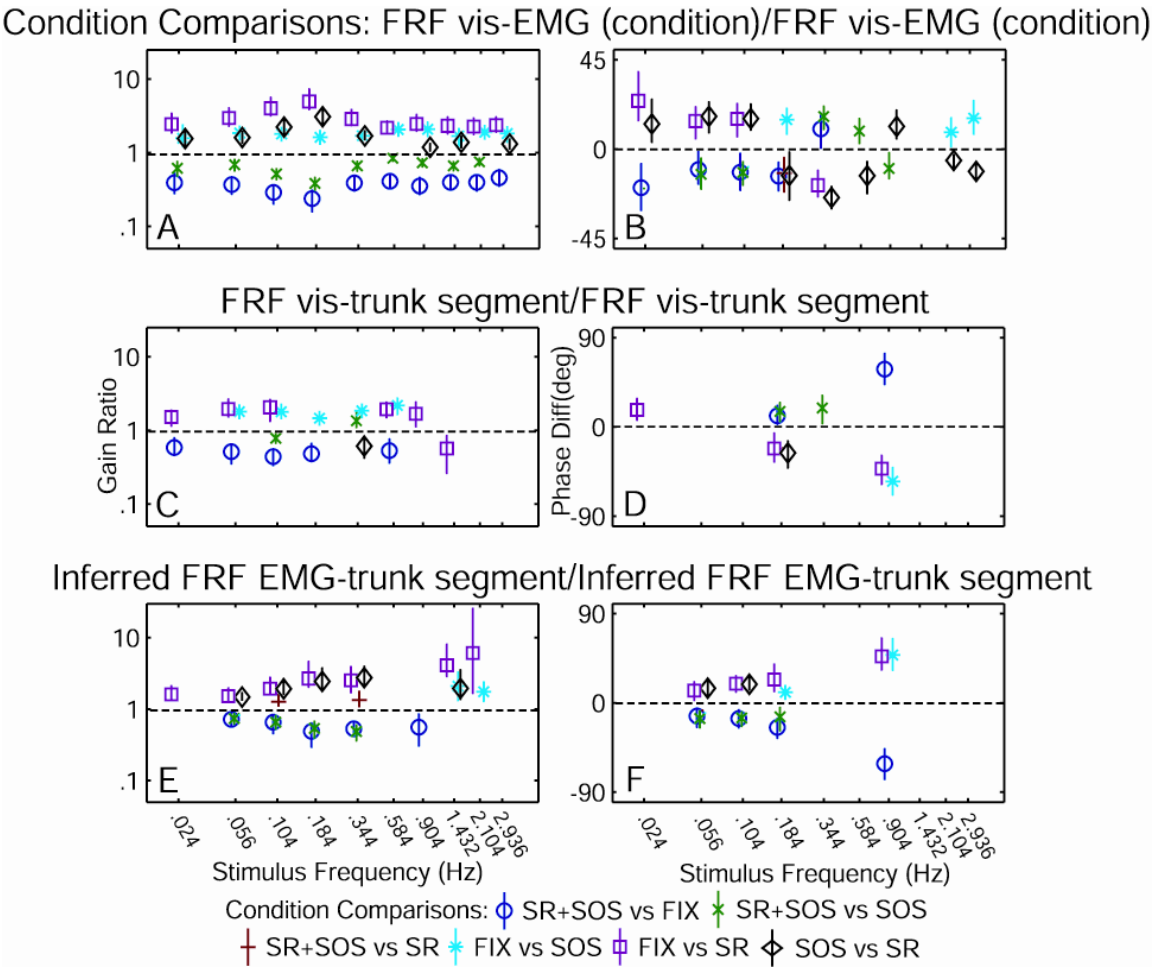

Figure 9. Ratios of FRF(condition1)/FRF(condition2) showing significant differences for the trunk segment between conditions. Only significant differences are shown.

Figure 10

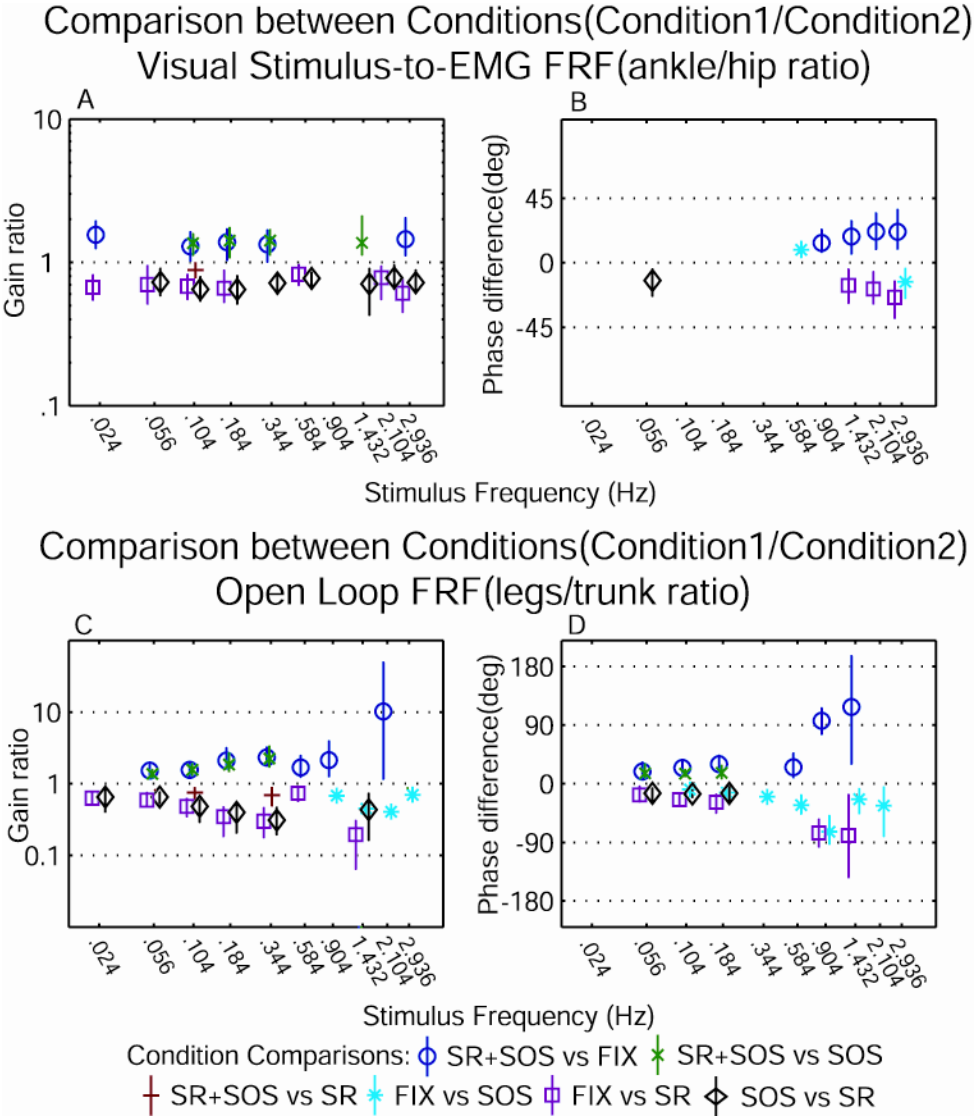

Figure 10. A&B compares conditions as the gain ratio (Condition1/Condition2) and phase difference (Condition1-Condition2) of the visual stimulus-to EMG FRFs of the weighted ankle EMG/weighted hip EMG. C&D compares conditions as the gain ratio (Condition1/Condition2) and phase difference (Condition1-Condition2) of the open loop FRFs of the legs/trunk. Only significant differences are shown.

Figure 11

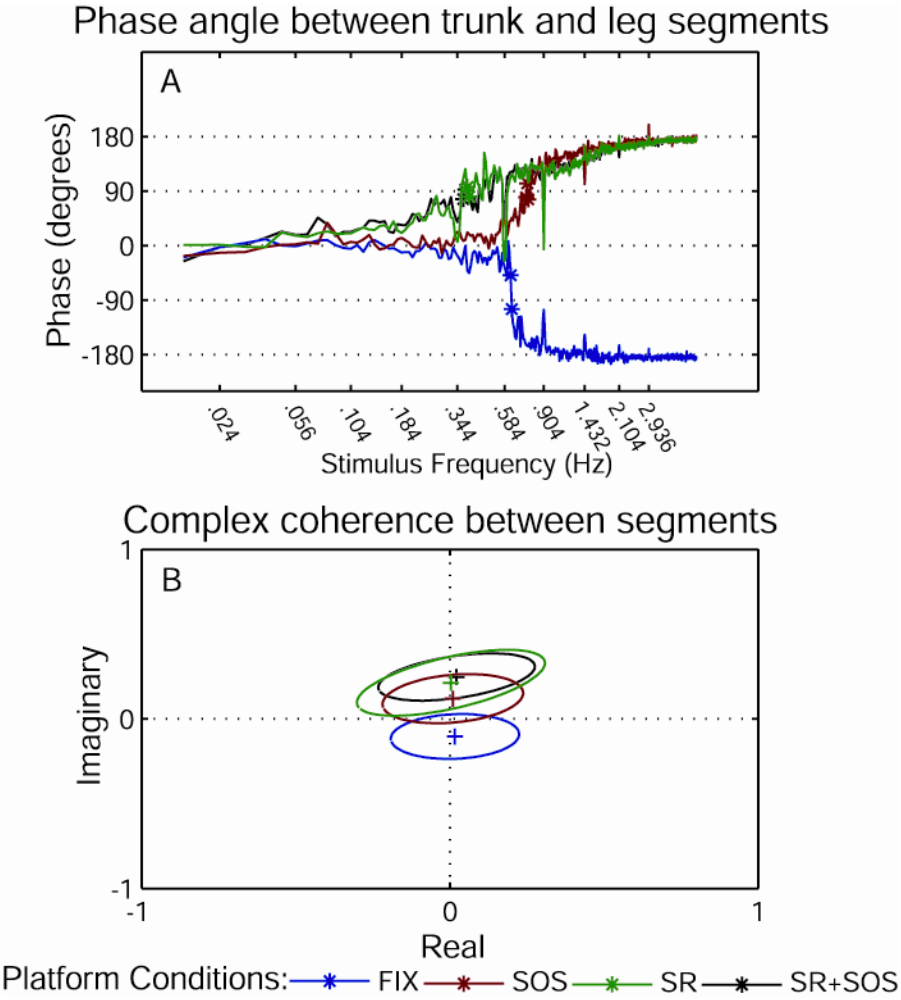

Figure 11. Cophase (A) and the complex form of the coherence (B) between trunk and leg segments. Asterisks in B used to calculate complex coherence are the average of the two data points identified as asterisks in A. Elliptical regions in B are 95% confidence regions.

References

Alexandrov AV, Frolov AA,Massion J, Biomechanical analysis of movement strategies in human forward trunk bending. I. Modeling. *Biol Cybern*. (2001) 84(6):425-34.

Alexandrov AV, Frolov AA,Massion J, Biomechanical analysis of movement strategies in human forward trunk bending. II. Experimental study. *Biol Cybern*. (2001) 84(6):435-43.

Alexandrov AV, Frolov AA, Horak FB, Carlson-Kuhta P, Park S, Feedback equilibrium control during human standing. *Biol Cybern*. (2005) Nov; 93(5):309-22.

Allum JH, Zamani F, Adkin AL, Ernst A. Differences between trunk sway characteristics on a foam support surface and on the Equitest ankle-sway-referenced support surface. *Gait Posture* (2002) 16(3): 264-70

Allum JH, Honegger F. Interactions between vestibular and proprioceptive inputs triggering and modulating human balance-correcting responses differ across muscles. *Exp Brain Res.* (1998) 121(4): 478-94

Allum JH, Honegger F, Schicks H. The influence of a bilateral peripheral vestibular deficit on postural synergies. *J Vestib Res.* (1994) 4(1): 49-70

Arnold L. *Stochastic Differential Equations: theory and applications* Wiley, (1974) New York

Ashmead DH, McCarty ME. Postural sway of human infants while standing in light and dark. *Child Dev.* (1991) 62(6):1276-87

Bardy BG, Warren WH Jr, Kay BA. The role of central and peripheral vision in postural control during walking. *Percept Psychophys.* (1999) 61(7): 1356-68

Bardy BG, Marin L, Stoffregen TA, Bootsma RJ, Postural Coordination modes considered as emergent phenomena. *J Exp Psychol Hum Percept Perform*. (1999) 25(5):1284-301.

Bardy BG, Oullier O, Bootsma RJ, Stoffregen TA, Dynamics of Human Postural Transitions. *J Exp Psychol Hum Percept Perform*. (2002) 28(3):499-514.

Benjamini Y, Hochberg Y, Controlling the false discovery rate: a practical and powerful approach to multiple testing, *J R Stat Soc Ser B* (Methodological) (1995) 57 (1):289-300.

Benson, A.J. The vestibular sensory system. In H.B. Barlow & J.D. Mollon (Eds.), The Senses (pp. 333-368). (1982) New York: Cambridge University Press.

Berencsi A, Ishihara M, Imanaka K. The functional role of central and peripheral vision in the control of posture. *Hum Mov Sci.* (2005) 24(5-6): 689-709

Berthoz A, Lacour M, Soechting JF, Vidal PP. The role of vision in the control of posture during linear motion. *Prog Brain Res.* (1979) 50: 197-209

Black FO, Shupert CL, Horak FB, Nashner LM, Abnormal postural control associated with peripheral vestibular disorders. *Prog Brain Res*. (1988) 76:263-75

Black FO, Wall C 3rd, Nashner LM. Effects of visual and support surface orientation references upon postural control in vestibular deficient subjects. *Acta Otolaryngol.* (1983) 95(3-4): 199-201

Black FO, Wall C 3rd, Rockette HE Jr, Kitch R. Normal subject postural sway during the Romberg test. *Am J Otolaryngol.* (1982) 3(5): 309-18

Brenière Y. Why we walk the way we do. *J Mot Behav* (1996) 28: 291–298.

Buchanan JJ, Horak FB. Vestibular loss disrupts control of head and trunk on a sinusoidally moving platform. *J Vestib Res.* (2001-2002) 11(6): 371-8

Buchanan JJ, Horak FB. Role of vestibular and visual systems in controlling head and trunk position in space, Society for Neuroscience Abstracts (1998) 24:153.

Buchanan JJ, Horak FB. Emergence of postural patterns as a function of vision and translation frequency. *J Neurophysiol*. (1999) 81(5):2325-2329.

Burgess PR, Perl ER. Cutaneous mechanoreceptors and nociceptors. In A Iggo (Ed.), Handbook of Sensory Physiology (pp 29-78) (1973) Berlin: Springer.

Carver S, Kiemel T, van der Kooij H, Jeka JJ. Comparing internal models of the dynamics of the visual environment. *Biol Cybern.* (2005) 92(3): 147-63

Chiari L, Bertani A & Cappello A. Classification of visual strategies in human postural control by stochastic parameters. *Human Movement Sci,* (2000) 19: 817-842.

Chong RK, Horak FB, Woollacott MH. Parkinson's disease impairs the ability to change set quickly. *J Neurol Sci.* (2000) 175(1): 57-70

Chong RK, Horak FB, Frank J, Kaye J. Sensory organization for balance: specific deficits in Alzheimer's but not in Parkinson's disease. *J Gerontol A Biol Sci Med Sci*. (1999) 54(3): M122-8

Chong RK, Jones CL, Horak FB. Postural set for balance control is normal in Alzheimer's but not in Parkinson's disease. *J Gerontol A Biol Sci Med Sci*. (1999) 54(3): M129-35

Coats AC. The sinusoidal galvanic body-sway response. *Acta Otolaryngol.* (1972) 74(3): 155-62

Collins JJ, De Luca CJ. Open-loop and closed-loop control of posture: a random-walk analysis of center-of-pressure trajectories. *Exp Brain Res.* (1993) 95(2): 308-18

Creath R, Kiemel T, Horak F, Jeka JJ. The role of vestibular and somatosensory systems in intersegmental control of upright stance. *J Vestib Res.* (2008)18(1):39-49.

Creath R, Kiemel T, Horak F, Jeka JJ. Loss of vestibular information affects trunk, but not leg segment control. Society for Neuroscience Abstracts (2006).

Creath R, Kiemel T, Horak F, Peterka R, Jeka J. A unified view of quiet and perturbed stance: simultaneous co-existing excitable modes. *Neurosci Lett.* (2005) 377(2): 75-80

Creath R, Kiemel T, Horak F, Jeka JJ. Limited control strategies with the loss of vestibular function. *Exp Brain Res.* (2002); 145(3): 323-33

Cremieux J, Mesure S. Differential sensitivity to static visual cues in the control of postural equilibrium in man. *Percept Mot Skills.* (1994) 78(1): 67-74

Diener HC, Dichgans J, Bruzek W, Selinka H, Stabilization of human posture during induced oscillations of the body. *Brain Res.* (1982) 45(1-2):126-32.

Dickstein R, Peterka RJ, Horak FB. Effects of light fingertip touch on postural responses in subjects with diabetic neuropathy. *J Neurol Neurosurg Psychiatry.* (2003) 74(5): 620-6

Dickstein R, Shupert CL, Horak FB. Fingertip touch improves postural stability in patients with peripheral neuropathy. *Gait Posture* (2001) 14(3): 238-47

Dietz V. Human neuronal control of automatic functional movements: Interaction between central programs and afferent input. *Physiol Rev*, (1992) 72: 33-69.

Dijkstra TM, Schoner G, Gielen CC. Temporal stability of the action-perception cycle for postural control in a moving visual environment. *Exp Brain Res.* (1994a) 97(3): 477-86

Dijkstra TM, Schoner G, Giese MA, Gielen CC. Frequency dependence of the action-perception cycle for postural control in a moving visual environment: relative phase dynamics. *Biol Cybern.* (1994b) 71(6): 489-501

Dornan J, Fernie GR, Holliday PJ. Visual input: its importance in the control of postural sway. *Arch Phys Med Rehabil.* (1978) 59(12): 586-91

Edwards WT. Effect of joint stiffness on standing ability. *Gait Posture* (2007) 25:432-439.

Elahi AJ, Kiemel T, Jeka JJ, Measuring Loop Gains During Human Balance Control. Society for Neuroscience Abstracts. 2006 Annual Conference, Atlanta, GA

Esteky H, Schwark H, Responses of rapidly adapting neurons in cat primary somatosensory cortex to constant-velocity mechanical stimulation. *J Neurophysiol.* (1994) 72: 2269-2279.

Fernandez C, Goldberg JM, Physiology of peripheral neurons innervating semicircular canals of the squirrel monkey. II. Response to sinusoidal stimulation and dynamics of peripheral vestibular system. *J Neurophysiol.* (1971) Jul; 34(4):661-75.

Fitzpatrick R, Burke D, Gandevia S, Loop Gain of Reflexes Controlling Human Standing Measured with the Use of Postural and Vestibular Disturbances, *J Neurophysiol.* (1996) 76(6):3994-4008.

Fitzpatrick R, McCloskey DI, Proprioceptive, visual and vestibular thresholds for the perception of sway during standing in humans. *J Physiol.* (1994) 478(1):173-186.

Gage WH, Winter DA, Frank JS, Adkin AL, Kinematic and kinetic validity of the inverted pendulum model in quiet standing, *Gait Posture* (2004) 19:124-132.

Goldberg JM, Fernandez C, Physiology of peripheral neurons innervating semicircular canals of the squirrel monkey. I. Resting discharge and response to constant angular accelerations. *J Neurophysiol.* (1971) Jul; 34(4):635-60.

Goldberg JM, Fernandez C, Physiology of peripheral neurons innervating semicircular canals of the squirrel monkey. 3. Variantions among units in their discharge properties. *J Neurophysiol.* (1971) Jul; 34(4):676-84.

Haslwanter T, Jaeger R, Mayr S, Fetter M, Three-dimensional eye-movement responses to off-vertical axis rotations in humans, *Exp Brain Res*. (2000) 134:96-106.

Hlavacka F, Shupert CL, Horak FB. The timing of galvanic vestibular stimulation affects responses to platform translation. *Brain Res.* (1999) 821(1): 8-16

Hlavacka F, Mergner T, Krizkova M. Control of the body vertical by vestibular and proprioceptive inputs. *Brain Res Bull.* (1996) 40(5-6): 431-4

Hlavacka F, Njiokiktjien C. Sinusoidal galvanic stimulation of the labyrinths and postural responses. *Physiol Bohemoslov.* (1986) 35(1): 63-70

Hlavacka F, Njiokiktjien C. Postural responses evoked by sinusoidal galvanic stimulation of the labyrinth. Influence of head position. *Acta Otolaryngol.* (1985) 99(1-2): 107-12

Hochberg Y, Tamhane AC. *Multiple Comparison Procedures*. Wiley, (1987) New York.

Holden M, Ventura J, Lackner JR. Stabilization of posture by precision contact of the index finger. *J Vestib Res.* (1994) 4(4): 285-301

Honrubia V, Jenkins HA, Baloh RW, Lau CGY, Evaluation of rotatory vestibular tests in peripheral labyrinthine lesions, In: Nystagmus and Vertigo: Clinical Approaches to the Patient with Dizziness, Academic Press Inc. (1982) pp. 5777.

Horak FB, Dickstein R, Peterka RJ. Diabetic neuropathy and surface sway-referencing disrupt somatosensory information for postural stability in stance. *Somatosens Mot Res.* (2002) 19(4): 316-26

Horak FB, Buchanan J, Creath R, Jeka J. Vestibulospinal control of posture. *Adv Exp Med Biol.* (2002) 508:139-45

Horak FB, Hlavacka F. Somatosensory loss increases vestibulospinal sensitivity. *J Neurophysiol* (2001) 86(2): 575-85

Horak FB, Earhart GM, Dietz V. Postural responses to combinations of head and body displacements: vestibular-somatosensory interactions. *Exp Brain Res.* (2001) 141(3): 410-4

Horak F, Kuo A, Postural adaptation for altered environments, tasks, and intentions, in Biomechanics and Neural Control of Posture and Movement, Winters JM and Crago, PE, Eds, Springer, NY, pp 267-281, 2000.

Horak FB, Macpherson JM. Postural orientation and equilibrium. In: Shepard J, Rowell L (Eds.), Handbook of Physiology. (1996) Oxford University Press, New York

Horak FB, Shupert CL, Dietz V, Horstmann G. Vestibular and somatosensory contributions to responses to head and body displacements in stance. *Exp Brain Res.* (1994) 100:93-106.

Horak FB, Nashner LM, Diener HC. Postural strategies associated with somatosensory and vestibular loss. *Exp Brain Res.* (1990) 82(1): 167-77

Horak FB, Diener HC, Nashner LM, Influence of central set on human postural responses. *J Neurophysiol.* (1989) 62(4):841-53.

Horak FB, Nashner LM. Central programming of postural movements: adaptation to altered support-surface configurations. *J Neurophysiol.* (1986) 55(6): 1369-81

Hsu W-L, Scholz JP, Schöner G, Jeka JJ, Kiemel T, Control and estimation of posture during quiet stance depends on multijoint coordination, *J Neurophysiol.* (2007) 97:3024-3035.

Hufschmidt A, Dichgans J, Mauritz KH, Hufschmidt M. Some methods and parameters of body sway quantification and their neurological applications. *Arch Psychiatr Nervenkr.* (1980) 228(2):135-50

Hytonen M, Pyykko I, Aalto H, Starck J. Postural control and age. *Acta Otolaryngol.* (1993) 113(2):119-22

Inglis JT, Shupert CL, Hlavacka F, Horak FB. Effect of galvanic vestibular stimulation on human postural responses during support surface translations. *J Neurophysiol.* (1995) 73(2): 896-901

Jeka J, Allison L, Saffer M, Zhang Y, Carver S, Kiemel T, Sensory reweighting with translational visual stimuli in young and elderly adults: the role of state-dependent noise. *Exp Brain Res.* (2006) 174(3): 517-27

Jeka J, Kiemel T, Creath R, Horak F, Peterka R. Controlling human upright posture: velocity information is more accurate than position or acceleration. *J Neurophysiol.* (2004) 92(4): 2368-79

Jeka JJ, Oie KS, Kiemel T. Multisensory information for human postural control: integrating touch and vision. *Exp Brain Res.* (2000) 134(1):107-125.

Jeka J, Oie K, Schoner G, Dijkstra T, Henson E. Position and velocity coupling of postural sway to somatosensory drive. *J Neurophysiol.* (1998) 79(4): 1661-74

Jeka JJ, Ribeiro P, Oie KS, Lackner JR. The structure of somatosensory information for human postural control. *Motor Control* (1998) 2(1):13-33

Jeka JJ, Schoner G, Dijkstra T, Ribeiro P, Lackner JR. Coupling of fingertip somatosensory information to head and body sway. *Exp Brain Res.* (1997) 113(3): 475-83

Jeka JJ. Light touch contact as a balance aid. *Phys Ther.* (1997) 77(5): 476-87

Jeka JJ, Easton RD, Bentzen BL, Lackner JR. Haptic cues for orientation and postural control in sighted and blind individuals. *Percept Psychophys.* (1996) 58(3): 409-23

Jeka JJ, Lackner JR. The role of haptic cues from rough and slippery surfaces in human postural control. *Exp Brain Res.* (1995) 103(2):267-76

Jeka JJ, Lackner JR. Fingertip contact influences human postural control. *Exp Brain Res.* (1994) 100(3):495-502

Johansson R, Magnusson M, Akesson M. Identification of human postural dynamics. *IEEE Trans BioMed Eng*. (1988) 35(10):858-869.

Kandel ER, Jessell & Schwartz JH & Jessell TM. Principles of Neural Science. McGraw-Hill (1991).

Kane TR, Levinson DA. Dynamics: Theory and Applications. McGraw-Hill (1985) New York.

Kearney RE, Hunter IW. System identification of human joint dynamics. *Crit Rev Biomed Eng.* (1990) 18(1):55-87.

Kiemel T, Elahi AJ, Jeka JJ. Identification of the plant for upright stance in humans: multiple movement patterns from a single neural strategy. *J Neurophysiol.* (2008) Oct 1. [Epub ahead of print]

Kiemel T, Oie KS, Jeka JJ. Multisensory fusion and the stochastic structure of postural sway. *Biol Cybern.* (2002) 87(4): 262-77

Konrad, P, The ABCs of EMG (2005). Noraxon Corporation, Scottsdale, AZ

Kuo AD, Speers RA, Peterka RJ, Horak FB. Effect of altered sensory conditions on multivariate descriptors of human postural sway. *Exp Brain Res.* (1998) 122(2):185-95

Kuo AD. An optimal state estimation model of sensory integration in human postural balance. *J Neural Eng.* (2005) 2(3): S235-49

Kuo AD, An optimal control model for analyzing human postural balance. *IEEE Trans Biomed Eng.* (1995) Jan; 42(1):87-101.

Lackner JR, Rabin E, DiZio P. Stabilization of posture by precision touch of the index finger with rigid and flexible filaments. *Exp Brain Res.* (2001) 139(4): 454-64

Lackner JR, DiZio P, Jeka J, Horak F, Krebs D, Rabin E. Precision contact of the fingertip reduces postural sway of individuals with bilateral vestibular loss. *Exp Brain Res.* (1999) 126(4): 459-66

Lackner JR. Multimodal and motor influences on orientation: Implications for adapting to weightless and virtual environments. *J Vestib Res.*, (1992) 2:307-322

Lacour M, Barthelemy J, Borel L, Magnan J, Xerri C, Chays A, Quakine M Sensory strategies in human postural control before and after unilateral vestibular neurotomy. *Exp Brain Res*. (1997) 115, 300-310.

Lee DN, Lishman JR. Visual proprioceptive control of stance. *J Hum Movement Studies*, (1975) 1:87-95.

Loram ID, Maganaris CN, Lakie M. The passive, human calf muscles in relation to standing: the non-linear decrease from short range to long range stiffness. *J Physiol.* (2007a) 584:661-675.

Loram ID, Maganaris CN, Lakie M. The passive, human calf muscles in relation to standing: the short range stiffness lies in the contractile component. *J Physiol.* (2007b) 584:677-692.

Loram ID, Lakie M. Direct measurement of human ankle stiffness during quiet standing: the intrinsic mechanical stiffness is insufficient for stability. *J Physiol.* (2002) 545(Pt 3): 1041-53

Loughlin PJ, Redfern MS, Spectral characteristics of visually induced postural sway in healthy elderly and healthy young subjects. *IEEE Trans Neural Syst Rehabil Eng*. (2001) Mar; 9(1):24-30.

Marple SL, *Digital spectral analysis with applications*. (1987) Englewood-Cliffs, NJ Prentice-Hall.

Magnusson ME, Johansson R, Wiklund J. Significance of pressor input from the human feet in lateral postural control. *Act Otolaryngol* (Stochl) (1990) 110: 321-327.

Masani K, Popovic MR, Nakazawa K, Kouzaki M, Nozaki D. Importance of body sway velocity information in controlling ankle extensor activities during quiet stance. *J Neurophysiol*. (2003) 90: 3774-3782.

Matthews PBC, Mamallian muscle receptors and their central actions. (1972) London: Edward Arnold.

Maurer C, Mergner T, Peterka RJ. Multisensory control of human upright stance. *Exp Brain Res.* (2005) 24: 1-20

Maurer C, Mergner T, Bolha B, Hlavacka F. Vestibular, visual, and somatosensory contributions to human control of upright stance. *Neurosci Lett.* (2000) 281(2-3): 99-102

McCollum G, Leen TK, Form and exploration of mechanical stability limits in erect stance. *J Mot Behav*. (1989) 21(3): 225-44.

Mergner T, Schweigart G, Maurer C, Blumle A. Human postural responses to motion of real and virtual visual environments under different support base conditions. *Exp Brain Res.* (2005) 167(4): 535-56

Mergner T, Maurer C, Peterka RJ. A multisensory posture control model of human upright stance. *Prog Brain Res.* (2003) 142: 189-201

Mergner T, Rosemeier T. Interaction of vestibular, somatosensory and visual signals for postural control and motion perception under terrestrial and microgravity conditions--a conceptual model. *Brain Res Brain Res Rev.* (1998) 28(1-2): 118-35

Mergner T, Huber W, Becker W. Vestibular-neck interaction and transformation of sensory coordinates. *J Vestib Res.* (1997) (4): 347-67

Miles FA, Braitman DJ, Long-term adaptive changes in primate vestibuloocular reflex. II. Electrophysiological observations on semicircular canal primary afferents. *J Neurophysiol.* (1980) May; 43(5):1426-36.

Miller EF, Evaluation of otolith function by means of ocular counter-rolling measurements, In: Vestibular Function on Earth and in Space, Proceedings of the Barany Society Vestibular Symposium. J. Stahle (ed.). Pergammon Press (1970), New York.

Mirka A, Black FO. Clinical application of dynamic posturography for evaluating sensory integration and vestibular dysfunction. *Neurol Clin.* (1990) 8(2): 351-9

Mittelstaedt H. Somatic versus vestibular gravity reception in man. *Ann N Y Acad Sci.* (1992) 656: 124-39

Morasso PG, Sanguineti V. Ankle muscle stiffness alone cannot stabilize balance during quiet standing. *J Neurophysiol.* (2002) 88: 2157-2162.

Morasso PG, Schieppati M. Can muscle stiffness alone stabilize upright standing? *J Neurophysiol.* (1999) 82(3): 1622-6

Nashner LM, Black FO, Wall C 3rd. Adaptation to altered support and visual conditions during stance: patients with vestibular deficits. *J Neurosci.* (1982) 2(5): 536-44

Nashner LM. Adapting reflexes controlling the human posture. *Exp Brain Res.* (1976) 26(1): 59-72

Nashner LM. Analysis of stance posture in humans. In Towe A, Luschei E (Eds.) *Handbook of Behavioral Neurobiology* (Vol 5), motor coordination (pp 527-555). (1981) Plenum, New York

Newell KM, Slobounov SM, Slobounova ES, Molenaar PC. Stochastic processes in postural center-of-pressure profiles. *Exp Brain Res.* (1997) 113(1): 158-64

Oie KS, Kiemel T, Jeka JJ. Multisensory fusion: simultaneous re-weighting of vision and touch for the control of human posture. *Brain Res Cogn Brain Res.* (2002) 14(1):164-76

Oie KS, Kiemel T, Jeka JJ. Human multisensory fusion of vision and touch: detecting non-linearity with small changes in the sensory environment. *Neurosci Lett.* (2001) 315(3): 113-6

Park S, Horak FB, Kuo AD, Postural feedback responses scale with biomechanical constraints in human standing. *Exp Brain Res.* (2004) Feb; 154(4):417-27.

Paulus WM, Straube A, Brandt T. Visual stabilization of posture. Physiological stimulus characteristics and clinical aspects. *Brain.* (1984) 107(Pt 4): 1143-63

Peterka RJ, Black FO, Schoenhoff MB, Age-related changes in human vestibulo-ocular and optokinetic reflexes: Psuedorandom rotation tests, *J Vestib Res.* (1990) 1:61-71.

Peterka RJ, Loughlin PJ. Dynamic regulation of sensorimotor integration in human postural control. *J Neurophysiol.* (2004) 91(1): 410-23

Peterka RJ. Sensorimotor integration in human postural control. *J Neurophysiol.* (2002) 88(3): 1097-118

Peterka RJ. Postural control model interpretation of stabilogram diffusion analysis. *Biol Cybern.* (2000) 82: 335-343

Peterka RJ, Benolken MS. Role of somatosensory and vestibular cues in attenuating visually induced human postural sway. *Exp Brain Res.* (1995) 105(1): 101-10

Reginella RL, Redfern MS, Furman JM. Postural sway with earth-fixed and body referenced finger contact in young and older adults. *J Vestib Res.* (1999) 9(2):103-9

Rickards C, Cody FW. Proprioceptive control of wrist movements in Parkinson's disease. Reduced muscle vibration-induced errors. *Brain.* (1997) 120(Pt 6): 977-90

Rogers MW, Wardman DL, Lord SR, Fitzpatrick RC. Passive tactile sensory input improves stability during standing. *Exp Brain Res.* (2001) 136(4): 514-22

Runge CF, Shupert CL, Horak FB, Zajac FE. Role of vestibular information in initiation of rapid postural responses. *Exp Brain Res.* (1998) 122(4): 403-12

Schmid-Priscoveanu A, Straumann D, Kori AA. Torsional vestibulo-ocular reflex during whole-body oscillation in the upright and the supine position: I. Responses in healthy human subjects. *Exp Brain Res* (2000)134:212-219.

Scholz JP, Schöner G, Hsu WL, Jeka JJ, Horak F, Martin V. Motor equivalent control of the center of mass in response to support surface perturbations. *Exp Brain Res.* (2007) Jun;180(1):163-79.

Scholz JP, Schöner G, Latash ML. Identifying the control structure of multijoint coordination during pistol shooting. *Exp Brain Research*, (2000) 25(3):382-404.

Schöner G. Dynamic theory of action-perception patterns: the "moving room" paradigm. *Biol Cybern.* (1991) 64(6): 455-62.

Schweigart G, Heimbrand S, Mergner T, Becker W. Perception of horizontal head and trunk rotation: modification of neck input following loss of vestibular function. *Exp Brain Res.* (1993) 95(3): 533-46

Scott DE, Dzendolet E, Quantification of sway in standing humans. *Agressologie.* (1972) 13: Suppl B: 35-4.

Shupert CL, Hlavacka F, Horak FB. Somatosensory loss increases responses to galvanic vestibulospinal stimulation. Society for Neuroscience Abstracts (1998) 24:152.

Shupert CL, Horak FB. Effects of vestibular loss on head stabilization in response to head and body perturbations. *J Vestib Res.* (1996) 6(6): 423-37

Shupert CL, Horak FB, Black FO. Hip sway associated with vestibulopathy. *J Vestib Res.* (1994) 4(3): 231-44

Soechting J, & Berthoz A. Dynamic role of vision in the control of posture in man. *Exp Brain Res*, (1979) 36, 551-561.

Trousselard M, Barraud PA, Nougier V, Raphel C, Cian C. Contribution of tactile and interoceptive cues to the perception of the direction of gravity. *Brain Res Cogn Brain Res.* (2004) 20(3): 355-62

van Asten WN, Gielen CC, van der Gon JJ. Postural movements induced by rotations of visual scenes. *J Opt Soc Am A.* (1988) 5(10): 1781-9

van der Kooij H, van Asseldonk E, van der Helm FC. Comparison of different methods to identify and quantify balance control. J Neurosci Methods. (2005) Jun 30;145(1-2):175-203. Epub 2005 Mar 19.

van der Kooij H, Jacobs R, Koopman B, van der Helm F. An adaptive model of sensory integration in a dynamic environment applied to human stance control. *Biol Cybern.* (2001) 84(2): 103-15

van der Kooij H, Jacobs R, Koopman B, Grootenboer H. A multisensory integration model of human stance control. *Biol Cybern.* (1999) 80(5): 299-308

Wei, WWS, *Time Series Analysis: Univariate and Multivariate Methods* (1990) Addison-Wesley, Reading, Ma.

Wilson V, Melvill Jones G. Mammalian Vestibular Physiology (1979) Plenum, New York

Winter DA, Patla AE, Prince F, Ishac M, Gielo-Perczak K. Stiffness control of balance in quiet standing. *J Neurophysiol.* (1998) 80(3): 1211-21

Zajac F, Muscle coordination of movement: a perspective. *J Biomech.* (1993) 26:109-124.

Zhang Y, Kiemel T, Jeka J, The influence of sensory information on two-component coordination during quiet stance, *Gait Posture.* (2007) Jul;26(2):263-71.

Zoubir AM and Boashash B, The bootstrap and it's application in signal processing. *IEEE Signal Processing Magazine*, (1998) 15:56-76.